Magnetic Resonance Augmented Cardiopulmonary Exercise Testing

Dr. Nathaniel Barber

A dissertation submitted in partial fulfillment
of the requirements for the degree of

Doctor of Philosophy
of
University College London

Institute of Cardiovascular Science
2018

I, Nathaniel Barber confirm that the work presented in this thesis is my own. Where information has been derived from other sources, I confirm that this has been indicated in the thesis.

Abstract

The clinical quantitative assessment of exercise capacity is usually achieved through measurement of peak oxygen consumption (VO_2) during cardio-pulmonary exercise testing (CPET). In most patients with cardiovascular disease reduced peak VO_2 is primarily the result of a limited capacity to augment cardiac output (CO). An important secondary cause is reduced peripheral oxygen extraction. As conventional CPET does not measure CO or tissue oxygen extraction it cannot comprehensively determine the causes of exercise limitation. Invasive CPET combining conventional exercise testing with pulmonary and systemic arterial catheterisation can differentiate the causes of exercise impairment however it is practically challenging, suitable only for limited groups of patients and precluded in children. We developed an alternative non-invasive approach to exercise testing combining real-time magnetic resonance imaging (MRI) flow measurement with respiratory gas analysis, using a system modified for safe use in the MRI environment. Using the Fick equation it is possible to determine the arterio-venous oxygen concentration difference (a-vO_2) in addition to CO and VO_2 throughout exercise.

The first part of this work describes the development of MR-augmented CPET (MR-CPET) and validation in 17 healthy adults. MR-CPET was well tolerated and demonstrated strong correlations with conventional CPET metrics. MR-CPET allowed differentiation of the contributions of a-vO_2 and CO to peak VO_2.

The second part of this work describes the application of MR-CPET in 10 healthy children, 10 with repaired Tetralogy of Fallot (ToF) and 10 children with Pulmonary Arterial Hypertension (PAH). MR-CPET was found to be safe and feasible in all three groups and demonstrated different patterns of abnormal response to exercise in the two disease groups with a significantly lower peak a-vO_2 in the PAH group and a greater rest to peak difference in CO but lower peak CO in the ToF group.

The final part of this work describes the application of MR-CPET in 13 young adults with the Fontan circulation and 13 matched controls. Adults with the Fontan circulation demonstrated chronotropic incompetence with an inability to augment CO. Although a-vO_2 was lower in patients than controls this was not significant.

Impact Statement

Exercise intolerance is a common feature of cardiopulmonary disease. In addition to its negative impact on quality of life, impairment in exercise capacity is known to be a powerful prognostic indicator in several conditions. This research focused on three patient groups: children with PAH, children with repaired ToF and young adults with the Fontan circulation. To varying degrees reduced exercise capacity is present in all three groups and has a diagnostic and/or prognostic role. In all three groups the mechanisms of reduced exercise capacity have not been fully explored. Increasingly the multisystem nature of exercise intolerance is recognised. We sought to develop a non-invasive MR-CPET methodology combining innovative real time CMR imaging with elements of conventional CPET in order to better understand the determinants of reduced exercise capacity in these groups.

In order to ensure that this approach could be readily translated into clinical practice we worked with a commercial CPET manufacturer to inexpensively modify a system widely used in clinical practice for safe use in the MR environment. We found that MR-CPET is safe and well tolerated in patient groups and able to demonstrate physiology not revealed using conventional non-invasive techniques. Improved evaluation of reduced exercise capacity may enable better management and prognostication. MR-CPET has a potential role in clinical trials, for example in investigating the mechanisms of response to pharmacological treatment or exercise intervention. Beyond potential direct clinical applications this approach may be useful for better understanding of exercise physiology in health, particularly in children where invasive techniques are not ethically or practically possible.

Acknowledgements

I would like to express my deepest thanks and appreciation to everyone who has contributed to realising this work.

To Dr Vivek Muthurangu and Dr Jennifer Steeden for their insight and expert supervision.

To the Cardiac MRI team at Great Ormond Street Hospital and in particular Ms Wendy Norman, Dr Grzegorz Kowalik, Mr Rod Jones, Mr Steven Kimberley, Dr Emmanuel Ako, Dr Mun Cheang and Dr Preeti Choudhary for their hard work, creativity and support. To the Pulmonary Hypertension and Transition teams at Great Ormond Street Hospital and the Adult Congenital Heart Disease team at Bart's Heart Centre for their assistance in recruiting patients. To Great Ormond Street Hospital Children's Charity for their generous funding.

Finally, I would like to thank all the children, young people and adults who participated, for their time, energy and enthusiasm and without whose altruism this research would not have been possible.

Table of Contents

List of Tables

List of Figures

Abbreviations

2D	Two Dimensional
31-P	Phosphorous 31
3D	Three Dimensional
4D	Four Dimensional
6MWT	Six Minute Walk Test
a-vO_2	Arteriovenous Oxygen Content Gradient
ACCP	American College of Chest Physicians
ACE	Angiotensin Converting Enzyme
ANOVA	Analysis Of Variance
ASL	Arterial Spin Labelling
ATP	Adenosine Triphosphate
ATS	American Thoracic Society
BLAST	Broad-use Linear Acquisition Speed-up Technique
BOLD	Blood Oxygen Level Dependent
BPM	Beats Per Minute
BTPS	Body Temperature And Pressure Saturated
CHD	Congenital Heart Disease
CI	Confidence Interval
CMR	Cardiac Magnetic Resonance
CO	Cardiac Output
CO_2	Carbon Dioxide
CPAP	Continuous Positive Airway Pressure
CPET	Cardio Pulmonary Exercise Test
CPMS	Central Portfolio Management System
CT	Computed Tomography
CTEPH	Chronic Thromboembolic Pulmonary Hypertension
DcO_2	Arterio-venous Oxygen Content Gradient
DICOM	Digital Imaging and Communications in Medicine
ECG	Electrocardiogram
EDV	End Diastolic Volume
EF	Ejection Fraction
EOV	Exercise Oscillatory Ventilation
EPI	Echo Planar Imaging
ESC	European Society of Cardiology
ESV	End Systolic Volume
FAIRER	Flow sensitive Alternating Inversion Recovery with an Extra Radiofrequency pulse
FOV	Field Of View
FVC	Forced Vital Capacity
GESV	Gas Exchange System Validation
GPU	Graphics Processing Unit
GRAPPA	GeneRalized Autocalibrating Partial Parallel Acquisition
GUCH	Grown-up Congenital Heart Disease

HLA	Horizontal Long Axis
HR	Heart Rate
ICC	Intra class correlation
iCPET	Invasive Cardio Pulmonary Exercise Test
IDEAL	Iterative Decomposition of water and fat with Echo Asymmetry and Least squares estimation
IGR	Inert Gas Rebreathing
iPAT	Integrated Parallel Imaging Technique
IRAS	Integrated Research Approval System
IVC	Inferior Vena Cava
k-t	k-space and temporal dimension
LGE	Late Gadolinium Enhancement
LV	Left Ventricle
LVEDV	Left Ventricular End Diastolic Volume
LVEF	Left Ventricular Ejection Fraction
LVESV	Left Ventricular End Systolic Volume
LVSV	Left Ventricle Stroke Volume
METS	Metabolic Equivalents
mPAP	Mean Pulmonary Artery Pressure
MR	Magnetic Resonance
MR-CPET	Magnetic Resonance Augmented Cardio Pulmonary Exercise Test
MRI	Magnetic Resonance Imaging
MRS	Magnetic Resonance Spectroscopy
MVV	Maximum Voluntary Ventilation
NIRS	Near Infrared Spectroscopy
O_2 Pulse	Oxygen Pulse
PA	Pulmonary Artery
PAH	Pulmonary Arterial Hypertension
$PcCO_2$	Endcapillary CO_2
PCMR	Phase Contrast Magnetic Resonance
PPM	Parts Per Million
PPVI	Percutaneous Pulmonary Valve Implantation
PR	Pulmonary Regurgitation
PRF	Pulmonary Regurgitant Fraction
PVE	Partial Volume Effect
Qp:Qs	Ratio of flow in the pulmonary artery to flow in the aorta
RER	Respiratory Exchange Ratio
RF	Radio Frequency
RFOV	Reduced Field Of View
ROI	Region Of Interest
RPM	Revolutions Per Minute
RV	Right Ventricle
RVEDV	Right Ventricular End Diastolic Volume
RVEF	Right Ventricular Ejection Fraction
RVESV	Right Ventricular End Systolic Volume

RVSV	Right Ventricle Stroke Volume
SaO_2	Oxyhaemoglobin Saturation
SAX	Short Axis
SENSE	SENSitivity Encoding
SNR	Signal to Noise Ratio
SSFP	Steady State Free Precession
STPD	Standard Pressure Dry
SV	Stroke Volume
SVC	Superior Vena Cava
SVR	Systemic Vascular Resistance
T	Tesla
TCPC	Total Cavo Pulmonary Connection
TE	Echo Time
TEFPI	Turbo Field Echo Planar Imaging
TOF	Tetralogy of Fallot
TR	Repetition Time
TSENSE	Temporal Filtering Combined With Spatial Sensitivity Encoding
UKCRN	United Kingdom Clinical Research Network
UNFOLD	Unaliasing by Fourier-encoding the overlaps in the temporal dimension
VCG	Vectorcardiogram
VCO_2	Carbon Dioxide Output
V_E	Minute Ventilation
V_E/VCO_2	Ventilatory Equivalent For Carbon Dioxide
VEDV	Ventricular End Diastolic Volume
VENC	Velocity Encoding
VESV	Ventricular End Systolic Volume
VLA	Vertical Long Axis
VNR	Velocity To Noise Ratio
VO_2	Oxygen Uptake
VO_{2max}	Maximum Oxygen Uptake
VO_{2peak}	Peak Oxygen Uptake
VO_{2AT}	VO_2 At Anaerobic Threshold
VT	Ventilatory Threshold
VTI	Velocity Time Interval
W	Watts
WHO	World Health Organisation

Chapter 1 Introduction and Motivation

For many patients with cardiopulmonary disease reduced exercise tolerance and exercise induced symptoms are central features. Exercise capacity and functional status are often closely interrelated with clinical symptoms and prognosis. Exercise impairment may significantly limit quality of life. For the majority of patients with cardiopulmonary disease the primary cause of reduced aerobic capacity is an impaired ability to augment cardiac output (CO)(1) but other mechanisms of exercise intolerance may be important contributory factors.

Despite symptoms frequently presenting or worsening with exercise, conventional cardiac imaging and therefore the imaging markers used to guide treatment are typically obtained at rest. Advances such as real time cardiac MRI mean that robust methodologies for exercise imaging now exist. Cardiopulmonary exercise testing (CPET) is an established exercise investigation and recognised as a powerful prognostic tool. CPET variables including oxygen uptake (VO_2), ventilatory equivalent for carbon dioxide slope (V_E/VCO_2) and exercise oscillatory ventilation (EOV) have all individually been proven to be significant prognostic markers in heart failure(2). Importantly, whilst CPET provides highly useful information about overall aerobic capacity alone it cannot provide accurate information on CO and tissue oxygen extraction.

The work in this thesis set out to develop a new modality integrating CPET with exercise cardiac magnetic resonance imaging (MRI) as a comprehensive, non-invasive means of assessing exercise capacity and causes of impairment. The clinical importance of improved identification and understanding is the potential to better target therapies and thereby treat disease.

1.1 Exercise Limitation

In health the body acts as a highly integrated system matching the response of multiple organs to the demands of exercise. Exercise starts with a neurological stimulus; a command from the motor cortex leading to motor neurone activation and depolarization of the motor neurone endplate. In turn this results in muscle action

potential propagation, calcium release and the formation of actin-myosin cross bridges and muscle shortening. This mechanical energy production is dependent on chemical energy in the form of adenosine triphosphate (ATP). Myocytes only contain sufficient stores of ATP for 10-15 seconds of activity. Sustained exercise is dependent on carbohydrate and fat oxidation to regenerate ATP and continue the cross bridge cycle(3). The continued supply of oxygen to mitochondria and removal of carbon dioxide are essential to maintain this. Ventilation, gas-exchange and circulation correspondingly adjust to meet these requirements. In healthy adults CO may increase to as much as 5-6 times resting levels in response to strenuous exercise(4). Similarly, ventilation becomes more efficient with exercise and ventilation perfusion matching improves. A rightward shift in the oxygen dissociation curve at the level of the exercising myocytes favouring oxygen unloading as well as multiple other factors all support increased metabolic demands(5). Established models of investigation and treatment of impaired exercise tolerance have centred on individual organ systems, however it is clear even from this very brief overview that a multisystem approach is needed to interpret exercise limitation.

The skeletal muscle hypothesis in heart failure(6) provides a model for an integrated, multisystem approach to understanding exercise limitation in patients with cardiopulmonary disease. The hypothesis proposes that a feedback loop links changes in skeletal muscle structure and function with abnormal reflex cardio-pulmonary control in a negative cycle, limiting exercise and resulting in further deterioration in disease progression and symptom generation. This hypothesis is backed by findings including an exaggerated and inefficient ventilatory response to exercise (increased V_E/VCO_2), poor correlation between functional class and conventional measures of haemodynamics / systolic function as well as little impact of inotropic therapy on exercise performance despite improvement in CO(6). These cardiovascular findings occur in the context of reduced skeletal muscle mass due to myocyte atrophy and apoptosis, predominance of fast glycolytic fibres and reduced mitochondrial density (7,8). The skeletal muscle hypothesis has contributed to a dramatic change in the treatment of chronic heart failure from a position where exercise was strongly discouraged to current guidelines actively recommending

exercise in this group of patients(9). There is significant crossover between peripheral findings in (acquired) heart failure and changes found in skeletal muscle in the two groups of patients studied in this work, patients with congenital heart disease (CHD)(10) and pulmonary arterial hypertension (PAH)(11).

Exercise intolerance is a cardinal feature of PAH (12). In PAH a range of factors including hypoxaemia, inflammation, insulin resistance and increased sympathetic nerve activity have been implicated in contributing to both respiratory and limb muscle dysfunction and in turn fatigue, dyspnea and exercise limitation (11). The role of limb muscle dysfunction in PAH exercise limitation are supported by the landmark findings of Mereles' study of adults with pulmonary arterial hypertension undergoing a 15 week exercise programme (13). Endpoints in this study including peak VO_2 and six-minute walk test distance increased significantly without significant changes in echocardiographic findings. This suggests that skeletal muscle dysfunction is an important target for therapeutic intervention in PAH.

Despite the very broad range of conditions that make up CHD a degree of exercise intolerance is a near universal finding across this group (14). Even where patients describe themselves as asymptomatic, cardiopulmonary exercise testing reveals impaired aerobic capacity. There is building evidence of acquired skeletal myopathy in congenital heart disease(10). Some of the mechanisms behind these findings are believed to be in common with recognised inflammatory and neurohormonal interactions found in acquired heart failure. Increased muscle fatigability has been demonstrated in patients with repaired Tetralogy of Fallot, Fontan circulation and post atrial switch operation(15). Reduced skeletal muscle mass has been found in adults with Fontan circulation and at a cellular level reduced muscle aerobic capacity has been identified using ^{31}P MR spectroscopy techniques(16). Again these findings have led to trials of exercise training programmes in patients with congenital heart disease with demonstrated improvement in exercise capacity after such interventions (17,18) .

1.2 Developing a New Approach to Exercise Assessment

Conventional approaches to the clinical investigation of exercise intolerance have tended to focus on individual systems and are unable to differentiate impairment in oxygen uptake due to cardiac output and tissue oxygen extraction. Given the emerging understanding of the multisystem causes of exercise limitation in patients with cardiopulmonary disease it is clear that more comprehensive approaches to assessment are needed. The complexity of factors involved in exercise limitation and the fact that assessing them requires the measurement of a moving target makes developing tools to allow a fully integrated assessment challenging. Invasive (cardiac catheter) exercise testing is a proven modality(19) but this technique is not appropriate for use in many patient groups and is particularly unsuitable for use in children.

As stated above this project set out to develop a non-invasive integrated approach combining cardiac MRI (CMR) and CPET (MR-CPET) that could differentiate cardiac, respiratory and skeletal muscle insufficiency as causes of exercise limitation. CMR is the reference standard for non-invasive assessment of CO. Maximum oxygen uptake (VO_{2max}) is the recognised primary measure of aerobic fitness. By simultaneously measuring CO and VO_2 and using the Fick principle it is possible to calculate arterio-venous oxygen concentration difference (a-vO_2) a proxy of tissue oxygen extraction. The Fick principle states that blood flow over a given time period is equal to the amount of substance entering the stream of flow over the same time period divided by the difference between the concentrations of that substance in the blood upstream and downstream from its entry point(20). In clinical practice the Fick principle is used as the gold standard for assessing cardiac output using cardiac catheter data. The Fick equation states:

$$Q = \frac{VO_2}{Ca - Cv\,O_2}$$

Where Q is flow, VO_2 oxygen uptake and Ca-CvO_2 the arteriovenous difference in oxygen content. The Fick equation can also be rearranged to calculate oxygen concentration gradient, a proxy for tissue oxygen extraction:

$$Ca - Cv\ O_2 = \frac{Q}{VO_2}$$

Achieving this integrated MR-CPET approach presents multiple challenges. Like other forms of imaging most CMR imaging is performed at rest. Conventional gated sequences are unreliable in exercise due to both respiratory motion and motion from the exercise stressor. In addition they do not accurately reflect short-term changes in flow as they average signal over multiple cardiac cycles. Novel high temporal and spatial resolution real time sequences have helped overcome these problems. This project sought to leverage these advances as well as innovative approaches to image reconstruction to facilitate imaging over the relatively long time periods required for exercise testing.

There are also several constraints to performing exercise testing in the MRI scanner. For most people the MRI scanner is an unfamiliar and uncomfortable environment in which to exercise. The amount of space available is limited by the size of the scanner bore, and visual and verbal cues that are an intrinsic part of conventional exercise testing are less readily accessible. Cardiopulmonary exercise test metabolic carts contain multiple ferromagnetic parts and cannot safely be brought into the scanner room. In order to develop the MR-CPET approach to a standard that would allow translation into clinical practice required solutions to these practical constraints.

Finally, the processing of the very large data sets produced by the proposed methodology presents new problems in terms of image processing and integration of the different data sources.

Before implementing MR-CPET in paediatric and adult disease populations it was necessary to validate the technique, testing its feasibility and tolerability in healthy adults. The results of this work make up the first results chapter. The second results chapter investigates MR-CPET in three paediatric groups, children with PAH, repaired Tetralogy of Fallot and healthy controls. Invasive CPET is not possible in children and MR-CPET may represent a useful tool for understanding the mechanisms of exercise impairment in paediatric populations. The final results chapter explores the causes of exercise limitation young adults with the Fontan

circulation and represents a development of the technique with the addition of measurement of leg muscle mass and multiple flows at rest and peak exercise in an attempt to better understand exercise limitation in this group.

Chapter 2 Conventional Cardiopulmonary Exercise Testing and Noninvasive Measurement of Cardiac Output in Exercise

2.1 Use and Limitations of Cardiopulmonary Exercise Testing

CPET is a widely used clinical tool that provides an objective integrative assessment of cardiac, respiratory and musculoskeletal response to exercise. This integrated approach provides additional value in understanding exercise physiology compared to testing individual systems. Conventional CPET addresses three main questions:

1) Is exercise capacity reduced in comparison to standardized data for age, sex, height and weight?
2) Is metabolic demand increased? For the same amount of work does peripheral muscle consume more oxygen or produce more carbon dioxide?
3) If limitation is present is this due to cardiac or respiratory limitation (other causes of limitation are inferred but not by conventional CPET)?

Psychological and behavioural causes of exercise limitation can also be identified through exclusion of other causes. A significant deficit of conventional CPET is an inability to measure CO. One approach to address this is invasive CPET (iCPET). Whilst this technique overcomes the limitations of conventional CPET it is technically challenging and only suited for use in limited patient groups. Because of the importance of CO in determining exercise capacity and the challenges of invasive testing a range of non-invasive methods have been developed.

This chapter summarises the technology used in conventional CPET, the design and performance of CPET protocols, the interpretation of key CPET variables and the clinical use of CPET. iCPET and a selection of alternative non-invasive techniques for exercise CO assessment are described at the end of the chapter.

2.2 Cardiopulmonary Exercise Test Equipment

Performing cardiopulmonary exercise testing requires an ergometer and analyser consisting of a gas analyser, flow and volume transducers. Guidelines recommend

that CPET is performed in a quiet, temperature and humidity controlled laboratory with full resuscitation equipment by appropriately trained staff.

2.2.1 Ergometers

An ergometer is an apparatus for measuring work performed by a person exercising. Typically an ergometer is mechanically or electrically braked to control resistance and work rate. The two most commonly used groups of ergometer are cycle and treadmill, however a range of other forms of ergometer from arm cranks (21) to simulated swimming (22) exist for specific roles / populations. Peak heart rate, ventilation and power-output are similar across all upright techniques. Peak VO_2 is consistently found to be approximately higher using a treadmill than cycle ergometer with differences of up to 7-10% reported (23). This difference has been explained by a higher whole body oxygen uptake due to more muscle groups being used with treadmill exercise(23). Where smaller groups of muscle are tested (non whole-body exercise) at any given sub-maximal VO_2 values for heart rate, ventilation and blood lactate have been found to be higher (24).

2.2.2 Supine Versus Upright Exercise

Supine ergometers are less widely used for cardiopulmonary exercise testing than upright techniques; they are however widely used in exercise imaging. There is known to be less use of stabilising and weight bearing muscles with supine ergometers as well as a lower non-exercising metabolic cost of work

The haemodynamics of supine exercise are clearly very different to upright exercise performed in daily life. Transitioning from a supine to upright position results in a fall in both ventricular end diastolic pressure and volume (25). Endurance and fatigue are influenced by body tilt with increased endurance when the active muscle is below the heart. A shorter duration of graded exercise and lower peak power and peak heart rate have all been associated with supine posture(26) however this is not an entirely consistent finding with similar peak power output and heart rate using both techniques demonstrated in children(27).

It has been suggested that a fully supine position with an elevated leg position (as with most MRI ergometers) increasing venous return to the heart results in maximal or near maximal EDV(28). The interaction between exercise and supine position is more challenging to assess and subject to longstanding discussion(25). The complexity of mechanisms behind positional differences in haemodynamics is increasingly recognised, for example differences in sympathetically mediated increase in heart rate and stroke volume via muscle metaboreflex activation have recently been demonstrated to be absent in supine exercise(29).

The differences in CPET values obtained by upright and supine exercise have been extensively investigated(30-32). Supine exercise is consistently found to result in a lower VO_2 capacity(27), although a higher VO_2 at sub-maximal exertion with supine than with upright exercise has been reported (33). In a large 2014 cohort healthy children peak VO_2 during upright exercise was found to be significantly higher with upright exercise but strongly correlated with supine peak VO2 (r=0.94) (27). This relationship has also been demonstrated in patient populations for example in adults with heart failure with preserved ejection fraction where a strong correlation (r=0.64) was found but with a ~60% higher peak VO_2 was found with upright exercise (34).Postulated mechanisms for a higher peak VO_2 in upright exercise include a postural effect on muscle endurance with greater blood flow to the legs (26) and greater overall muscle involvement and less localised muscle fatigue (35).

2.2.3 Gas Analysers

CPET systems use gas analysers to quantify exhaled carbon dioxide and oxygen concentrations in order to calculate oxygen consumption and carbon dioxide production.

In clinical CPET systems three main types of oxygen analyser are in use: Electrochemical, Paramagnetic and Zirconium Oxide. Mass spectrometry systems are also available and provide even greater precision in measurement. However, these systems are less widely used in clinical settings primarily because of the significantly higher financial cost. Because of their accuracy and cost-effectiveness electrochemical (also known as fuel cell) analysers are most often used for oxygen

sensing in commercial systems. Electrochemical analysers use a sensing membrane and thin layer of electrolyte. Molecules reach the cathode surface where they undergo reduction to produce OH^- ions that then migrate to the anode where oxidation occurs. Flow of electrons produces a current proportional to the concentration of oxygen in the sample gas. Carbon dioxide (CO_2) is typically measured using a nondispursive infrared type analyser. An infrared beam is passed alternately through the sample and through a reference. A detector is used to sense change in absorption in detected infrared wavelengths with the calculated fractional concentration proportional to the infrared absorption.

Accurate and reproducible CPET is dependent on regular calibration. Oxygen analyser calibration is performed against gases of known concentration and performed over the sample range expected of measurements in testing (12% to 21%) CO_2 calibration is typically preformed against a gas containing no carbon dioxide known as the "zero" gas and a "span" gas containing above the expected physiological upper limit of normal (7% to 8% CO_2).

2.2.4 Flow and Volume Measurement

Flow transducers measure flow at a set frequency, integration of flow and time data provides calculated flow volume data. The four types of flow transducer most commonly used in commercial systems are pneumotachograph, pitot tube, hot-wire anemometer and turbine. The pneumotachograph works by measuring change in pressure across an obstruction within the pneumotachograph tube. Across all types of flow transducer calibration is essential prior to use. Standard calibration is with a 3 litre calibration syringe(36). An accuracy of no greater than 3% error is considered acceptable in clinical testing.

2.2.5 Water Vapour

Water vapour is a significant practical concern in cardiopulmonary exercise testing and warrants specific note. As water vapour pressure contributes to total pressure it decreases the partial pressure of all other gases in sample. Underestimation of the amount of water vapor in a sample results in falsely elevated gas concentration

measurements and conversely overestimation results in falsely low gas concentration measurement. In order to attempt to overcome this problem systems may include sampling tubes composed of polymers such as Nafion(37). These polymers work as ion exchange membranes selectively reducing water vapor content in the sample line. Appropriate line storage and intervals between uses also combat this problem.

2.2.6 Other Monitoring

Other standard monitoring equipment used during CPET includes a 12 lead ECG, pulse oximeter and sphygmomanometer. ECG monitoring during exercise is required to assess heart rate and rhythm and also used to detect ischaemic and QT interval changes. Exercise ECG systems require a muscle artifact filter system in order to minimize distortion to signal(38).

2.3 Exercise Protocols

Various approaches exist to designing exercise protocols. General principals of exercise protocol design are that exercise should last for more than six minutes (to provide an adequate physiological stressor) and should not exceed twenty minutes (primarily due to inattention / boredom associated with longer tests). The optimal test duration to assess aerobic capacity is 8-12 minutes in adults and adolescents and between 6-10 minutes in younger children(38). Significantly shorter tests do exist, for example the Wingate Anaerobic Test, a test of peak anaerobic power and anaerobic capacity. Within clinical cardiopulmonary exercise testing there are two predominant approaches to determining maximal predicted workload used. The most widely used is the Wasserman approach using reference standards of expected VO_{2max} to calculate work rate increment in Watts per minute. Other groups have advocated a standardised pragmatic approach with a set work rate for health and disease. Within graded exercise testing there are two major groups of protocol, stepped protocols (typical of treadmill testing) and continuous ramp protocols (associated with cycle ergometers). Proponents of ramp protocols argue that the continuous small increments in this kind of design increase the likelihood of reaching $VO_{2max,}$ however this has not been proven(39). It is recognized that large, unequal

increments in work can disrupt the linear relationship between VO_2 and work rate (40).

2.4 Measures in Cardiopulmonary Exercise Testing

2.4.1 Work

The endurance time (total time of exercise including warm up time) in itself is an important variable for understanding functional capacity. In incremental exercise testing it is dependent on the rate of increase in work rate. Work rate or power is normally reported in Watts. Low values for work rate on their own are not informative, as they do not explain the cause of low work rate.

2.4.2 VO_2, VCO_2, Respiratory Exchange Ratio

Oxygen uptake (VO_2) is calculated as described above throughout exercise testing. It is conventionally presented as ml/minute or ml/kg/minute. Peak VO_2 (VO_{2peak}) is the highest VO_2 measured during exercise testing whereas maximum VO_2 (VO_{2max}) is the value for VO_2 at which further increase in work will not increase VO_2. In adults VO_{2max} is considered to be the best indicator of a subject's aerobic fitness. Up to 50% of healthy children will not reach a plateau, rendering VO_{2max} less relevant in paediatric studies (41). Clinically (with the exception of testing of athletes in sports medicine practice) it is rare for adult patients to reach a plateau in VO_2 and therefore other parameters are used to determine whether a test was maximal. The CPET metric with the highest reliability is VO_{2peak} and whilst a familiarization effect does exist with repeat testing it is not clinically significant(42).

Factors considered when deciding if a test was maximal include the percentage of predicted heart rate achieved, respiratory exchange ratio and whether the ventilatory threshold was surpassed. Respiratory exchange ratio (RER) is the ratio of VCO_2 (measured exhaled carbon dioxide eliminated through respiration) to VO_2 over a unit time. A RER of greater than 1.1 is used as an indicator that a subject has exercised beyond their anaerobic threshold.

2.4.3 Ventilatory Threshold

The ventilatory threshold (VT) is the point at which there is an exponential increase in V_E relative to VO_2. VT is believed to correspond to the anaerobic threshold, the point at which at a given work rate there is insufficient oxygen supply to meet demand. At this point anaerobic glycolysis is used to meet energy demand with the production of lactate as a byproduct. Increased V_E is required to remove the resulting excess CO_2. In untrained healthy adults VT typically occurs at between 45-65% of VO_{2peak} and at a higher percentage of VO_{2peak} in athletes.

2.4.4 Ventilatory Efficiency

The efficiency of the ventilatory response is evaluated by assessing the increase in minute ventilation (V_E) relative to work rate, VO_2 or VCO_2. Ventilatory equivalent for carbon dioxide (V_E/VCO_2), the ratio of minute ventilation to carbon dioxide production is the most commonly used of these variables. In healthy adults 25-30 litres per minute ventilation are required to expire 1 litre of CO_2 therefore a normal V_E/VCO_2 slope is 25-30. In heart failure this slope becomes much steeper. V_E/VCO_2 slope is recognised as an important prognostic indicator in heart failure(2).

2.4.5 Oxygen Pulse

Oxygen pulse (O_2 pulse) is a CPET derived measure defined as peak VO_2/peak HR and is expressed in ml/beat. O_2 pulse can be used as an indicator of stroke volume and arterio-venous O_2 difference. Normal values may be calculated by dividing the predicted peak VO_2 by the predicted peak HR. Although not one of the primary CPET metrics, O_2 pulse merits more detailed discussion here as it may be erroneously interpreted as a method for non-invasively measuring CO. O_2 pulse was described by Whipp (43)for estimation of a single average value for SV in steady state exercise. Whipp tested O_2 pulse performing cycle-ergometer CPET testing with simultaneous invasive catheter monitoring via pulmonary artery and brachial artery catheters in 23 healthy adults. Exercise was performed up to a steady state at 125 Watts. Predicted SV during steady state exercise was found to reflect measured values with a correlation coefficient of 0.8. Several factors mean that oxygen pulse may be unreliable(44). O_2 pulse under-estimates stroke volume in patients who have

reduced arterial oxygen concentration at peak exercise (for example in anaemia or significant arterial desaturation). In patients with increased arterial oxygen concentration (polycythaemia) stroke volume will be over estimated(45). Other confounding factors include fitness level with athletes displaying plateau in O_2 pulse at higher workloads, a need to account for body habitus and unreliability in patients with diastolic dysfunction (46-48).

2.4.6 Other Measures

Prior to CPET standard spirometry is usually performed providing data including Forced vital capacity (FVC) Forced expiratory volume in 1 second (FEV1) and Maximum voluntary ventilation (MVV). Other variables measured during CPET include heart rate and blood pressure response and oxygen saturation. In health there is an immediate increase in heart rate in response to exercise as a result of decreased vagal tone and increased sympathetic stimulation(49), during dynamic exercise there is a linear relationship with work rate, with the magnitude dependent on age, conditioning and type of exercise(50). Heart rate response is assessed for example to check adequate beta blockade or to assess chronotropic incompetence (defined as either failure to meet 85% of age predicted maximum HR or low chronotropic index; low heart rate adjusted for metabolic equivalents (METs)). In health systolic blood pressure is expected to rise in response to increasing work rates whilst in contrast diastolic blood pressure remains relatively stable. An inadequate rise or fall in blood pressure is associated with a range of disease processes as well as antihypertensive treatment and dehydration. Pulse oximetry (measuring differential absorption of infrared light) is used to provide general trends in oxygenation and is recognized to be less accurate during exercise during exercise with underestimation of true saturation due to motion artifact and poor capillary perfusion. A fall of >5% in saturations during exercise is considered to represent abnormal exercise induced hypoxaemia(36).

2.5 Standardised Reference Values

Multiple standardised reference values used to compare exercise performance exist for upright ergometer cardiopulmonary exercise testing in both healthy adults and

children(51). Because of the relative heterogeneity of exercise performance and population changes in lifestyle and fitness over time it is recommended that regularly updated datasets representative of the population from which the subject is drawn are used(52).

2.6 Safety

Cardiopulmonary exercise testing is in general, very safe. The incidence of death in adults due to CPET is 0.5 per 10,000(50) tests. As the major risk, ischaemic heart disease is far rarer in children than adults, the risks of CPET are believed to be correspondingly far lower in children. In relation to the disease conditions studied in this thesis there is evidence supporting the safety of conventional cardiopulmonary exercise testing in children with pulmonary hypertension(53) and in children and adults with congenital heart disease(14).

2.7 Diagnostic and Prognostic Value of CPET

CPET is a powerful and established prognostic tool routinely used in the management of heart failure in adults. Peak VO_2 has been demonstrated to be prognostic of worse outcome in adult heart failure with impaired and midrange ejection fraction and most recently in heart failure with preserved ejection fraction(54). V_E/VCO_2 slope independently predicts adverse cardiac events (55) (death, ventricular assist device, heart transplantation) as well as providing incremental prognostic value to peak VO_2 (54). Beyond heart failure use of CPET is indicated in a wide range of conditions and situations. Indications listed by the American Thoracic Society and the American College of Chest Physicians is summarized in Table 1.

Table 1 Summary of indications listed in the ATS / ACCP statement on CPET

Indication	Example
Evaluation of exercise capacity	Determination of functional capacity (peak VO_2) Determination causes of exercise limitation and mechanisms
Evaluation of exercise intolerance	Assessment of symptoms disproportionate to resting cardiac / pulmonary test findings Assessment of unexplained dyspnea
Cardiovascular disease	Functional evaluation / prognosis in heart failure Heart / heart-lung transplant assessment Baseline for exercise rehabilitation / monitoring response
Respiratory disease	Chronic obstructive pulmonary disease (functional impairment, assessment of contributing factors to exercise limitation) Interstitial lung disease assessment Cystic fibrosis assessment Assessment of exercise-induced bronchospasm
Pre-operative	Evaluation prior to lung resection Assessment / risk stratification in elderly patients prior to major abdominal surgery

Pertinent to the populations described in this thesis CPET also has an established role in both adult and paediatric congenital heart disease and pulmonary hypertension. Comprehensive disease specific, age and gender standardised reference values for CPET metrics exist for adults with congenital heart disease for use in interpreting disease severity and guiding treatment(56). For example, CPET has been advocated for as an adjunct for the decision making on timing of pulmonary valve replacement in repaired tetralogy of Fallot (57). CPET also has a prognostic role, for example in adults with the Fontan circulation a decline in percentage of predicted VO_{2peak} has recently been shown to be associated with an increased risk of cardiac adverse event (death or surgery) (58).

In adult pulmonary hypertension CPET has been used to demonstrate response to treatment with increases in peak VO_2 following treatment with IV prostacyclin(59) and increased peak VO_2 and decrease in V_E/VCO_2 slope with inhaled iloprost(60). CPET variables have also been used prognostically in adults with PAH. Baseline V_E/VCO_2 slope and deterioration in peak VO_2 have been shown to be predictive of survival (61) and peak VO_2 to be predictive of time to clinical worsening(62). Because of concerns over safety use of CPET in paediatric pulmonary hypertension has historically been less widespread (53) however it is now regularly used in

clinical practice. Elevated V_E/VCO_2 has been demonstrated to be associated with poor outcome (death / transplant) in children with PAH(63).

2.8 Invasive CPET

Invasive cardiopulmonary exercise testing (iCPET) involves a full conventional cardiopulmonary exercise test with the addition of invasive central haemodynamic assessment using radial and pulmonary artery catheters. For safety and practical reasons it is normally undertaken in the catheter laboratory(64).

This technique is only performed at a limited number of specialized centres in adults, typically for the investigation of unexplained exercise intolerance. It is not routinely performed in children. iCPET can be used to differentiate diagnoses including exercise induced pulmonary hypertension, exercise induced heart failure with preserved ejection fraction and impaired pre-load augmentation during exercise (19). It can also be used to identify patients where there is abnormal oxygen uptake by skeletal muscle from arterial blood (characterized by a high oxygen uptake relative to CO and relatively blunted fall in venous oxygen concentration). Mitochondrial disorders, errors of metabolism and haemoglobinopathies with high oxygen affinity all fall into this group.

The potential power of iCPET is highlighted in a paper from Huang(65). 530 patients with unexplained dyspnea underwent iCPET over 3 ½ years. Patients had undergone a median of 6 non-laboratory and 15 laboratory tests prior to referral for iCPET. In all patients there was sufficient information to make a diagnosis after iCPET. The authors recognize that conventional CPET does objectively measure exercise capacity, allowing evaluation of VO_2 and VCO_2 response to exercise but argue that it is primarily useful for establishing normal from abnormal. They highlight that abnormal findings identified by conventional CPET are not necessarily specific to a single disease.

The safety of iCPET is not widely discussed in published literature. Authors from a leading group undertaking this technique describe the safety profile and considerations of iCPET as being ‘akin’ to those for conventional CPET with the

need for additional considerations with regard to radial and pulmonary artery catheters and recommends exercise testing with a team of two physiologists a doctor and nurse present(64).

2.9 Non-invasive Methods of Assessing Cardiac Output in Exercise

Invasive assessment of CO in exercise using iCPET is clearly challenging and resource intensive. The desirability of non-invasive CO monitoring in a range of settings from surgery to intensive care and basic physiology research has led to the development of multiple approaches. This section discusses some of the most clinically relevant of currently favoured approaches to non-invasive CO monitoring in exercise to provide context (echocardiography, bioimpedance and bioreactance, oxygen pulse, gas re-breathing techniques and pulse contour analysis) but is not exhaustive.

2.9.1 Exercise echocardiography

The echocardiographic assessment of CO is based on the Doppler principle, the frequency shift in ultrasound waves reflected by a moving reflector; as the target approaches the receiver the frequency of reflected waves increases and as it moves away from the observer decreases. Doppler ultrasound used in conjunction with measured cross sectional area can be used to estimate the volume of blood flowing through the vessel. The measured velocity of blood flow over time is plotted and the area under this curve, the velocity time interval (VTI) is calculated. Stroke volume is calculated by multiplying the VTI by the cross sectional area of the vessel (usually the aorta at the level of the aortic valve or ascending aorta). Exercise echocardiography can be performed using both treadmill and supine / semi-recumbent cycling approaches, however where cardiac output is to be assessed supine/semi-recumbent cycling is preferred. Reflecting the established nature of exercise echocardiography there are recognised guidelines for use of exercise echocardiography across a wide range of conditions (66). Where exercise and imaging are not simultaneous (typically for upright exercise) 2 minutes is specified as the maximum time in which imaging should be completed.

Advantages of exercise echocardiography include that it is non-invasive, may be more readily accessible than some other modalities, can be performed at any level of exercise intensity and because it provides instantaneous high temporal resolution data does not require steady state exercise. Disadvantages include risks of error caused by transducer angulation, change in vessel cross sectional area during exercise and alterations in velocity profile with increased flow. Where exercise echocardiography results are inconclusive European (ESC) guidelines recommend CMR as the next approach(67).

2.9.2 Impedance Cardiography

Impedance cardiography is a technique used to determine CO, first developed in the late 1960s. Bio-impedance systems pass an electric current across the thorax and measure transthoracic direct current resistance. The resistance, known as impedance is proportional to the amount of fluid in the thorax and can be used to determine stroke volume and cardiac output. Impedance techniques have been used in a range of critical care settings with mixed findings.

Exercise impedance cardiography has been described in both adult and paediatric populations. A study directly comparing CO determined by an impedance device and simultaneous direct Fick method during supine exercise was undertaken by Charloux (68). A population of 40 adults with sleep apnoea or chronic obstructive pulmonary disease underwent simultaneous impedance cardiography and right heart catheterisation with continuous breath-by-breath VO_2 measurement. Low intensity exercise at a consistent workload dependent on fitness (10-50 watt) was performed on a supine ergometer. There was acceptable correlation between methods in assessing CO at rest $r = 0.89$ and at exercise $r = 0.85$. Limits of agreement (mean difference ± 2 SD) were -1.34 to +1.41 l/min at rest and -2.34 to +2.92 l/min in exercise. The authors concluded that reliability and accuracy were not definitively established but that the technique had potential advantages, because of its cost, ease of use and potential for ambulatory use over longer periods.

Welsman and colleagues investigated the reliability of thoracic impedance in 20 healthy children performing repeated cardiopulmonary exercise testing to exhaustion

on 3 occasions 3 weeks apart(69). There was no 'gold-standard' comparator in this study design. Instead, pairwise comparisons were made across the three sets of tests to assess reliability with the finding of error as a coefficient of variation for CO and stroke volume of 9.3%. The authors conclude that the technique is a valuable non-invasive tool in children although slightly less reliable than exercise echocardiography with previous studies demonstrating it to have coefficients of variation between 4.9 and 5.7% (70,71).

Recently published findings on impedance cardiography at rest and during exercise in adults with pulmonary arterial hypertension concluded that it was not a reliable technique in this group(72). Resting and exercise impedance cardiography and resting and exercise cardiac catheterisation were performed in 16 patients with the finding of unsatisfactory correlation and agreement between CO measured using these techniques. In contrast there was excellent correlation between resting CO measured by thermodilution and using PCMR.

There continue to be strong advocates for the use of impedance cardiography during exercise in clinical practice. Legendre performed a retrospective analysis of peak stroke volume measured by impedance cardiography during CPET in a mixed group of adolescent patients with residual right ventricular outflow tract lesions following surgery for congenital heart disease(73). 30 patients underwent repeat CPET testing with impedance cardiography within a time period of 18 months. Overall there was a relatively high intra class correlation coefficient between tests for both stroke volume and cardiac index (ICC 0.8), however this was significantly lower when patients with higher indexed stroke volumes (>50ml/m2) were considered (ICC <0.5). No alternative method of assessment was compared in this study. The authors maintain that the technique may have a role in decision making for these patients.

Circumstances where bioimpedance may fail include arrhythmia, and factors that impact on electrical conduction including patients body habitus, factors affecting contact between electrodes and skin (e.g. temperature, humidity) (74).

In summary although there are many appealing features to bio-impedance techniques there remain concerns over their reliability and accuracy limiting their appropriateness for use in clinical practice.

The bioreactance method for CO assessment is a newer technology. Bioreactance techniques take into account both changes in resistance to blood flow but also the changes in thoracic volume in estimating cardiac output. In healthy adults good test-retest reliability has been demonstrated during exercise with these technique(75). Bioreactance has been used in patient populations during CPET, for example in adults with heart failure demonstrating a good correlation with oxygen uptake in 23 adults with heart failure(76). Currently studies validating bioreactance against invasive CO assessment during exercise are lacking.

2.9.3 Gas rebreathing techniques

Rebreathing techniques are based on the principle that pulmonary blood flow can be determined through analysis of alveolar gas exchange. Commonly used gas rebreathing techniques include inert gas rebreathing (IGR) and CO_2 rebreathing techniques.

CO_2 rebreathing techniques involve the measurement of CO_2 elimination under normal conditions followed by a period (up to 50 seconds) when CO_2 elimination is stopped (rebreathing period). Stopping CO_2 elimination results in increased endcapillary CO_2 ($PcCO_2$) that plateaus over the non-rebreathing time. The ratio in differences between VCO_2 and $PcCO_2$ and the known CO_2 dissociation curve are used to estimate pulmonary capillary blood flow(77). Although CO_2 rebreathing been extensively used in studies estimating CO both at rest and during exercise their accuracy and reliability are contested(78).

IGR techniques compare the fall in the concentration of a blood soluble gas with the concentration of an insoluble gas within a closed rebreathing system. Several studies have validated IGR against CMR, direct Fick and thermodilution techniques(79-81) in adult populations. IGR techniques have been used in large patient populations including adults with heart failure and a large group of children and adults with a

broad range of congenital heart disease(82). In addition normal values for IGR derived CO have been published in a population of 500 healthy adults(83).

IGR techniques have been performed during exercise in studies comparing other non-invasive techniques and appear to perform well(84), however there are not studies comparing against a 'gold-standard' during exercise in health.

2.9.4 Pulse Contour Analysis

Pulse contour techniques have typically been used to invasively estimate CO in intensive care settings, however there are also descriptions of non-invasive pulse contour methodologies. Non-invasive pulse contour techniques use a finger pressure cuff to analyse the arterial wave form and calculate the area under the curve to model stroke volume in conjunction with inputted patient specific values(85). Non-invasive pulse contour analysis has been tested in exercise to a limited extent. One study of healthy adults performing cycle ergometry to a target HR of 150 bpm found good correlation with IGR derived CO($r=0.88$) with overall limits of agreement of 30.3%(86).

2.10 Summary

Exercise testing with conventional CPET provides objective data on functional capacity that cannot be determined using resting investigations. It has become an important prognostic tool across a range of conditions. A major deficit of conventional CPET is that it does not measure cardiac output and therefore is not a fully comprehensive assessment. Invasive CPET overcomes this limitation but is a major undertaking, generally requiring the use of a catheter laboratory and is not suitable for use in a range of patient groups including children.

Despite improvements in all of the non-invasive technologies described here they remain limited in their ability to estimate CO because of multiple sources of error. If these sources of error can be overcome potential advantages of these techniques may include lower cost, less intensive physiologist input and therefore relative ease in applying them to large populations. As described in the introduction and motivation

cardiac MRI is the reference standard for non-invasive measurement of CO. The next chapter sets-out fundamentals of cardiac MRI relevant to the work in this thesis.

Chapter 3 Cardiac Magnetic Resonance Imaging

Magnetic resonance imaging is a relatively new technology. The foundations of MRI go back to 1946 when Bloch and Purcell independently discovered the magnetic resonance phenomena. It was not until the late 1970's that the first human MRI scans were performed. With advances in the speed of computing the practicality and applications of clinical MRI rapidly increased and it now has an important role in medical imaging across a wide range of specialties.

Underlying MRI imaging is the principle that any spinning charged particle generates an electric field. MRI uses the body's magnetic properties to create detailed images, non-invasively providing structural and functional information.

This chapter will briefly summarise the basic theory of MRI followed by a more detailed description of challenges pertinent to this project and how they may be overcome.

3.1 MRI Physics

Felix Bloch theorized that any spinning particle will create an electromagnetic field. In humans hydrogen nuclei, consisting of a single spinning proton carrying a positive charge, are abundant. This moving charge generates a current, causing the nucleus to behave like a bar magnet with an associated dipole magnetic field.

The magnetic moment of a proton ($\vec{\mu}$) is proportional to its gyromagnetic ratio (γ) and to its angular momentum or spin ($\vec{J}$).

$$\vec{\mu} = \gamma \vec{J}$$

In normal conditions the orientation of the individual nuclei's magnetic moments are random due to thermal random motion, therefore there is no net-magnetic moment. When an external magnetic field (B_0) is applied the magnetic moments of individual nuclei can become aligned in parallel with the magnetic field (spin-up) or antiparallel (spin-down). More nuclei will align with B_0 than against it, as this requires the least

energy. Whilst the nuclei are aligned with B_0 spins continue to precess at a rate determined by the Larmor equation (ω_0);

$$\omega_0 = \gamma B_0$$

This equation shows that the precessional frequency is determined by the gyromagnetic ratio and the strength of the magnetic field.

3.1.1 Longitudinal Magnetisation

The application of B_0 causes the sum of magnetization of the sample (patient) in the scanner to align parallel with direction of B_0. This net magnetic vector can be measured by applying a radio-frequency (RF) pulse on the x-y plane. The RF pulse tips the net magnetic vector onto the transverse plane (where it can be measured), and brings the protons in phase (makes them all precesses in the same direction at the same time). This RF pulse is applied at the same frequency (the Larmor frequency) as the precessional frequency of the protons. This phenomenon is resonance.

3.2 MR Signal

The net magnetic vector in the transverse plane continues to precess. Therefore, when a receiver coil is placed on the subject, an alternating voltage will be induced across it generating electrical current; the magnetic resonance signal.

3.2.1 Relaxation

Once the RF pulse has been switched off, the magnetization returns to thermodynamic; described as T1 and T2 relaxation. T1 relaxation is the return to equilibrium of z magnetization Mz, and T2 relaxation is the destruction of the transverse magnetization, as the spins become misaligned Mxy.

3.3 Encoding Spatial Information

The received signal in MRI is the sum of magnetization from all of the excited spins within the object. Therefore it does not contain any spatial information. From the Larmor equation we see that the precessional frequency is proportional to the

external magnetic field. Therefore, by applying linearly varying magnetic field gradients, we can vary the frequency as a function of position along the gradient.

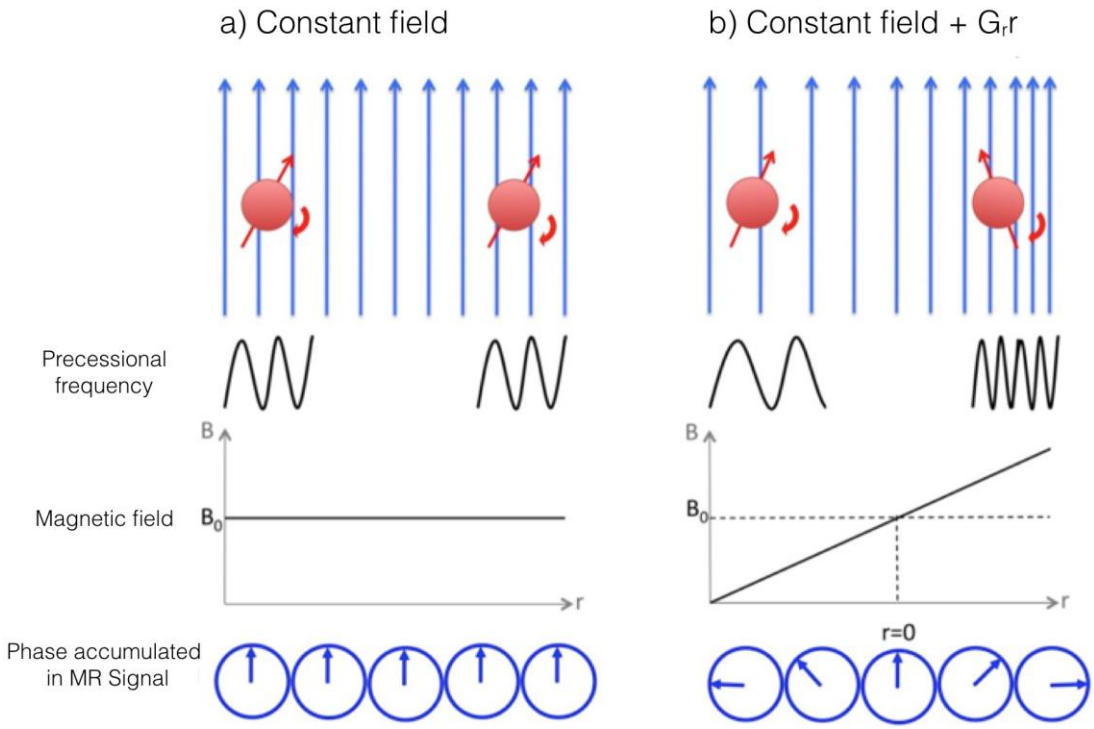

Figure 3.1 The effect of application of a gradient on the precessional frequency of spins.

A) All spins precess at the same frequency in a constant field B) Application of a linear gradient results in precessional frequency dependent on position. Reproduced with the kind permission of Dr Jennifer Steeden.

The resultant signal is therefore dependent on its 3D position;

$$S(t) = \iiint \rho(\vec{r}) \exp\left(-j\gamma \vec{G}_r . \vec{r}t\right) d\vec{r}$$

S = signal $\vec{G}_r$ = gradient

This raw data space is called *k-space*. The centre of k-space contains low spatial frequencies and at the periphery contains high spatial frequencies. Fourier transformation of this signal resolves the position of spins in space.

3.3.1 Slice selection

As previously described, the RF-pulse only affects spins that are precessing at the frequencies present in the RF-pulse. Therefore, by applying a linearly varying

gradient (Figure 3.2) at the same time as the RF-pulse, only a band of spins are excited. This is called slice selection, and reduces the problem to two dimensions.

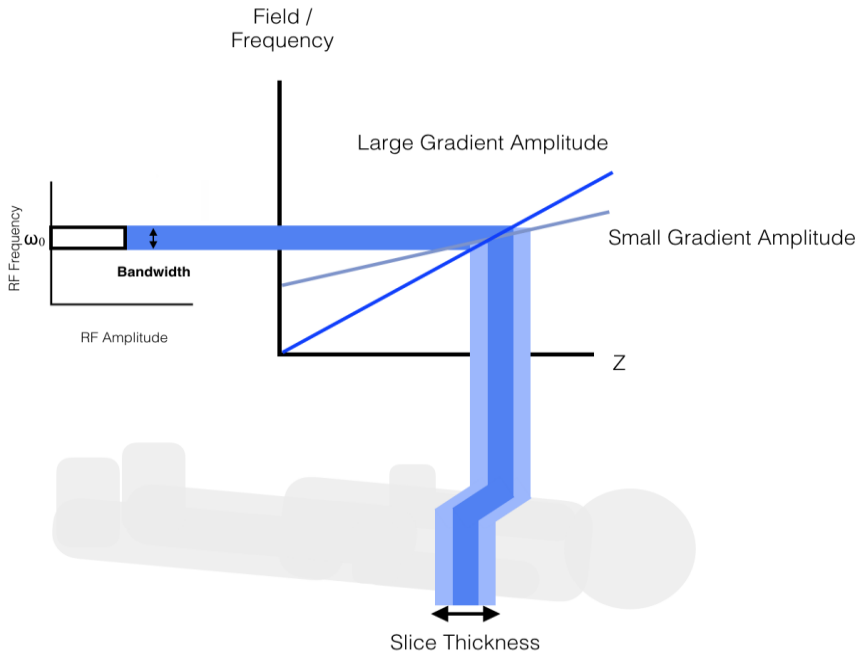

Figure 3.2 Slice selection: a linear gradient is applied simultaneously with the RF-pulse resulting in a band of spins being excited along the z-axis.
Adapted with the kind permission of Dr Jennifer Steeden.

3.3.2 2D Signal Localisation

In conventional Cartesian imaging, k-space data is acquired one row at a time by applying a phase-encoding gradient on the *y*-axis (to determine the line in k-space), followed by a readout gradient on the *x*-axis (to move across k-space). This sequence of gradients is repeated with a different phase-encoding gradient for each row in k-space.

Unfortunately, Cartesian filling is inefficient as only one line is filled after each RF pulse. This makes MRI a slow imaging methodology, which is particularly challenging when trying to image moving structures. The most common alternative trajectories include spirals and radials. One advantage of these trajectories is that they oversample the centre of k-space, making them less vulnerable to phase errors from flow and motion. Additionally, spiral trajectories are very efficient as they fill a large proportion of k-space after each RF pulse.

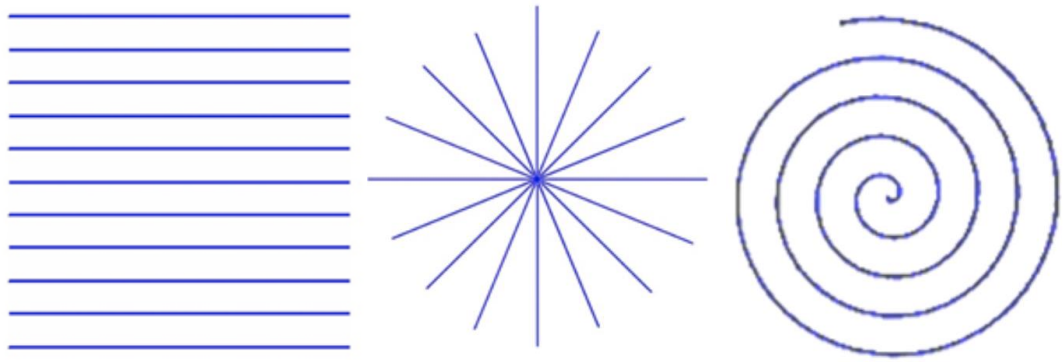

Figure 3.3 Cartesian, radial and spiral K space trajectories.
Reproduced with the kind permission of Dr Jennifer Steeden.

Cardiac imaging must address motion resulting from respiration, the cardiac cycle and voluntary and involuntary patient movement. Respiratory motion can be addressed by breath holding, use of respiratory navigators or the use of multiple signal averages. None of the conventional approaches to overcoming respiratory motion are optimal for use in exercise. Breath holding is the simplest way to address respiratory motion. Healthy adults may be able to comfortably hold their breath for 20-30 seconds at rest allowing full acquisition for shorter sequences. However the duration of breath holding tolerated by children and in disease(87) is shorter. Breath holding in exercise is challenging for all groups and does not reflect the physiology of exercise in daily life. Respiratory gating (using bellows or a signal navigator) has been associated with significantly longer scan duration and conventionally required regular breathing, again making it unsuited to exercise. Use of signal averaging to compensate for respiratory motion also significantly increases total scan time(88). Cardiac gating reduces the effects of motion from the cardiac cycle by limiting the filling of k space to a set phase of the cardiac cycle, with k space being completely filled over a number of cycles. Temporal resolution is increased by using shorter periods to fill k space but comes at the expense of a longer scan duration. Cardiac gated sequences require an ECG trigger; typically from a 3 lead vectorcardiogram and during intense exercise triggering may fail. Similarly, gating may fail in arrhythmia. A further disadvantage is that the resulting velocity information produced by segmenting this kind of data is a weighted temporal average of velocity over the duration of the acquisition and therefore does not reflect acute changes.

3.4 Undersampling and Parallel Imaging

The speed of image acquisition can also be increased by data under-sampling; acquiring a reduced amount of k-space data. The acceleration (reduction) factor R, is the ratio of k-space data needed for a fully sampled image to the k-space data acquired in the accelerated acquisition. Undersampling k-space data results in aliasing in the resultant images.

In Cartesian imaging, undersampling by a factor of 2, is achieved by missing out alternative lines of k-space, resulting in 2 overlaid replicas of the object, spaced at FOV/2;

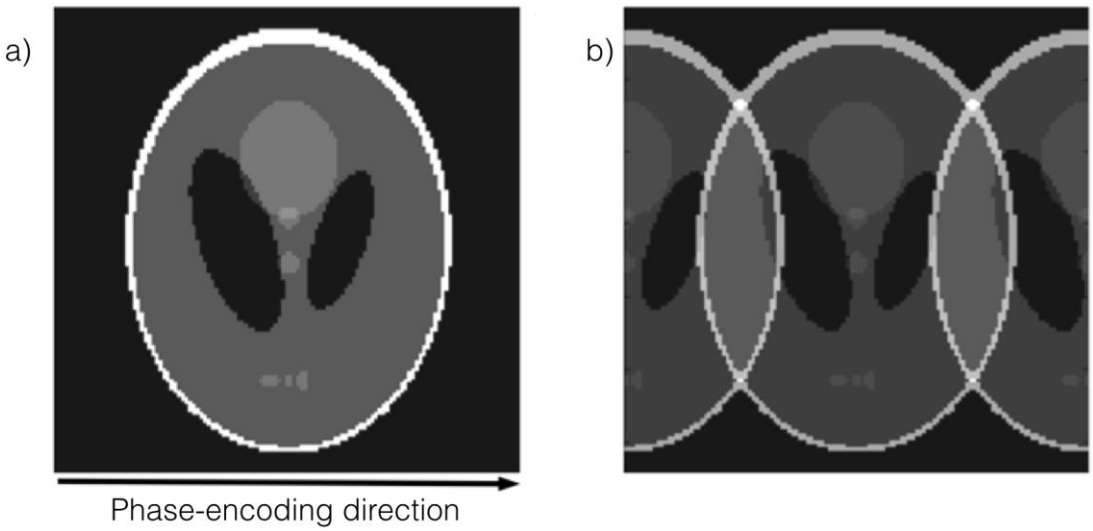

Figure 3.4 Simulation of Cartesian undersampling a) fully sampled b) with two-fold acceleration Reproduced with the kind permission of Dr Jennifer Steeden.

Parallel imaging, so called because data is acquired simultaneously (i.e. in parallel) using multiple coils, can be used to remove aliasing from undersampled data. Parallel imaging uses the spatial dependence of the individual coils (the coil sensitivities) to imply information about origin of the signal, and unwrap the aliasing. The most commonly used parallel imaging techniques include SENSitivity Encoding (SENSE, which works in imaging space) and GeneRalized Autocalibrating Partial Parallel (GRAPPA, which works in k-space).

The work in this thesis primarily uses UNFOLDed SENSE parallel imaging to speed up acquisition of data. The UNFOLD “unaliasing by Fourier-encoding the overlaps in the temporal dimension” techniques works by interleaving k-space lines in sequential images. Images reconstructed from any single frame contain aliasing, however as the aliased component is shifted between frames it can be removed by low-pass filtering of the data. The combined UNFOLDed SENSE approach allows for the very high temporal resolution required to accurately capture physiological data at the high heart rates associated with exercise. Further details of the techniques used are described in chapter 5 (methods).

3.5 Flow Imaging

MRI is inherently motion sensitive. Phase Contrast Magnetic Resonance (PCMR) uses the phase shift that occurs in spins as they move along a magnetic field gradient to encode velocity into the resulting signal. Applying a gradient causes a phase shift with an increase in the precessional frequency of spins in proportion to the field strength. Providing a spin does not move within this field, reversing the gradient for the same duration re-aligns spins creating no net phase shift. For spins moving in the direction of the gradient, the reverse gradient does completely realign spins, resulting in a net change in phase. This phase shift is proportional to the velocity of blood flow.

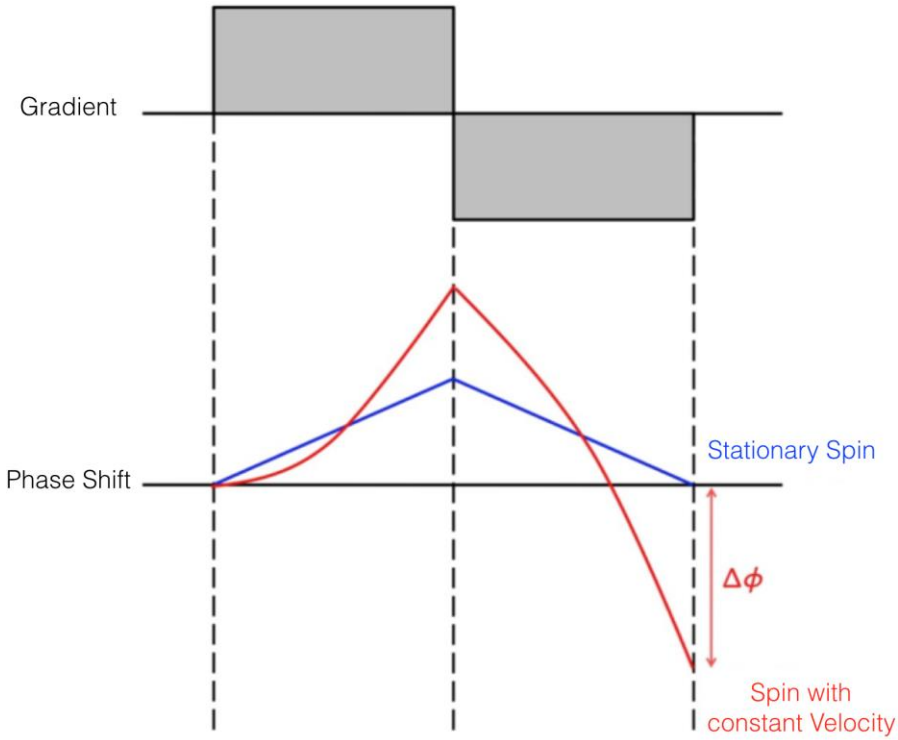

Figure 3.5 Application of a balanced bipolar gradient resulting in a phase shift proportional to the velocity of spins.
Reproduced with the kind permission of Dr Jennifer Steeden.

The bipolar gradient is altered, so that a phase shift of 180^{o} corresponds to the maximum expected velocity for the vessel. This process is known as velocity encoding (VENC) and is determined by the operator before running the sequence. Typically, each line in K-space is acquired twice with a different VENC; normally one with velocity- compensated gradients (i.e. with a VENC of zero) and the other with velocity- encoded gradients (i.e. with the expected VENC). The final phase image is formed from the subtraction of the velocity-compensated data from the velocity-encoded data, in order to subtract out any background phase shifts.

For each PCMR acquisition both a magnitude image (that can be used for anatomical segmentation) and a phase image (giving the velocity within each voxel used to calculate flow volumes) are reconstructed.

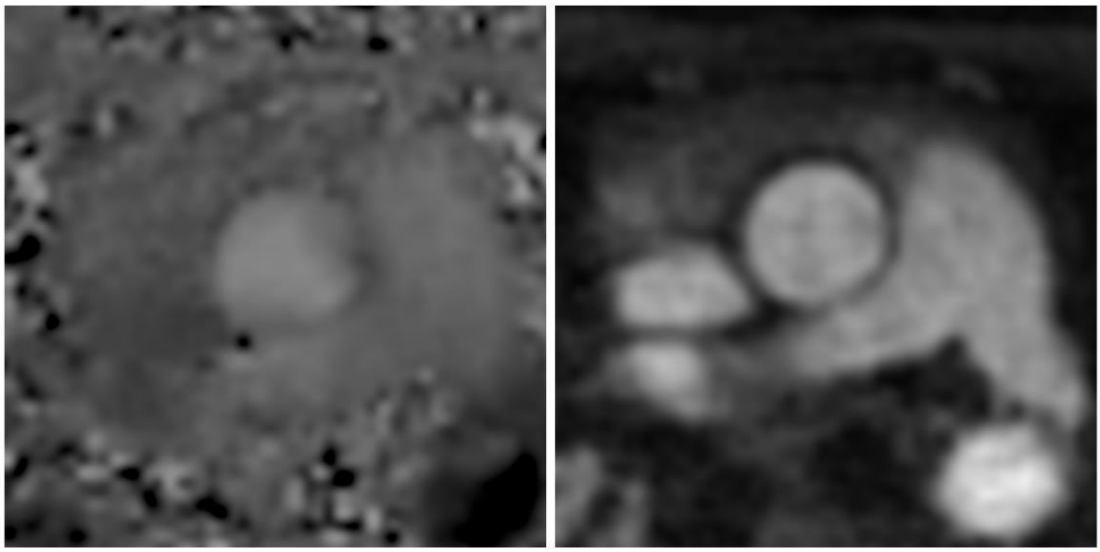

Figure 3.6 Phase and Magnitude flow images.

3.6 Accuracy of PCMR

Overall error of PCMR flow measurement is estimated to be less than 10%(89). This is generally not attributed to one predominant source of error but to the cumulative effect of multiple potential causes of error and can be minimised by using appropriate imaging parameters. The closer the VENC is set to the maximum expected velocity in the vessel of interest the greater precision of measurement. Setting the VENC below the peak velocity in the vessel results in velocity wraparound and manifests as aliasing. Overestimating the peak velocity and setting a VENC that is too high results in reduced signal to noise ratio potentially masking the true velocity(90). Although the ideal imaging plane is orthogonal to the vessel of interest, deviation up to 15 degrees and the associated increase in vessel area is tolerated. Temporal and spatial resolution also impact on the accuracy of PCMR. Inadequate temporal resolution will result in underestimation of peak velocity and flow. Inadequate spatial resolution may result in partial volume effect (PVE). PVE occurs in voxels that include vessel boundaries containing both stationary spins and spins moving in the blood pool; the signal intensity of the flowing spins is higher and consequently their velocity is given greater weighting(89).

Other potential sources of error include phase offset errors (primarily due to magnetic field inhomogeneities) and pulsation artefact from the ascending or descending aorta(91). Inaccurate segmentation will also clearly result in error.

Several validation studies demonstrate the accuracy of PCMR in assessing resting flow, both in phantoms and in vivo. For example, Powell and colleagues(92) tested the accuracy of PCMR in quantifying pulsatile blood flow both in vitro and in children and young adults showing excellent agreement between PCMR and phantom flow measurement in vitro and between pulmonary and systemic flow in patients. Beerbaum et al(93) demonstrated the accuracy of PCMR flow quantification against invasive measurement in a group of children with atrial or ventricular level left to right shunt showing minimal difference between Qp:Qs measured by catheterization and by MRI. With appropriate application of acquisition parameters PCMR is clinically robust. Greil and colleagues looked at the degree of tolerance in the effect of application of a range of acquisition parameters including VENC, angle of imaging plane to vessel direction and FOV on the accuracy of measurement, with only FOV significantly impacting on overestimation of flow when spatial resolution was decreased (94). Currently PCMR is recommended clinically to address multiple questions including assessment of cardiac output, shunts, differential lung perfusion, aortic and pulmonary regurgitation(95,96).

3.7 Real Time Imaging

Real time imaging techniques are defined as acquiring, reconstructing and displaying images as they happen. In the context of cardiac MRI specific constraints are that cardiac motion should be resolved without gating or synchronisation (97). Guidelines recommend a temporal resolution of at least 50 milliseconds to assess function in adults and therefore complete images should be acquired in this time. Real time CMR imaging requires continuous data acquisition with sequential filling of each k-space frame and the time taken to do this will determine the temporal resolution.

3.7.1 Real Time Flow Imaging

Implementation of real time PCMR flow measurement has been achieved through both the use of the efficient echo planar imaging (EPI) radial and spiral trajectories and parallel imaging techniques outlined above. Initial work in this field focused on the use of efficient trajectories. Nayak, et al (98) developed a spiral real-time PCMR sequence with a sliding window reconstruction demonstrating a good correlation with conventional PCMR in a phantom study however the low temporal resolution of 180ms rendered it likely to miss peak flow and unsuitable for use in exercise. Spatial resolution is also critical for accurate flow measurement. Klein and colleagues (99) used a turbo gradient-echo EPI PCMR sequence to measure flow in a patient population with comparison to a retrospectively gated PCMR sequence. Although correlation with conventional flow volumes was acceptable in larger vessels (r=0.87) this was not the case in medium sized vessels (r=0.67).

Through combining non-cartesian trajectories and shared encoding strategies it has been possible to meet the temporal and spatial resolution requirements of implementing real time PCMR. Körperich et al (100) used echo planar imaging (EPI) in combination with sensitivity encoding to create a real time PCMR sequence with a frame rate of 25/second. Validating the sequence in children the authors found excellent agreement with a conventional retrospectively cardiac gated PCMR sequence, with a 3% difference in aortic SV and 2% difference in pulmonary SV. Signal to noise ratio (SNR) in the magnitude image was significantly reduced in the real time sequence however velocity to noise ratio (VNR) in the phase images was preserved (93% in the aorta). The authors intentionally used a relatively large FOV (30x34cm2) demonstrating the robustness of the real time sequence for use in a range of body sizes and slice angulations.

Although EPI sequences fill k-space efficiently a long TE means that moving spins can dephase before the centre of k-space is sampled. In contrast spiral trajectories are ideal for flow measurement as they sample from the centre of k-space first. Nezafat and colleagues validated a real time PCMR sequence combining a spiral trajectory and SENSE reconstruction (101). Although there was preserved spatial resolution and a temporal resolution of 60.8ms this remains too low for use in exercise. Steeden

and colleagues developed a spiral PCMR sequence with SENSE reconstruction and validated it for use in exercise (102). The temporal resolution of 40 ms allowed the accurate assessment of exercise haemodynamic response. The correlation between conventional PCMR and real time PCMR flow at rest was very high (r=0.99) and remained high (compared to real time LVSV) during exercise (r=0.98).

The combination of high temporal resolution, lack of cardiac gating and compatibility with free breathing mean that real time PCMR sequences are well suited for use in exercise. This is supported by validation studies both at rest and during exercise.

3.7.2 Real time Assessment of Ventricular Function

CMR is the reference standard imaging modality for volumetric assessment(103,104). Conventionally in cardiac MRI a stack of cine images is acquired from the base to the apex of the heart allowing quantification / calculation of variables including end systolic and diastolic volumes, stroke volume, ejection fraction and ventricular mass. Conventional Cartesian imaging of the ventricles is time consuming and requires multiple breath-holds rendering it unsuitable for use in exercise where there maybe rapid changes in haemodynamics and breath-holding is both unpleasant and unrepresentative of physiology in daily life.

Various approaches can be used to accelerate the process of image acquisition for (function and volume) assessment including reduced field of view (RFOV) and partial Fourier techniques. The parallel imaging techniques and Cartesian trajectories described above have been implemented for real time quantification of ventricular volumes. These approaches reduce the effects of cardiac and respiratory motion by rapid filling of k space and therefore overcome the need for breath holding and the limitations of longer acquisitions in capturing acute changes in physiology. The high spatiotemporal resolution radial k-t SENSE sequence developed at Great Ormond Street Hospital combines efficient radial filling of k space with k space and time (k-t) sensitivity encoding. k-t SENSE uses spatial and temporal correlations in addition to coil sensitivity maps allowing further acceleration of acquisition with reduced undersampling artefacts(105). This sequence has been demonstrated to accurately

quantify ventricular volumes and function in patients with congenital heart disease at rest and been validated for use at rest and during exercise in healthy volunteers. In the validation of this sequence it was compared against a vendor supplied standard real time sequence and subsequently through agreement in right and left ventricular stroke volume as a surrogate of accuracy well as image quality scoring at exercise. Reproducibility was tested by repeating the experiment within one month. Agreement between RV and LVSV was higher using the radial k-t sequence (SD of difference ±3.43 vs. ±8.97 mL, P < 0.001). Although agreement in RV and LVSV was lower at heart rates of greater than 130 compared to at rest (SD ± 4.5 mL; *P* < 0.001) it remained superior to the vendor supplied real time sequence(106).

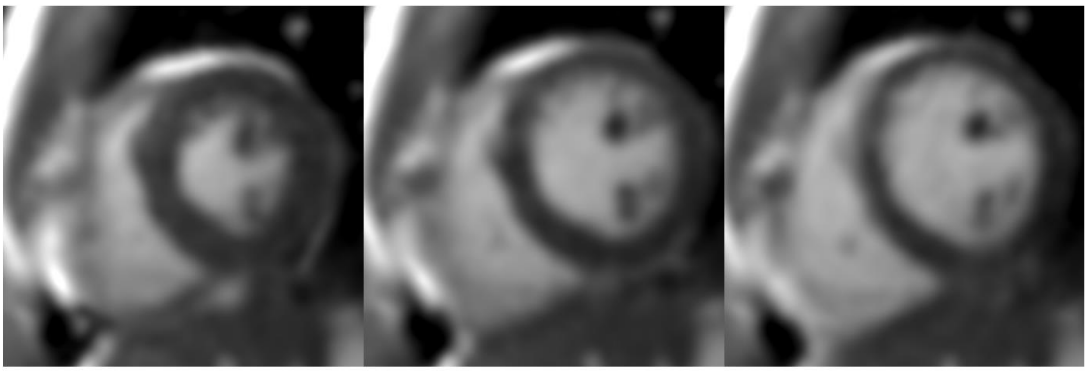

Figure 3.7 High spatial and temporal resolution k-t SENSE short axis images used for assessment of ventricular function.

3.8 Summary

This chapter has described the physics underlying CMR, including the inherent limitations of MRI and how these have been addressed in the development of real time sequences able to meet the demands of accurately measuring flow and assessing cardiac function in exercise.

Chapter 4 Review of Exercise CMR Literature

The motivation to this work was to develop a comprehensive non-invasive exercise assessment combining elements of conventional CPET with cardiac MRI. This chapter summarises literature on exercise cardiac MRI with a focus on flow measurement and describes alternative MRI techniques for determining oxygen uptake.

4.1 Stress MRI

For the purposes of imaging, the cardiovascular system can be challenged with either exercise or pharmacological agents. Using exercise as a stressor in CMR is appealing for a number of reasons. Exercise as opposed to the use of pharmacological stressors more closely resembles real life physiology, testing all of the systems involved in exercise limitation and providing insight into functional limitation. The development of faster imaging and improved post processing techniques means that the challenges of body motion in exercise can be overcome. Some groups of patients however cannot safely or adequately exercise in the scanner and for this reason pharmacological stressors remain necessary.

4.1.1 Pharmacological Stress CMR

The use of drugs as stressors to assess coronary artery disease is well established in adult cardiac MRI(107) and is the on-going focus of a large body of research (108-110). Two main groups of pharmacological agents are commonly used, coronary vasodilators (adenosine, regadenoson, dipyridamole) and catecholamine (dobutamine)(111). Vasodilators are used in conjunction with an extracellular magnetic resonance contrast agent to demonstrate areas of myocardium with decreased perfusion. Adenosine is a purine nucleoside with effects mediated through A_1, A_{2A}/A_{2B} and A_3 receptors(112), binding to A_{2A} receptors causes vasodilation. As adenosine is non selective it is associated with a range of side-effects, most commonly flushing (up to 40%), chest pain (35%) and dyspnoea (35%) as well as gastro-intestinal symptoms and headache(113). These side effects are short lived due to the very short half-life of Adenosine but are nevertheless unpleasant. Interaction with A_1 receptors causes bronchoconstriction and therefore contraindications include

use in patients with asthma. Other contraindications are recent myocardial infarction, unstable angina and hypertension(114)). Caffeine and Theobromine (present in chocolate) are antagonists of Adenosine and failure to exclude food and drink containing these substances 24 hours before testing is a not infrequent cause of failure of testing. Dipyridamole works by reducing reuptake of endogenous adenosine resulting increased extracellular adenosine and indirectly causing vasodilation. It has similar side-effect profile to adenosine but with longer lasting effects. Regadenoson is a newer selective A_{2A} receptor agonist and has fewer undesired side-effects.(115)

Dobutamine, a synthetic catecholamine, is the most frequently used catecholamine in stress testing. Dobutamine's effects are predominantly mediated through agonism of β_1 receptors with positive inotropic and chronotropic effects, causing increased oxygen consumption. It is also a weak agonist of α_1 and β_2 receptors causing vasodilation and bronchodilation(116). In coronary heart disease Dobutamine is used to induce either wall motion abnormalities or perfusion deficit. Dobutamine is contraindicated in a range of conditions including hypertrophic obstructive cardiomyopathy, myocarditis and critical aortic stenosis(114).

Despite the high frequency of side-effects the overall safety of pharmacological methods is good with low rates of serious complications (117). Because of the unpleasant dose related effects that may be less well tolerated in children as well as the different profile of disease in children there is less experience of pharmacological stress testing in paediatric populations. Even at centres performing high volumes of paediatric CMR overall the use of pharmacological stressors is generally limited(118,119).

To summarise, pharmacological agents are safe if used in appropriately selected patients and have a well-established role particularly in adult CMR. Major disadvantages of pharmacological stressors are their side effects, even in newer agents, and their inability to fully reproduce exercise conditions.

4.2 Approaches to Exercise in the MRI Environment

Three main groups of approaches to exercise MRI have been described 1) in scanner isometric techniques 2) aerobic exercise adjacent but outside of the MRI scanner 3) in scanner aerobic exercise.

4.3 Isometric Techniques

Isometric exercise increases HR, CO, blood pressure and myocardial oxygen consumption and can be performed with minimal upper body motion. For this reason isometric exercise techniques are an attractive non-pharmacological stressor for use in cardiac MRI. Several approaches to isometric exercise in the MRI scanner have been described. Using a commercial dynamometer von Knobelsdorff-Brenkenhoff (120) was able to demonstrate a small but significant increase in HR from 68±12 bpm to 81±13 bpm. Using a breath-held retrospectively gated PCMR sequence it was possible to demonstrate an increase in increase in CO from 5.4 ± 0.8 l/min to 6.9 ± 1.1 l/min. Although the effects of exercise were modest a benefit was that no exercise images were rejected due to motion artefact. Another advantage of this kind of approach is that it can effectively be introduced with relatively little expense. Mortensen (121)performed a three minute biceps exercise using a low-cost custom made pulley system. The exercise elicited an increase in HR from 65.9±10.2 to 76.7±12.2 bpm. Aortic flow was measured using a prospectively gated spiral PCMR sequence with a 4-8 second breath hold and left ventricular volumes assessed using a free-breathing real-time radial k-t SENSE sequence. CO increased from 3.2±0.6 l/min/m2 to 3.7±0.7 l/min/m2. Both LVEDV and LVESV increased with this exercise.

Isometric exercise techniques have been applied to a limited extent in clinical research. Alegret (122) described maximal isometric exercise (elevation of weight using leg muscles) in a group of asymptomatic patients with aortic regurgitation. Hays and colleagues (123) used a isometric handgrip exercise using a commercial dynamometer in a 3.0 T MRI scanner to obtain coronary artery cross-sectional area and blood flow measurements before and during exercise stress in patients with

known coronary artery disease and in healthy controls demonstrating decreased coronary area and blood flow velocity in patients during exercise .

Isometric techniques have been demonstrated to be easily implemented, effective stressors and feasible in both healthy populations and patient groups. However they cannot reproduce the same cardiovascular response as aerobic exercise and would therefore not be an adequate alternative to dynamic exercise for functional assessment.

4.4 'Near Scanner' Exercise

The use of aerobic exercise adjacent to rather than inside the MRI scanner has been favoured by some investigators over in-scanner exercise. Primarily this is because of the higher work rates achieved with whole body exercise and reduced motion artefact as well as comfort and familiarity of upright exercise to subjects. Further advantages of upright exercise include the possibility of twelve lead ECG monitoring and the extensive diagnostic and prognostic literature validated using upright exercise. To date studies using this type of design using upright exercise in the same room as the MRI scanner has focused on using MRI compatible treadmill ergometers rather than other types of ergometer. Over the past 15 years there has been a progression from reduction (124,125) to complete removal of ferromagnetic parts allowing exercise to be performed increasingly adjacent to the scanner. Studies in this area (summarised in Table 2) have focused on the use of exercise as a stressor for detection of regional wall motion abnormalities and or myocardial perfusion. Apart from the very earliest studies which had variable success (124) real time sequences have been used, avoiding the need for cardiac gating and breath-holding.

A major disadvantage of this type of design is that there is inevitably a delay between the end of exercise and the onset of imaging. This is exacerbated in perfusion studies when there is added delay connecting contrast (126). Although across studies there appears to be a trend in increasingly rapid transfer and positioning (in some studies aided by the use of a moldable vacuum lock cushion and practice transfers before testing) patient groups are likely to take longer to transfer

than healthy volunteers. As heart rate recovery is rapid (127) this approach means that peak exercise is never truly captured.

Table 2 Summary of 'near-scanner' exercise CMR studies

Author / Paper	N	Indication	Scanner / Sequence	Breath hold	Exercise Protocol	Delay	Heart rate change	Conclusion
Rerkpattanapipat,et al. Feasibility to detect severe coronary artery stenoses with upright treadmill exercise magnetic resonance imaging. Am J Cardiol. 2003	27	Wall motion Patients	1.5T multiphase, SSFP 3 x SAX slices	yes	Exercise to exhaustion / ST changes / angina	Imaging complete 60-90 seconds post exercise	130 ± 20 bpm at peak exercise to 113 ± 16 bpm during imaging	Some limitations in adequate acquisition. Further development needed for wider use.
Jekic et al Cardiac function and myocardial perfusion immediately following maximal treadmill exercise inside the MRI room. Journal of Cardiovascular Magnetic Resonance. BioMed Central; 2008	20	Wall motion / perfusion Healthy volunteers	1.5T Real time SSFP TSENSE, 5x SAX slices, 1 x HLA,1x VLA. Perfusion imaging GRE EPI 3x SAX slices	no	Exercise to exhaustion / maximum predicted heart rate	30 ± 4 seconds to start	98% ± 7% maximum predicted heart rate at peak exercise 84% ± 11% at start of imaging	Successful in healthy volunteers
Foster et al. MR-compatible treadmill for exercise stress cardiac magnetic resonance imaging. Magn Reson Med. 2012	10	Wall motion / perfusion Healthy volunteers	1.5T Real time cine TGRAPPA 5 SAX 3 VLA 1 HLA. Perfusion imaging GRE EPI 3x SAX slices	no	Bruce protocol to maximum predicted heart rate	24 ± 4 seconds	86% ± 9% maximum predicted heart rate at peak to 81% ± 9% 1 minute post exercise	Successful in healthy volunteers
Thavendiranathan et al. Comparison of treadmill exercise stress cardiac MRI to stress echocardiography in healthy volunteers for adequacy of left ventricular endocardial wall visualization: A pilot study. J Magn Reson Imaging. 2014	28	Wall motion (v/s echo) Healthy volunteers	1.5T Real time SSFP TGRAPPA 5x SAX, 4x H/VLA slices	no	Bruce protocol to 'fatigue'	21 ± 2 seconds	173 (146–196) bpm at peak to 148 ± 14 bpm during imaging	Performed as rapidly as echo
Raman et al. Real-time cine and myocardial perfusion with treadmill exercise stress cardiovascular magnetic resonance in patients referred for stress SPECT. Journal of Cardiovascular Magnetic Resonance. 2010	43	Wall motion / perfusion (v/s SPECT) Patients	1.5T Real time SSFP TSENSE 5 SAX 3 HLA/VLA slices GRE EPI 3x SAX slices	no	Bruce protocol to 90% predicted heart rate	68 ± 14 seconds to completion of imaging	156 ± 21 bpm at peak to 126 ± 19 bpm during imaging	Feasible need to confirm relative effectiveness
Raman et al. Diagnostic Performance of Treadmill Exercise Cardiac Magnetic Resonance: The Prospective, Multicenter Exercise CMR's Accuracy for Cardiovascular Stress Testing (Trial. J Am Heart Assoc. AHA, 2016	94	Patients Wall motion / perfusion (+ LGE)	1.5T Real time SSFP GRE EPI SSFP LGE	no	Bruce protocol *"symptom limited"*	25±13 seconds	97.1±10.3% maximum predicted heart rate at peak to 83±11% at start of imaging.	*"excellent diagnostic value"*

HLA indicates horizontal long axis; SAX, short axis; VLA, vertical long axis, LGE, late gadolinium enhancement

CPET has not been widely attempted in the MR environment however interest in bringing the two modalities closer together led LaFountain (128) to undertake CPET testing in a standard laboratory and then with a modified CPET system with extended umbilical and bespoke treadmill in the scanner room. Imaging was performed before and immediately after CPET in the MRI scanner room. An ungated real time SSFP short axis stack as well as two long axis images were acquired with an interval of 35.6 ± 3.8 seconds between end of exercise to the start of imaging and completion of imaging within a minute 55.7 ± 4.9 seconds. HR fell from 191.2 ± 12.2 bpm at maximum exercise to 166.3 ± 20.2 bpm during imaging. The increased interval between end of exercise and start of imaging compared to studies using a similar methodology is attributed to the removal of the CPET headgear. The authors do not expand on why testing in the same room but not simultaneously would be beneficial.

To summarise, near scanner treadmill methodologies are attractive in that the exercise technique is familiar to patients and allow 12 lead ECG monitoring in exercise. These types of study design have bought the advantages of conventional exercise testing and MRI imaging closer together. A fundamental disadvantage is that imaging is always in recovery rather than at peak exercise when subjects are most likely to have symptoms / functional limitation.

4.5 Exercise Within the MRI Scanner

Attempts to quantify cardiac function and output during exercise within the MRI scanner have been made since the mid 1980's. A device for supine exercise MR imaging were described as early a 1986 (129). Although it was demonstrated to provide an adequate stimulus with an appropriate HR response, sequences at the time meant that acquisitions were too long to obtain meaningful exercise data. This illustrates the constraints on the development of in-scanner exercise techniques that have included not only the adequacy of MRI compatible ergometers and the size of the MRI bore but most importantly the unsuitability of conventional sequences for use in dynamic exercise.

4.5.1 Upright Exercise MRI

Upright / open MRI scanners are rare in contemporary clinical practice because of the lower magnetic field and signal to noise ratio, however there have been some attempts to perform exercise cardiac MRI using this type of scanner. Cheng and colleagues developed an MR compatible cycle ergometer for use in an open 0.5T scanner(130). Subsequently the same group used the open magnet and cycle ergometer to measure main and branch pulmonary artery flow as well as systemic venous return in 10 healthy children and teenagers(131). Exercising subjects to 150% of their resting HR and using a free-breathing cardiac gated PCMR with respiratory bellows to compensate for respiratory motion it was possible to demonstrate increased ratio of IVC to SVC flow in exercise. Unfortunately following this initial work the approach has not been reproduced at a larger scale or in patient populations.

4.5.2 Supine Exercise MRI

Various approaches have been taken to attempt supine exercise within the MRI scanner. A summary of studies using in-scanner supine exercise to assess flow is provided in Table 3. One of the earliest successful attempts at cardiac imaging in supine exercise was published by Mohiaddin and colleagues in 1995(132). Using a bespoke cycle apparatus a 0.5T whole body magnet and real-time cardiac gated breath-held spiral velocity mapping sequence, with a temporal resolution of 50 ms the authors were able to demonstrate an increase in descending aortic flow immediately after dynamic exercise in ten healthy volunteers (from 41±8 ml/beat to 57±11 ml/beat). A description of the exercise protocol used is not given other than the subject was ‘asked to perform maximum exercise’ and although there was a mechanism to control resistance there was not a formal measurement of workload. Despite the constraints described in this study design there was a significant increase in HR from 68 ±6 to 101±12 bpm. In an attempt to avoid some of the challenges of segmenting exercise data the authors acquired flow in the descending aorta, avoiding the variation in shape/size seen in the ascending aorta through the cardiac cycle. It was possible to segment the flow with the same region of interest propagated over all frames in the study. The benefits of using a spiral trajectory in acquiring flow data particularly in exercise are emphasized by this paper where it was chosen because of

its early acquisition of data from the centre of k-space and reduction in signal loss and flow artefacts. In their discussion the authors stress the rapid haemodynamic changes which occur after stress and therefore their attempts to measure flow ‘before recovery can take place’ although it is now evident that, as changes are so rapid this is not a realistic ambition.

Niezen et al tested the feasibility of assessing great vessel flow in submaximal exercise using PCMR and describe one of the first uses of a commercial cycle ergometer for this purpose(133). This study highlights both the advantages of supine cycle ergometers in conventional scanners in that a higher workload was achieved than with other types of ergometer (100 watts) but also the disadvantages, subjects performed supine cycling positioned outside the isocentre of the scanner to prevent obstruction of leg movement from contact with the scanner bore. Images were acquired using a retrospectively gated PCMR sequence (using a peripheral pulse unit placed on a finger) with a temporal resolution of 30-35 ms. The authors were able to show good correlation between aortic and pulmonary flows obtained at rest and exercise ($r=0.9$) and an increase in aortic flow from 64 ± 13 ml/beat at rest to 79 ± 13 ml/beat at 100 W. Limitations identified by this study included motion artefact and breath-motion artefact particularly at peak exercise.

Table 3 Summary of exercise CMR aortic flow studies

Author / Paper	N =	Ergo-meter	Vessel	Scanner / Sequence	Breath hold	Protocol / Image Timing	Response
Mohiaddin RH, Gatehouse PD, Firmin DN. Exercise-related changes in aortic flow measured with spiral echo-planar MR velocity mapping. J Magn Reson Imaging. 1995	10	Bespoke cycle	DA	0.5T Real time cardiac gated spiral velocity map	Yes	*"maximum exercise"* Immediately post exercise	HR 68±5 to 101±12 bpm CO 41±8 to 57±11 ml/beat
Niezen RA, Doornbos J, van der Wall EE, de Roos A. Measurement of aortic and pulmonary flow with MRI at rest and during physical exercise. J Comput Assist Tomogr. 1998	16	Lode cycle	AA / MPA	1.5T Retrospectively gated PCMR	No	10 W/min to 50 then 100 W Immediately post exercise	HR 63±8 to 106±21 bpm CO (Ao) 64±13ml/beat to 79±13 ml/beat
Steeden JA, Atkinson D, Taylor AM, Muthurangu V. Assessing vascular response to exercise using a combination of real-time spiral phase contrast MR and noninvasive blood pressure measurements. J Magn Reson Imaging. 2010	20	Lode up down	AA	1.5 T Real time k-t sense PCMR	No	2 W/min to 8 W During exercise	HR 68.2±12.5 bpm to 108.6±21.1 CO 5.8±1.4 to 9.1±1.7 l/min
Weber TF, Tengg-Kobligk von H, Kopp-Schneider A, Ley-Zaporozhan J, Kauczor H-U, Ley S. High-resolution phase-contrast MRI of aortic and pulmonary blood flow during rest and physical exercise using a MRI compatible bicycle ergometer. Eur J Radiol. 2011	20	Lode cycle	AA	1.5T HR PCMR	No	Watts increased to target HR During (steady state) exercise	HR acceleration 1.77 ± 0.16 Average flow velocity 22.35 ± 4.45 to 36.39 ± 6.78 cm/s
Pieles GE, Szantho G, Rodrigues JCL, Lawton CB, Stuart AG, Bucciarelli-Ducci C, et al. Adaptations of aortic and pulmonary artery flow parameters measured by phase-contrast magnetic resonance angiography during supine aerobic exercise. Eur J Appl Physiol. 2014	9	Lode up down	AA / DA / MPA	1.5 T Real time PCMR	No	Watts increased to target HR During (steady state) exercise	HR 69±9 to 117 ±12 bpm CO 6.5±1.4 to 12.5±1.8 l/min
Forouzan O, Flink E, Warczytowa J, Thate N, Hanske A, Lee T, et al. Low Cost Magnetic Resonance Imaging-Compatible Stepper Exercise Device for Use in Cardiac Stress Tests. J Med Device. 2014	21	Bespoke stepping	AA / DA / MPA	1.5T Retrospectively gated PCMR	Yes	*"3 to 4 min of physical exercise"* Interrupted exercise (stop-start)	HR 59±8.9 to 83.6 ± 22.2 bpm CO 5.9±1.4 to 8.2±1.9 l/min
Heiberg J, Asschenfeldt B, Maagaard M, Ringgaard S. Dynamic bicycle exercise to assess cardiac output at multiple exercise levels during magnetic resonance imaging. Clinical Imaging. 2017	40	Lode cycle	AA / MPA	1.5T Real time TEFPI	No	25 W 2 min then 25W / 75s During (steady state) exercise	HR 61±9 to 150±16 bpm CO 5.5±1.5 to 13.7±3.7 l/min

AA indicates ascending aorta; DA, descending aorta; MPA, main pulmonary artery; W, watts

Steeden(102) developed an innovative real time spiral PCMR sequence with SENSE acceleration for use in exercise, validating it in a population of 20 healthy volunteers against a standard vendor supplied gated sequence at rest, and against left ventricular volumes obtained using a validated real time k-t SENSE sequence at peak exercise. Subjects performed exercise using a Lode up-down ergometer over six minutes using a staged protocol up to a workload of 8 watts. Motion artefacts from exercise and breathing were not significant and no images were rejected. HR increased from 68.2 ± 12.5 bpm to 108.6 ± 21.2 bpm and CO increased from 5.8 ±1.4 to 9.1 ±1.7 l/minute. In addition simultaneous blood pressure measurements were made throughout exercise allowing SVR and arterial compliance measurement, both of which were demonstrated to fall significantly with exercise. There was a good level of agreement and correlation with validated techniques at rest and at peak exercise (bias 0.83ml/cycle, limits of agreement -4.18 to 5.84 ml/cycle, r = 0.98). This was an important advance in exercise CMR as it avoids the need to suspend exercise during imaging giving a closer insight into true exercise physiology. In addition low temporal resolution, a barrier to accurate measurements at higher heart rates associated with exercise, was overcome through the use of a spiral trajectory, efficiently filling K-space and through under sampling.

In contrast to other studies using cycle ergometers Weber (134) and colleagues were successful in performing cycle ergometry within the bore of the scanner with the subject's mid-thorax at the isocentre of the magnet. Unfortunately the paper's methodology does not expand on how this was achieved using the Lode cycle ergometer common to many studies. Sub-maximal exercise was performed in conjunction with high resolution PCMR in a group of healthy volunteers. Imaging was performed at 4 predetermined levels (rest, unloaded exercise and at 140% and 180% of resting HR). Importantly flow parameters were significantly different from rest at 'medium' intensity exercise and the authors suggest that 140% of resting heart rate is a sufficient exercise stimulus in assessing haemodynamics.

Pieles (135) studied aortic and pulmonary artery flow during exercise using a real time free breathing PCMR sequence, using the up-down Lode MRI ergometer in 9 healthy volunteers. The exercise protocol consisted of measuring resting HR then

starting with unloaded exercise for 2 minutes increasing resistance until HR reached 180% of the resting HR. A maximum of 50 watts resistance was used over a period of 2-3 minutes, the rate / design of increment is not given. Resting HR increased from 69±9 bpm to 117± 12 bpm. Ascending aortic flow increased from 6.5±1.4 to 12.5±1.8 l/minute, descending aortic flow from 4.4±1.0 to 9.3±1.5 l/minute, main pulmonary artery flow increased from 4.4±1.0 to 9.3±1.5 l/minute. Strengths of this study were the use of a real time free breathing sequence allowing more physiological exercise. Although using a target HR is easily reproducible a disadvantage of this study design is that work is not formally quantified. Once the target HR was achieved PCMR images of the ascending and descending aorta and subsequently main pulmonary artery were acquired.

Forouzan (136) developed a custom made stepping ergometer with the goal of studying main pulmonary artery stiffness using pulse wave velocity and relative area change techniques. 21 healthy volunteers under went exercise at two workloads, 35 and 45 Watts. Each stage of exercise lasted 3-4 minutes. Exercise was paused after each stage and breath-held (retrospectively gated) phase contrast images acquired in the main pulmonary artery, with breath-holds lasting 15-17 seconds. 6 of the 21 studies were considered unsuitable for segmentation, either due to motion artefact or movement completely out of the imaging plane. Using this technique HR increased by 50% at the second stage (45 Watt workload). CO increased from 5.9 ± 1.4 l/minute to 8.2 ± 1.9 l/minute. Exercise resulted in an increase in main pulmonary artery pulse wave velocity from 1.6 ± 0.5 m/s to 3.6 ± 1.4 m/s.

Heiberg and colleagues (137) also used a conventional commercial MRI cycle ergometer and were able to perform ergometry in the bore of the scanner through the use of a restraining system that prevented knee extension beyond 30 degrees. In addition volunteers were positioned to ensure no contact between the legs and the scanner bore, they report this resulted in a maximum displacement from the isocentre of 10cm. In a preliminary phase the authors of this paper reviewed real time flow sequences with a range of techniques including k-t SENSE, k-t BLAST and turbo field echo planar imaging (TEFPI), concluding that (subjectively) optimal images were obtained using the TEFPI sequence. Reflecting the higher workloads

achievable with cycle ergometers a stepped protocol increasing 25 watts every 75 seconds was used, with real-time flow acquisitions prior to each increment. Exercise was continued until volunteers reached 75% of predicted maximal HR. All 40 volunteers completed the exercise protocol with a mean workload of 153 ± 41 watts and an increase in CO from 5.5 ± 1.5 l/minute baseline to 13.7 ± 3.7 l/minute at peak exercise. Images from six scans at peak exercise were rejected because of upper body movement. This may represent a compromise of the greater workload achieved with cycle ergometry. 4 lead ECG monitoring was possible throughout exercise in this study. This has been a significant concern in previous exercise MRI studies particularly where exercise has been used in patients with ischaemic heart disease. Unfortunately the reasons for successful ECG monitoring are not expanded on.

An example of clinical application of flow measurement in exercise MRI is the work of Wei et al (138) who studied respiratory modulation in patients with TCPC. Subjects cycled on a cycle ergometer to a targeted heart rate, outside the bore of the scanner before acquisition of flow measurement in each of the SVC, IVC, ascending and descending aorta (as heart rate fell cycling was repeated for vessel). Free breathing images were acquired with a real time EPI sequence with shared velocity encoding. This study is of note as post processing included use of semi-automated chest wall tracking to synchronise flow wave forms with the respiratory cycle, concluding there was higher respiratory variation in SVC and IVC flow immediately post exercise but no effect on mean flow

The studies outlined above demonstrate that in healthy subjects exercise CMR using real time PCMR flow measurement is now feasible and able to demonstrate changes in heart rate and cardiac output between rest and exercise. As relatively few groups have worked in this area with limited numbers of subjects there is not a consensus on the optimal exercise technique or protocol. Cycle ergometry, which allows exercise at higher work rates has become more viable with larger bore scanners and recent studies do not report a compromise in the quality of data acquired. This negates previous arguments in favour of ‘near-scanner’ exercise MRI. The use of standardised stepped exercise protocols and heart rate targeted increase in work rate are both described. The reasoning behind choice of protocol is often not the focus of

these papers and therefore not widely expounded upon, however in translating these techniques into clinical practice further justification will be required.

4.6 Exercise MRI Ventricular Assessment

Four major studies examine ventricular response to in-scanner exercise in healthy volunteers. All but the most recent of these have used breath holding. All of the studies here are relatively small and reveal discrepancies in the understanding of the mechanism of change in stroke volume with supine exercise.

Roest et al (139) performed used cycle ergometry to a target heart rate determined by conventional CPET prior to MRI. Exercise was performed to steady state heart rate followed by a pause in exercise and breath held acquisition of turbo-field EPI images. To maintain heart rate, exercise was repeated at intervals. The main finding of this study was an increase in left and right ventricular stroke volume and ejection fraction due to a decrease in end systolic volume A criticism of this kind of study design must be the frequent stopping and starting of exercise to maintain a sub-maximal energy level although feasible in healthy volunteers may be too demanding for patient groups.

Gusso and colleagues (140) used a low-cost bespoke cycle ergometer to perform exercise to a target heart rate of 110 beats per minute (the rationale is not fully expanded upon) Imaging of the LV was performed using a an integrated parallel imaging technique (iPAT) Trufisp cine sequence with breath holds. The authors found no significant change in LVEDV but LVESV did significantly fall with exercise.

Steding-Ehrenborg (141) studied a population of 26 healthy volunteers. A breath held retrospectively gated SSFP sequence was used to acquire short axis and long axis images of the left and right ventricle during exercise using a bespoke ergometer designed for knee extension of one leg. The authors concluded that total heart volume was decreased in exercise. In this study LVEDV was unchanged and LVESV decreased in exercise, both RVEDV and RVESV decreased with exercise.

Le (142) and colleagues performed cycle ergometry in athletes and normal controls using the Lode cycle ergometer with the volunteer in the bore of the MR scanner. Non breath held real time balanced SSFP cine images were acquired at incremental stages of exercise with pauses in exercise during image acquisition to reduce motion artefact (of note pause in exercise resulted in immediate drop in heart rate of 9±6 bpm in the normal / control group and 16±9 bpm in athletes). In both groups LVESV fell with each step in exercise. EDV increased in athletes up to 75% of peak heart rate then remained elevated whilst in controls EDV initially increased (up to 50% peak heart rate) then fell.

An example of successful application of volumetric measurement in exercise is the work of Lurz et al (106) who investigated the impact of percutaneous pulmonary valve implantation (PPVI) in patients with pulmonary stenosis and pulmonary regurgitation on ventricular function using exercise cardiac MRI. Subjects underwent scans pre and post PPVI exercising within the scanner on an up down ergometer to their maximum capacity following stepped protocol. Real time k-t SENSE images were acquired every three minutes. This study shows the potential of exercise MRI to elicit important differences in physiology between groups. For example in patients with primarily pulmonary stenosis there was no reserve in right ventricular ejection fraction prior to PPVI. Following intervention patients in this group were demonstrated to have reserve in right ventricular ejection fraction.

4.7 In-scanner Exercise with Invasive Haemodynamic Measurement

In one of the most ambitious approaches to exercise CMR LaGerche (143) and colleagues performed real time exercise cardiac MRI with simultaneous cardiac catheterisation allowing direct comparison of MRI derived values with the invasive reference standard. 19 adult volunteers (10 athletes, 6 arrhythmia patients, 3 heart failure patients) underwent cardiopulmonary exercise testing. 24 hours later they undertook exercise cardiac MRI with both a pulmonary artery catheter in the right pulmonary artery (inserted via the internal jugular vein) and a radial arterial catheter in situ. Exercise was performed using the Lode cycle ergometer to workloads equivalent to 25%, 50% and 66% of maximal workload established on CPET. Each level of exercise was maintained for around 4 minutes, 1 minute to establish a steady

state followed by 2-3 minutes of image acquisition. As the integral (Philips) ECG monitoring was found to be ineffective in exercise during a pilot stage an external MRI ECG system was used for gating. Images were acquired firstly using a retrospectively gated SSFP cine sequence with a temporal resolution of 34 milliseconds to acquire a short axis stack followed by a horizontal long axis stack. The short axis stack took up to 70 seconds to acquire and long axis stack up to 60 seconds. Subsequently an ungated real time SSFP cine sequence was performed with 40-75 frames per 36-38 milliseconds in the same short and long axis stacks. In addition to continuous ECG monitoring a plethysmograph allowed synchronisation with respiratory data. Using VO_2 data gained from prior cardiopulmonary exercise testing and haemoglobin, oxygen saturations, and arterial and venous oxygen partial pressure measured with an automated analyser using samples taken from catheters during exercise, the direct Fick method was used to determine cardiac output. The authors found that the ECG gated images acquired in exercise were unsuitable for segmentation in over 50% of cases. In contrast the real-time sequence provided easily segmented images with good inter-observer variability. Most importantly there was a high level of agreement between CO determined by real time MRI and by the direct Fick method with an intraclass correlation coefficient of 0.96. Whole group data is not published however in the athlete group (n=10) using the cycle ergometer the maximum workload was 230±35 Watts. HR increased from 59±14 bpm at rest to 164±10 bpm at peak exercise. Both left and right ventricular stroke volume increased in exercise due to a decrease in end systolic volume from 91±19 to 67±15 ml in the left ventricle and 106±25 77±34ml in the right ventricle. CO increased from 8.4±2.6 l/minute to 25.4±4.5/l minute.

The same group went on to investigate the effects of respiration on left and right ventricular interaction(144) at rest and during exercise in 9 healthy subjects. Using the exercise protocol and ungated real time SSFP cine sequence the authors found that both at rest and in exercise ventricular volumes oscillate with the respiratory cycle with RV volumes maximal at peak inspiration and LV volumes maximal on expiration. Again highlighting the potential for exercise studies to elicit findings that would not be apparent at rest the same group have used combined exercise cardiac MRI and invasive systemic and pulmonary artery pressure been used to investigate

exercise limitation in adults with chronic thromboembolic pulmonary hypertension (CTEPH) as well has the acute effects of pulmonary vasodilator treatment(145). Most recently working with the same methodology Van De Bruaene(146) and colleagues performed exercise cardiac MRI with invasive monitoring in 10 adult/adolescent patients with the Fontan circulation before and after a single dose of Sildenafil. Stroke volume and cardiac index both increased significantly following Sildenafil and to a greater extent with exercise. Cardiac index increased post Sildenafil from 4.1±0.9 to 4.8±1.0 L/[min·m2] with an exercise effect: of +0.9±0.4 L/[min·m2]). The authors concluded that the pulmonary vasculature plays an important role in physiological limitation in this group, the haemodynamics of which are best demonstrated with exercise.

4.8 Other Approaches to Assessing Oxygen Uptake in the MRI Environment

An alternative approach to investigating exercise limitation using MRI focuses on assessing oxygen extraction at the level of individual or groups of exercising muscle. There are fewer studies in this field, using a diverse range of methodologies.

Blood oxygen level dependent (BOLD) MRI is a technique commonly used in functional neuro imaging. BOLD measures magnetic field inhomogeneities resulting from changes in blood oxygen concentration. Oxygenated blood is diamagnetic and therefore has no signal loss. Where there is a low ratio of deoxygenated to oxygenated blood there will be a slow decline in the MRI signal. As deoxygenated blood is paramagnetic when there is a high ratio of deoxygenated blood to oxygenated blood there is a rapid decrease in MR signal. Some studies have looked at muscle oxygenation during or immediately after exercise using this technique. Caterini and colleagues measured BOLD signal recovery in the quadriceps muscle immediately post exercise in ten healthy volunteers(147). Exercise was performed on the Lode up/down MRI compatible ergometer. In this study volunteers exercised to 65% of a pre-determined maximal work-load for three minutes followed by immediate recovery T2* weighted BOLD imaging of the non dominant quadriceps muscle using a gradient echo EPI sequence. Regions of interest were then drawn in the muscle groups recruited and BOLD signal fitted to a sigmoid function. The authors proposed that the same technique could be used to determine microvascular

response in patients with chronic disease to further understanding of exercise intolerance. Muller and colleagues(148) have described a methodology for assessing BOLD signal during low intensity exercise using a bespoke plantar flexion ergometer and were able to demonstrate both sudden decrease in BOLD signal at the onset of exercise and lower BOLD signal intensity at higher resistance.

Hall and colleagues (149)performed exercise MRI with the goal of assessing pulmonary blood flow using arterial spin labeling (ASL) . ASL is a technique where water molecules in arterial blood are 'labeled' immediately below the region of interest using a 180-degree inversion pulse. Following a time interval (transit time) the labeled molecules flow into the region of interest. Tissue magnetisation is reduced by the inflowing inverted spins. An image is acquired known as the 'tag' image. Subsequently a control image is acquired. Subtracting magnetisation of the tag image from the control image produces a perfusion image with the difference between tag and control images proportional to blood flow. Interestingly Hall's study design used VO_2 rather than HR to stratify exercise intensity using a modified CPET system with 6-metre expiratory line. Subjects exercised to a target oxygen consumption less than 1 1/minute, equivalent to around 27% of VO_{2max}. This approach was primarily used to maintain exercise within a narrow window, sufficient to elevate pulmonary vascular pressure but not to impair gas exchange and to ensure imaging was undertaken in steady state conditions for V_E and VO_2. Exercise was performed on a Lode 'stepping ergometer' to a target intensity and after 10 minutes at steady state, images acquired using an ASL-FAIRER sequence (requiring up to 9 second breath-holds). The authors comment that the studies were 'exceptionally difficult to conduct' due to both upper body motion impacting on ECG gating and on image registration at post processing. In the six subjects studied the authors were able to demonstrate redistribution of blood flow to non-dependent lung and decreased lung perfusion heterogeneity at low-intensity exercise.

Another approach to assessing muscle metabolism is phosphorous-31 magnetic resonance spectroscopy (^{31}P-MRS). This technique assesses oxidative phosphorylation and anaerobic glycolysis and has been performed in exercise in

healthy children and in groups including children with cystic fibrosis, demonstrating lower resting ATP concentrations and delayed phosphocreatine recovery (150).

Near infrared spectroscopy (NIRS) is a technique that works by using the differential in absorption of near infrared light to approximate the ratio of oxygenated to total haemoglobin. A recent study with the goal of providing a surrogate of exercise PCMR for computational fluid dynamics studies of the aorta under stress conditions (151)used a bespoke ergometer to measure exercise flows in the ascending aorta innominate, left common carotid and subclavian arteries at between 130 and 170% of resting HR and subsequently measured NIRS values in corresponding locations at the same levels of exercise outside the MRI scanner. Data were then combined to relate oxygen extraction acquired with NIRS with PCMR findings. Although there were limitations in the study design around the exercise protocol and details of the PCMR sequence, as MRI compatible NIRS probes are now available a combined exercise MRI/NIRS approach may provide important information on the coupling of oxygen delivery and consumption during exercise in the future.

Finally a complex-difference projection method has also been described in healthy volunteers at low intensity exercise. Using this technique it was possible to simultaneously measure femoral venous blood flow and saturations immediately following but not during exercise (152)

Whilst techniques described in this section may not translate into first line clinical investigations alone they present useful potential research tools and could also be integrated into more comprehensive clinical protocols.

4.9 Summary of Literature Review

Building on the established diagnostic and prognostic role of conventional CPET we set out to develop a comprehensive exercise assessment including non-invasive CO measurement using MRI. Cardiac MRI represents a gold standard for non-invasive assessment of CO and ventricular volumes at rest. The development of real time PCMR has allowed accurate measurement of CO in exercise. The wider context of stress imaging includes the use of pharmacological stressors. Whilst these have a

proven role they also have significant disadvantages and are not a true surrogate for exercise. Various approaches to use of exercise as a stressor have been considered. Treadmill exercise adjacent to the scanner has the advantage that higher workload achieved and availability of 12 lead ECG monitoring. Benefits of this approach are to an extent negated by the rapid changes in physiology that occur on termination of exercise. Isometric techniques are associated with less upper body movement but do not reproduce the conditions limiting dynamic exercise. There is now a body of literature on in-scanner dynamic exercise including in both healthy volunteers and patient populations. As this is an evolving field with small study populations questions remain on the optimal form of exercise and exercise protocols. A range of other MRI approaches to assessing tissue oxygen extraction during exercise have been proposed however the potential clinical utility of these techniques is unclear.

Chapter 5 Methods

The aim of this work was to develop and test a comprehensive, non-invasive approach to assess exercise physiology differentiating exercise intolerance caused by cardiac, respiratory and skeletal muscle insufficiency. As stated in the introduction this novel approach combines simultaneous cardiac magnetic resonance measurement of CO and cardiopulmonary exercise test measurement of VO_2.

In order to be clinically relevant this technique should be suitable (both practically and in terms of user experience) for use in health and disease and across a wide range of age groups. Additionally it should be easily reproducible at centres performing conventional CMR and CPET without excessive additional costs.

The methods common to all three of the studies presented are described in this chapter. Where there are differences in the methodology used they are presented in the relevant results chapter.

5.1 Ethical Approval

Ethical approval for the studies was sought and granted through the integrated research approval system (IRAS). Examples of ethics committee approved study materials are provided in appendix I. The study was registered with the UK clinical research network (UKCRN study ID: 17282) and subsequently transferred to the central portfolio management system (CPMS).

All studies were performed with full verbal and written consent and in addition written assent where appropriate.

5.2 Study Populations

As this is a relatively new field of research with limited prior experience, power calculation is challenging. Based on the findings of a previous exercise CMR study in patients with pulmonary stenosis an estimated six subjects were required to detect a difference in exercise stroke volume between patients and controls at the 0.8 level (α=0.05). Additional subjects were included in all studies for redundancy.

Standard exclusion criteria for CMR(153,154) (for example, pregnancy, conditional or unsafe implant, retained metal foreign body) applied across all studies. The MRI safety checklist used at Great Ormond Street Hospital, is included in appendix II. Standard exclusion criteria for CPET were also applied across all studies (for both conventional and MR-CPET). Joint American Thoracic Society (ATS) and the American College of Chest Physicians (ACCP) guidelines on absolute and relative contraindications to CPET are shown in Table 4.

Table 4 Absolute and relative contraindications to CPET

Absolute Contraindication	**Relative Contraindication**
Acute myocardial infarction in past 5 days	Left main coronary stenosis or equivalent
Uncontrolled arrhythmia with symptoms or haemodynamic compromise	Moderate stenotic valve disease
Syncope	Severe untreated arterial hypertension at rest
Active endocarditis	Tachyarrhythmia / Bradyarrhythmia
Acute endocarditis / myocarditis	High-degree A-V block
Severe aortic stenosis (symptomatic)	Hypertrophic cardiomyopathy
Uncontrolled heart failure	Significant pulmonary hypertension**
Acute pulmonary embolus / infarction	Advanced or complicated pregnancy
Lower limb thrombosis	Electrolyte imbalance
Suspected dissecting aneurysm	Orthopaedic impairment compromising exercise performance
Uncontrolled asthma	
Pulmonary oedema	
Room air desaturation at rest⩽85%*	
Respiratory failure	
Uncontrolled asthma	
Acute non cardiac /cardiopulmonary illness that may affect performance or deteriorate with exercise (i.e. acute infection, renal failure, thyrotoxicosis)	
Mental impairment precluding co-operation with testing	
*Exercise with supplemental O_2 **Can safely perform test but with extra caution	

Absolute and relative contraindications for cardiopulmonary exercise testing adapted from the American Thoracic Society (ATS) and the American College of Chest Physicians (ACCP) joint statement on Cardiopulmonary Exercise Testing, January 2003(36)

The specific inclusion and exclusion criteria for patient groups in individual studies are described in the respective study chapters.

5.3 CPET System

Because of the multiple ferromagnetic parts required in a standard CPET system it would not be practical to develop a metabolic cart for use in the scanner room. Instead, multiple vendors of CPET systems were contacted to discuss the adaptation of commercially available systems for use in an MRI environment. Following a site visit the manufacturer of the Ultima CPET system (MedGraphics, St. Paul, USA) developed an extended length MR compatible umbilical line. The Ultima system is a widely used commercially available CPET system (including use in the exercise laboratory at Great Ormond Street Hospital). The umbilical line consists of a gas drying Nafion sampling circuit (to remove water vapour from expiratory gas) within a protective hose. The length of the umbilical was increased from a standard length of 234cm to 470cm (Figure 5.1)

Figure 5.1 Standard (left) and Modified (right) Umbilical.

This modification allowed it to be passed from the CPET system in the control room through the wave-guide into the scanner room and to reach the subject within the bore of the magnet. The extended umbilical included additional length to allow for scanner table movements. Due to the narrow gauge of the sampling lines the dead space remained small (Figure 5.2).

This customised umbilicus was extensively tested by the manufacturer and met all of the prescribed quality control standards. All measured gas variables (VO_2, VCO_2) RER and volume measures at both standard pressure dry (STPD) conditions and body temperature and pressure saturated (BTPS) fell with in the same acceptable ranges as the standard length commercial umbilical. A copy of the gas exchange system validation (GESV) data set for the modified umbilical is provided in appendix III.

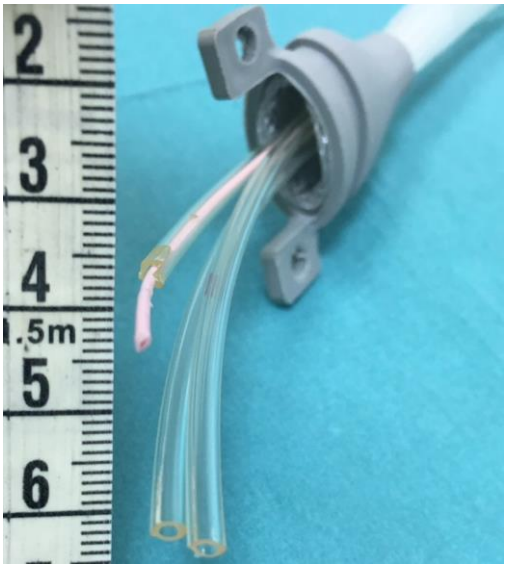

Figure 5.2 Sampling Lines

Subjects wore an appropriately sized Hans Rudolf reusable facemask and headgear set (Hans Rudolf, Shawnee, USA). This facemask has no metal parts. Once subjects were comfortably positioned in the scanner the flow sensor testing assembly was connected to the facemask (Figure 5.3). Reusable parts were cleaned between volunteers as per manufacturer and hospital infection control advice.

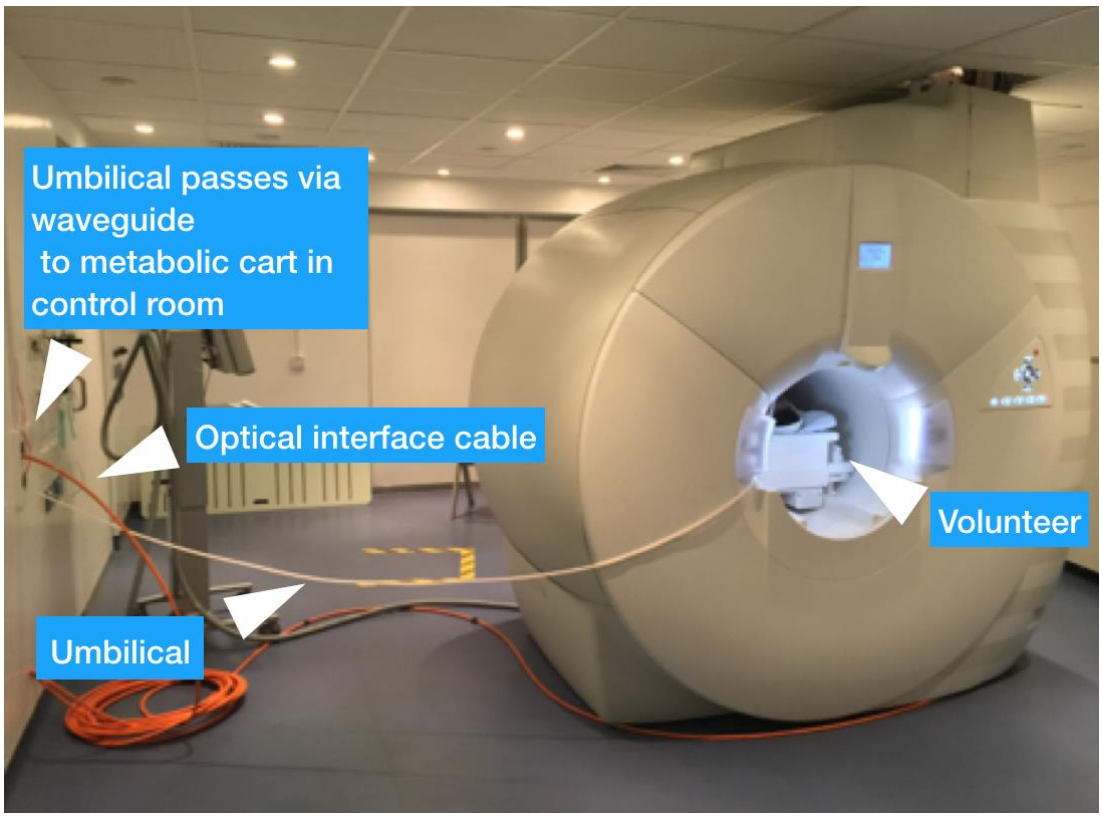

Figure 5.3 Demonstrating the Umbilical passing through the Wave Guide to a Volunteer.

The Ultima CPET system performs breath-by-breath gas exchange analysis using an electro galvanic oxygen sensor (range 0-100%, accuracy ±1%) and non-dispersive infrared carbon dioxide sensor (range 0-15%, accuracy ±0.1%). Airflow is measured using a differential pressure transducer. The scanner room was temperature controlled with regular humidity monitoring.

Gas and flow calibration was performed before each use. Flow sensor calibration was performed using a 3-litre calibration syringe, testing repeatedly at varied rates to test the linearity of the flow system. O_2 and CO_2 calibration was performed using an automated calibration feature of the Ultima system that automatically adjusts gain and offset values in relation to the measured signal. Data was recorded using the CPET system supplier's software (BreezeSuite, Medgraphics, St. Paul, USA) and exported as a text file.

5.4 MRI Compatible Ergometer

Exercise was performed on a supine MR compatible ergometer (MR Cardiac Ergometer Up/Down, Lode, Groningen, The Netherlands) (Figure 5.4). The ergometer is compatible with a wide range of MRI scanners up to 3.0 T and works using an electromagnetic breaking system. The minimum workload increment is 1 Watt and increases can be controlled remotely via an optical interface cable (either manually or using a pre-programmed ramp). The ergometer underwent routine servicing and calibration during the course of these studies.

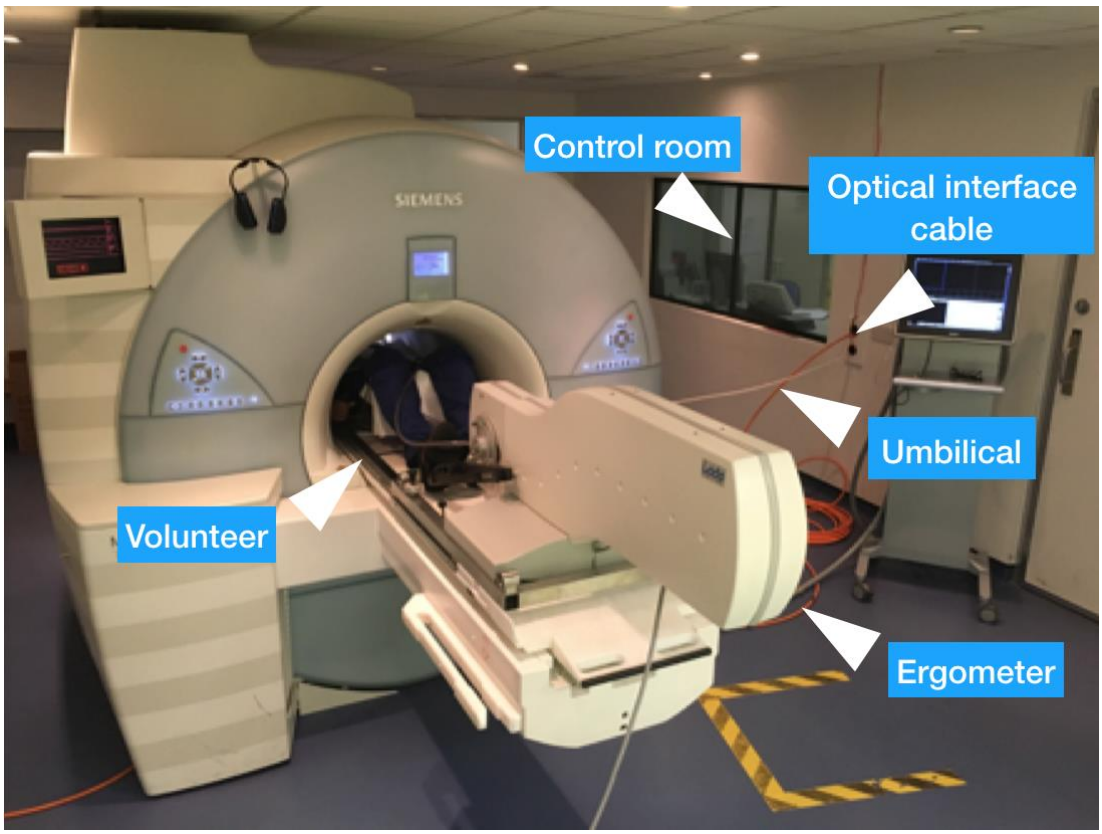

Figure 5.4 Lode Up Down MRI Ergometer.

The ergometer uses an up-down kicking motion with the thighs relatively immobilized using Velcro straps. This exercise allows full range of motion within a 60 cm scanner bore. The muscle groups primarily engaged during this exercise include the quadriceps extensor muscles, posterior thigh muscles and calf muscles.

5.5 Exercise Protocol

There was some variation in the exercise protocols used over the three studies because of the different populations investigated. Study exercise protocols are detailed in the individual study chapters. Prior to all studies volunteers underwent a standardized briefing on the exercise technique and protocol and were able to familiarize themselves with the equipment used. For the validation study the briefing involved a verbal description and physical demonstration. For subsequent studies a short video of the exercise was sent to participants by email before attending and was played again on the day of the study in addition to the same verbal description and physical demonstration as used in the validation study. For all studies three members of the research team were present throughout exercise. This was necessary in order to have one member of staff in the scanning room during exercise, one to run cardiopulmonary exercise testing and one to scan the subject. All had basic life support training and at least one had age appropriate advanced life support qualification. Prior to the validation study and again during the subsequent studies simulated evacuations of volunteers from the MR-ergometer out of the scanning room to the adjacent resuscitation area by three members of staff were run with safe evacuation completed within 90 to 120 seconds. Access to a full resuscitation team and full resuscitation facilities were always available. Stopping criteria for exercise applied across all studies: verbal or non verbal indication of desire to stop, signs of physical or mental distress, chest pain, arrhythmia/ECG change, syncope, chest pain, other parent/guardian or study team member concern.

5.6 MR Sequences

All imaging was performed on a 1.5 Tesla MR scanner (Avanto, Siemens Medical Solutions, Erlangen, Germany) using two six-element body-matrix coils. There was continuous ECG monitoring using the Siemens MRI vectorcardiogram (Siemens Medical Solutions, Erlangen, Germany).

5.6.1 Real Time Flow Assessment

Aortic flow was assessed just above the sino-tubular junction. Flow was continuously measured during exercise using a previously validated UNFOLDed-

SENSE spiral PCMR sequence (see chapter 3). This approach has previously been demonstrated to be a robust method with sufficient temporal resolution to accurately measure great vessel flow in exercise(102). The following parameters were used: field of view = 450 mm, matrix =160x160, voxel size = 2.8x2.8x7mm, TR = 5.8 ms, TE = 1.4 ms, flip angle = 20°, velocity encoding (VENC) = 250 cm/s, temporal resolution = 35 ms. An acquisition scheme was used that provided temporal encoding (for the UNFOLD) and allowed calculation of coil sensitivity maps from the data itself (for SENSE). As described in chapter 3, phase offset is a potential source of error in PCMR flow measurement. Phase offset error is a systematic phase error arising from three major effects; inhomogeneity in B0, concomitant gradients and eddy currents. The sequence used in this study uses coil sensitivity and regularisation data acquired over all of the frames acquired for reconstruction. Maxwell correction is performed to remove the effects of the concomitant flow-encoding gradients. Residual phase offset was removed through automated phase correction. Validation of this sequence has been previously published(102) and when indicated (for example for acquisition of flow data in infants) it is used in clinical practice.

The UNFOLDed-SENSE reconstruction was performed online using a GPU-equipped external computer (Tesla C2070, Nvidia, Santa Clara, CA, USA) that was networked to the native scanner reconstruction system. Undersampled k-space (R=6) was initially temporally filtered (UNFOLD), which reduced the undersampling by a factor of 2. The resultant data with reduced undersampling (R=3) then underwent SENSE reconstruction. The reconstructed images were sent back into the scanner-based reconstruction pipeline for final conversion to the DICOM format and image viewing on the scanner console. This approach had previously been developed and validated for use in computationally intensive reconstructions associated with large data sets acquired over long time periods that would otherwise take prohibitively long to reconstruct(155).

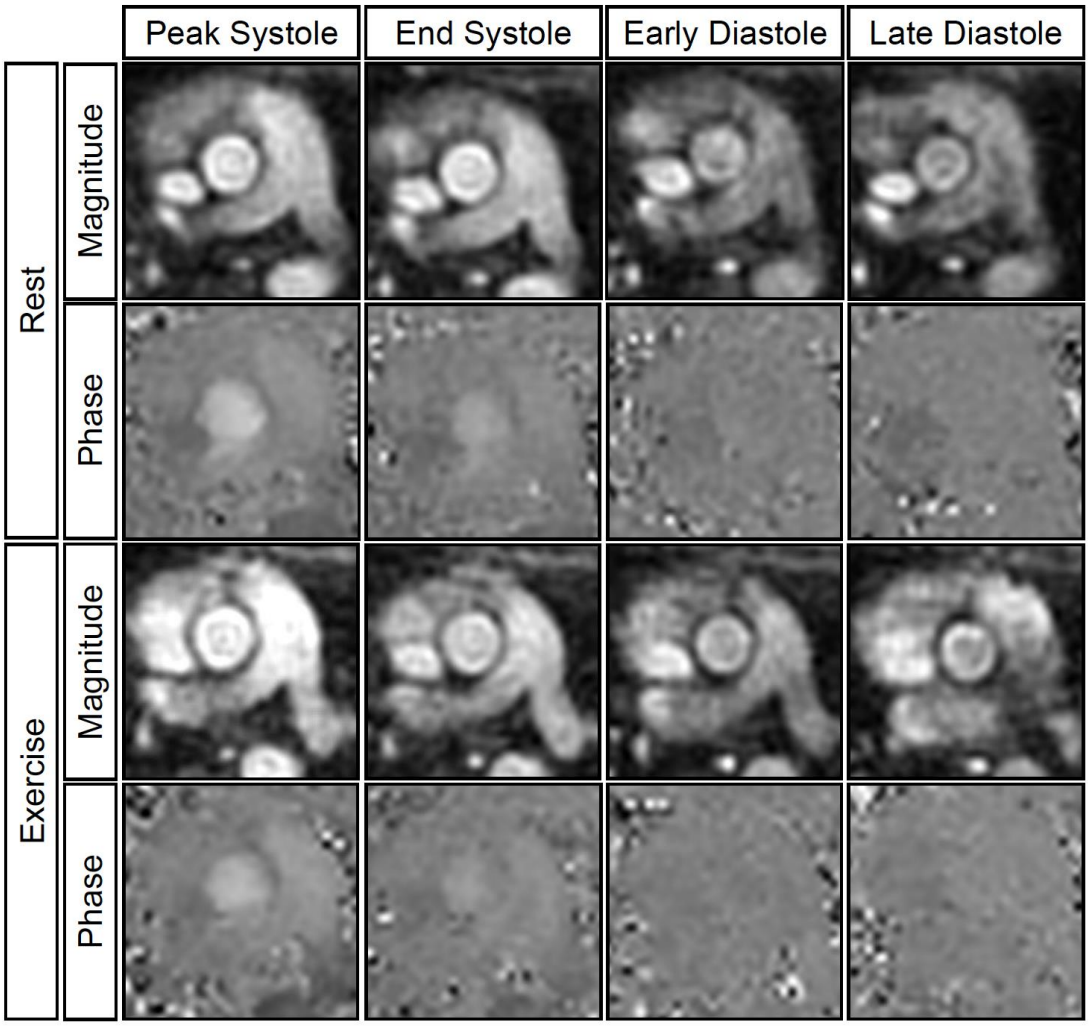

Figure 5.5 Examples of magnetic resonance flow images at rest and exercise throughout the cardiac cycle.

5.6.2 Ventricular Volume Assessment

Ventricular volume was assessed at rest and in exercise in the studies focussing on patient groups (second and third). A short axis stack was acquired using a real-time (free breathing) radial k-t SENSE steady state free precession sequence (described in chapter 3). Again this sequence was chosen because of a high temporal and spatial resolution had been previously validated in exercise(106). The parameters used were: field of view = 320 mm, matrix = 128x128, voxel size 2.5x2.5x8, TR = 2.4 ms /TE = 1.17 ms, flip angle = 47°, R = 8, temporal resolution = 36ms.

5.7 Image Analysis

All images were processed using in-house plug-ins for the open-source software OsiriX (OsiriX Foundation, Geneva, Switzerland). Image analysis was performed on a multicore workstation (12 core, Mac Pro, Apple, CA). Volumetric analysis varied between studies and is therefore described in the individual results chapters. Analysis of flow data is described below.

5.7.1 Flow

Because exercise was performed for up to 14 minutes with a frame rate of 28.6 frames per second a very large number of frames were generated (as many as 24000 frames per study). As described in chapter 3, segmentation of the vessel of interest (in this case the ascending aorta) is necessary in order to obtain accurate flow measurement. Segmentation is performed using anatomical data provided by the magnitude data set and ROIs then copied to the corresponding phase images to calculate flow. The very large data sets resulting from MR-CPET make manual segmentation prohibitive and necessitated semi-automatic segmentation of the data. As this kind of data set is not produced in routine clinical work applicable processing tools are not currently commercially available from vendors. Therefore it was necessary to develop specific plugins for use with MR-CPET flow data. This was a challenging task, primarily because of the size of the data sets but also due to the misalignments from frame to frame from free breathing, cardiac motion and exercise motion as well as lower spatial resolution and signal to noise ratio from the real-time data. Segmentation was parallelized across multiple cores by dividing the data into equally sized sub-sets, each processed by a separate thread. Firstly using the magnitude data set a large region of interest was drawn around the aorta ensuring that the vessel was within it throughout exercise (Figure 5.6).

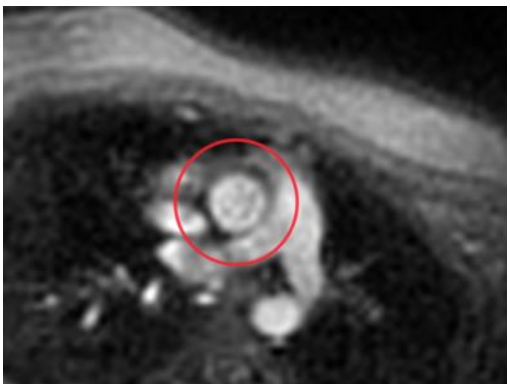

Figure 5.6 Magnitude data set with large region of interest drawn around the aorta.

This ROI was used to generate a ‘rough’ flow curve from the phase data, as seen in (Figure 5.7). Peak detection was then performed on this flow curve (shown in figure 1.7 as stars) and the data divided into approximate heartbeats.

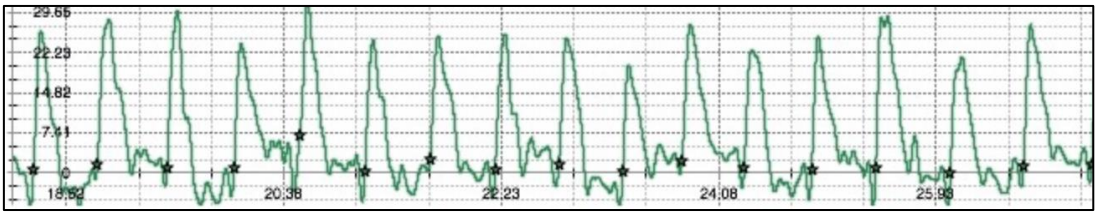

Figure 5.7 The 'rough' flow curve.

The data was then retrospectively cardiac gated, by placing each frame into 1 of 12 cardiac bins depending on its position in the approximate heartbeat (Figure 5.8). This resulted in each bin containing frames at a similar approximate position in the cardiac cycle but at different respiratory and exercise motion positions. In the second study flow data was first divided into ten equal sections by time before retrospective cardiac gating. This was done in attempt to overcome failure in segmentation due to large differences in position related to exercise motion between rest and peak exercise.

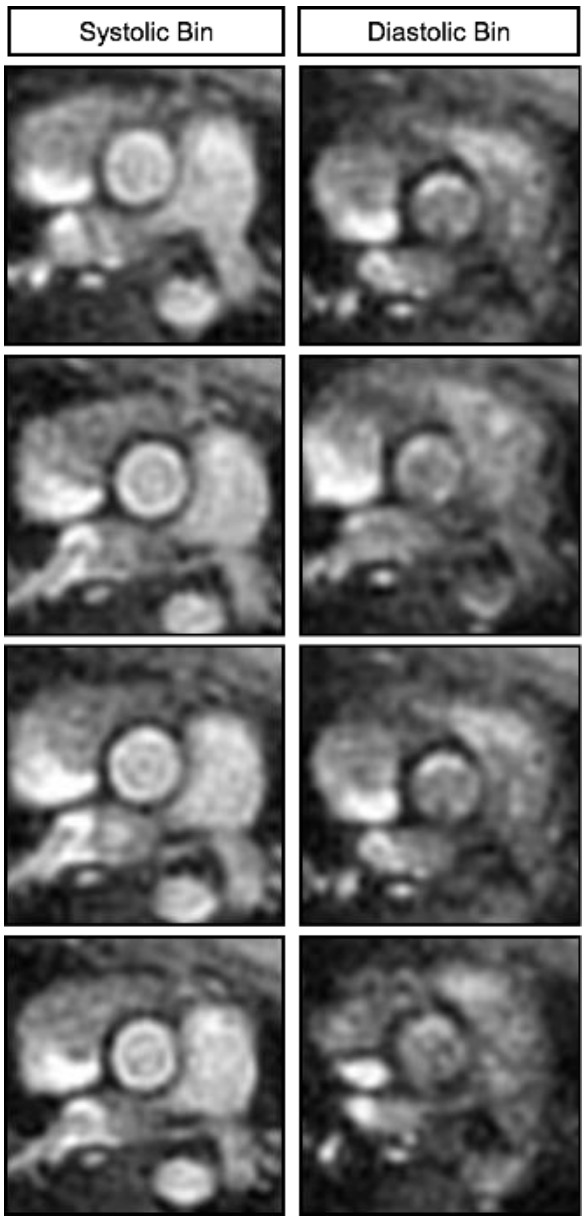

Figure 5.8 Examples of a systolic and diastolic 'bin'.

Manual segmentation of the aorta was performed on one reference frame in each sub-set by drawing a 5 point closed region of interest before starting the automatic registration. This used a previously developed fully deformable (non-rigid) registration based algorithm. Non-rigid registrations allow for non-uniform mapping between images deforming one image to match other images (in contrast rigid registration techniques use a simple transform where rotations and translations are uniformly applied). Only the magnitude image was used for the registration, the registration algorithm searches for a sequence of 2D displacement fields that

optimally match frames to the original reference frame. The polygonal contour was then propagated by applying displacement fields provided by the registration to the vertices of the polygon. This algorithm has been previously validated for use with real time images obtained in exercise(156).

The technique was chosen because of its ability to overcome some of the challenges present in the post-processing of real time data including the lower signal to noise ratio and spatial resolution as well as frame-to-frame misalignment. The reference frame was chosen to ensure similarity to the overall dataset as choice of a dissimilar or 'bad' reference frame could result in the registration problem being too difficult and result in failure of propagation. The resulting ROIs were visually assessed and where necessary, subsets were individually re-segmented to improve accuracy. Finally, the phase and magnitude data sets were recombined and flow curves generated. The output was displayed graphically in the plugin (Figure 5.9), and corresponding text files saved.

Figure 5.9 Example of exercise flow plugin graphical output

5.8 Integration of CPET and Real-Time Flow Data

Further processing of the raw flow curves and combination with the VO_2 data was performed in Matlab (Matlab, The Mathworks, Natick, MA). The start of ejection in each cardiac cycle from the flow curves was automatically calculated as the intersection of the tangent of the steepest part of ejection, allowing calculation of r-r interval and heart rate (HR) (Figure 5.10). Stroke volume (SV) was calculated by integrating the flow curve across each r-r interval and CO ($CO = HR * SV$).

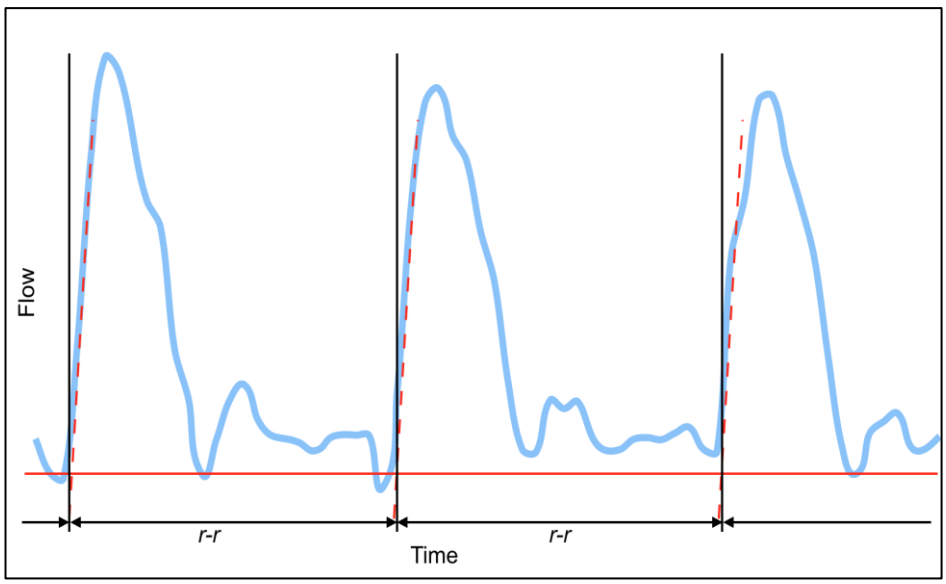

Figure 5.10 Identification of r-r interval.

The HR, SV, CO and VO_2 curves were filtered using zero-phase, low pass, second-order Butterworth filter with normalized cut-off frequency of 0.0125 Hz. This filter was chosen following visual inspection of filtering with a range of cut-off frequencies and was found to optimally reduce noise without loosing signal. Arterio-venous oxygen content gradient (a-vO_2) was then calculated as:

$$a - vO_2 = \frac{VO_2}{CO}$$

As described above the initiation of VO_2 and flow recording was simultaneous, temporal alignment of VO_2 and flow curves was ensured by creating a new time vector adjusted for the lengths of the individual MR and CPET time vectors. Minimum and peak values were extracted from the interpolated CO and VO2 data to which a Butterworth filter had been applied to remove noise. This is consistent with conventional exercise testing where absolute rather than averaged values are identified.

5.9 Experience

Acceptability to patients is a key criteria in assessing whether any health technology could or should be implemented(157). For this reason all volunteers were asked to complete a questionnaire adapted from a validated questionnaire used to assess the acceptability of coronary CT angiography in adults(158). Participants were asked to rate on 5-point Likert scale: i) degree of concern prior to the test (1=very intense concern, 3=moderate, 5=no concern), ii) comfort during the test (1=very poor, 3=moderate, 5=very good), and iii) degree of perceived helplessness (1=very intense helplessness, 3=moderate, 5=no helplessness). Responses ≥3 were considered clinically acceptable. Reported hours of exercise per week were also recorded in this survey order to investigate relationship between training and MR-CPET measures.

Chapter 6 Validation of MR-CPET in Healthy Adults

6.1 Introduction

The limitations of conventional exercise testing described in the motivation to this thesis support the need for alternative approaches to exercise assessment. As described in the literature review one approach is invasive CPET. However this is difficult even in healthy adults and more so in chronic disease. In children, who require general anesthetic for cardiac catheterization, invasive CPET is not a tenable clinical technique. A novel approach combining simultaneous cardiac magnetic resonance measurement of CO and cardiopulmonary exercise test measurement of VO_2 is a potential alternative, however to date this method has not been fully exploited. Partly this is because of the challenges of acquisition of adequate MR data in exercise and partly because of the lack of compatible CPET systems. Advances in MRI with non-breatheld high temporal and spatial resolution sequences as well as reconstruction pipeline development make MR-augmented CPET viable. In this study a combined MR-CPET approach was implemented using a modified commercially available CPET system. It was necessary to validate this technique in healthy adults in relation to conventional exercise testing before applying it in paediatric and disease populations.

6.2 Aims

The aims of this study were: 1) to evaluate feasibility and acceptability MR-CPET in healthy adults and 2) to test whether peak values obtained at conventional and MR-CPET correlate 3) to demonstrate how variation in VO_{2peak} is related to both peak CO and peak oxygen extraction.

6.3 Study Population

17 healthy volunteers (12 male, 5 female) with varying levels of (self-reported) regular physical activity were recruited between May and August 2014 through advertising within Great Ormond Street Hospital. Exclusion criteria were: i) cardiovascular disease (as assessed by clinical history), ii) contra-indications to

exercise testing (i.e. musculoskeletal injury, joint disease), and iii) contraindications to MR (i.e. MR-incompatible implants, pregnancy).

6.4 Methods

The methodology for this study was as described in the methods chapter with the addition that prior to MR-CPET volunteers underwent conventional cardiopulmonary exercise testing. A doctor and senior physiologist supervised conventional CPET. Testing was performed using an upright bicycle ergometer (Sensormedics Ergoline 800, Bitz, Germany). Cycle ergometery was chosen as although there are advantages and disadvantages of both treadmill and cycle techniques (discussed in chapter 2) cycle ergometers allow work rate measurement and better quantify the metabolic cost of exercise(50,159). Respiratory gases were continuously sampled via a mouthpiece and nose clip (sampling using a well fitted facemask and mouth piece are interchangeable (50)). Respiratory gas exchange analysis was performed using a SensorMedics CPET system and Vmax Encore software (Vmax Encore, Viasys Healthcare, UK). Like the Ultima system described in chapter 5 this metabolic cart uses an electro galvanic oxygen sensor and non-dispersive infrared carbon dioxide sensor with data being averaged over a peak width of 10 seconds at the end of exercise to determine maximum values. Gas analyser volume and flow calibration was performed before each test. Exercise was performed in a quiet, temperature and humidity controlled environment with full resuscitation facilities available. Work rate was increased following a standardized ramp protocol. Participants were asked to cycle to a target of 60 to 70 rpm and to continue to their maximal capacity (exhaustion). The ventilatory anaerobic threshold was calculated for conventional CPET data using the V-slope method (regression of the VO_2 and VCO_2 slopes which detects the beginning of excess CO_2 generated from H^+ buffering) (160).

As there was some variation between studies in the MR-CPET protocols used it is described here rather than in the methodology chapter. Adult volunteers (>16 years old) followed a standardised MR-CPET exercise protocol consisting of one minute rest followed by 2 minutes unloaded cycling then a 1 Watt increase every 20 seconds for the next 5 minutes and subsequent 2 Watt increase every 30 seconds to exhaustion followed by 2 minutes of recovery. This protocol was based on published

data on the optimal duration for conventional exercise testing and on prior experience of workloads achievable during supine exercise using the 'up-down' ergometer. As described in the methodology chapter continuous real-time flow data and breath-by-breath CPET data acquisition was performed from rest through to recovery.

6.5 Statistical Analysis

All statistical analysis was performed using StataSE 13.0 (StataCorp, College Station, USA). All results are expressed as the mean ± standard deviation. Measurements of agreement were performed using correlations and ratio Bland-Altman analysis. The most commonly used application of the Bland Altman technique is to plot difference in paired measurements against the mean of the two measurements but it is also possible to plot the differences as percentages and ratios. In order to assess agreement in paired samples independently from mean values it is most appropriate to use the ratio of the paired measurements(161). Differences between means were assessed using Student t-test and multiple linear regression analysis was used to assess the relationship between metrics. A p value <0.05 was considered statistically significant.

6.6 Results

6.6.1 Demographics

The mean subject age was 38.6 ± 10.6 years, 12/17 were male, with a mean height and weight of 1.72 ± 0.08 m and 73.36 ± 13.2 kg. The amount of regular exercise performed as reported by volunteers was 6.4 ± 5.23 hours per week (range 1-20 hours).

6.6.2 Feasibility and Tolerability

All subjects successfully completed conventional CPET and 15/17 subjects completed MR-CPET. One subject was unable to successfully complete MR-CPET due to claustrophobia (male, 39 years) and one subject was unable to successfully master the exercise technique using the MR compatible ergometer (male, 58 years).

The mean number of days between tests was 11.6 ± 11.4 days (range 1-32 days). There was no significant difference in perceived helplessness between the two tests (conventional CPET: 4.29 ± 1.01 vs. MR-CPET: 4.18 ± 1.0, p=0.58). There were small but significant differences in reported concern prior to testing (conventional CPET: 5.0 ± 0 vs. MR-CPET: 4.7 ± 0.47, p=0.02) and comfort during testing (conventional CPET: 4.35 ± 0.7 vs. MR-CPET: 3.88 ± 0.6, p=0.04). However, it should be noted that all MR-CPET results were still in the clinically acceptable range (≥3) (Figure 6.1).

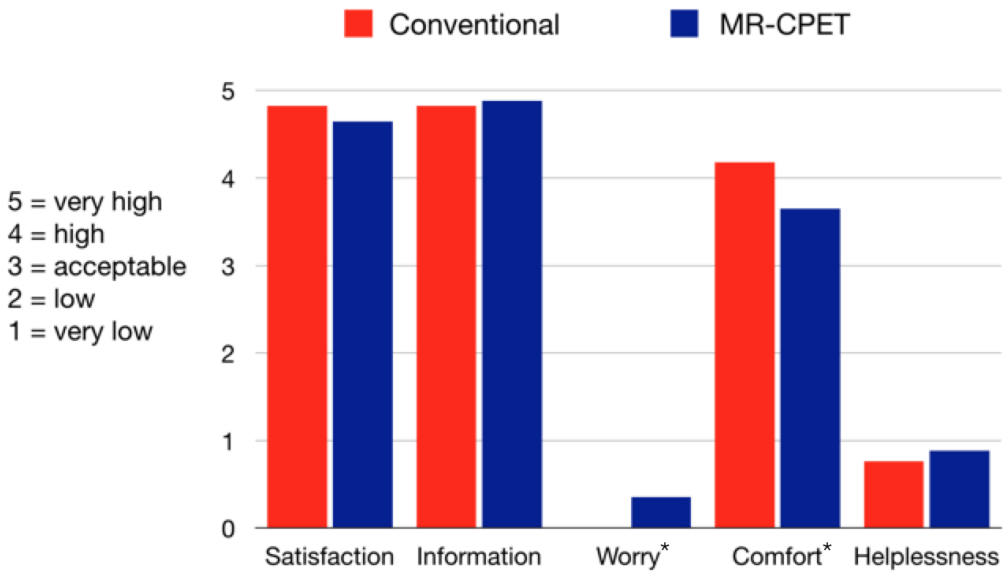

Figure 6.1 Acceptability survey results for conventional CPET and MR-CPET (*significant difference)

6.6.3 Conventional and MR-CPET Findings

VO_{2peak}, peak carbon dioxide production (VCO_2), and VO_2 at anaerobic threshold (VO_{2AT}) during conventional CPET and MR-CPET were strongly correlated (r=0.87-0.94, p<0.001)(Table 5) However as expected MR-CPET measurements were systematically lower, with a ratio bias of approximately 0.45-0.48 for VO_2 and VCO_2 and 0.68 for VO_{2AT} (Figure 6.2, Figure 6.3) There was also a strong correlation between peak HR during conventional CPET and MR-CPET (r=0.76, p=0.001) (Figure 6.5) although it was lower during MR-CPET (ratio bias = 0.78). Finally, peak work rate achieved during conventional CPET and MR-CPET was moderately

correlated (r=0.66, p=0.007), with MR-CPET work rate being much lower than during conventional CPET (ratio bias=0.12) (Figure 6.6)

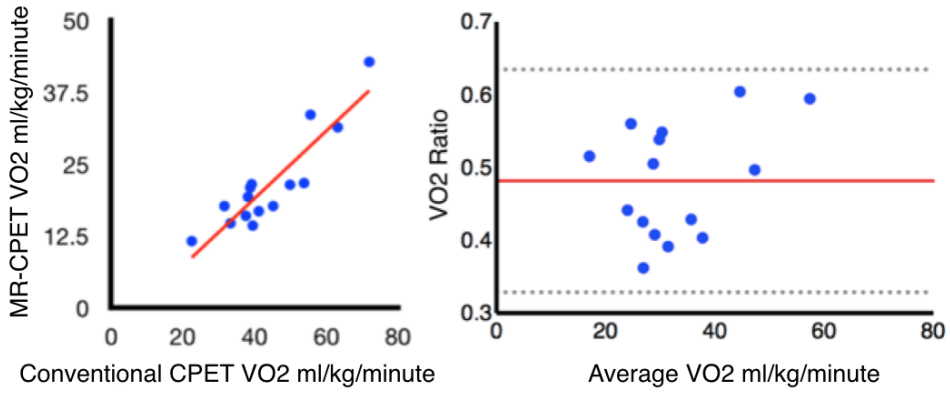

Figure 6.2 Scatter graph of peak VO_2 measured during MR-CPET against conventional CPET. b) Ratio Bland-Altman analysis of peak VO_2 as measured by conventional and MR-CPET. Ratio = VO_2 / Conventional CPET. Red line = bias, dotted line = limits of agreement.

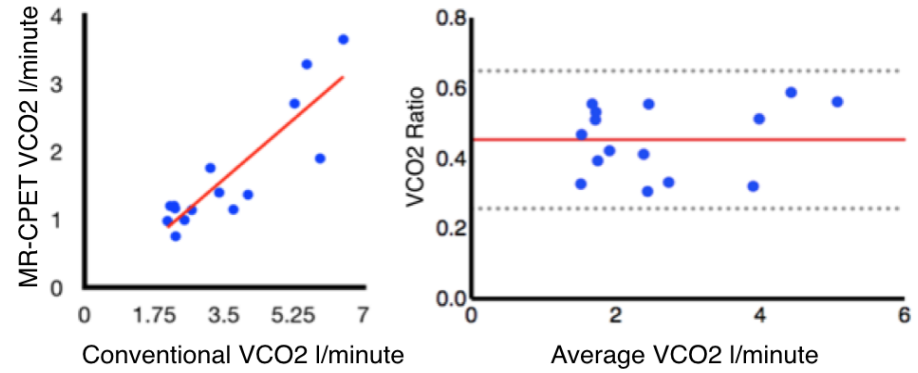

Figure 6.3 Scatter graph of peak VCO_2 measured during MR-CPET against conventional CPET. b) Ratio Bland-Altman analysis of peak VCO_2 as measured by conventional and MR-CPET. Ratio = VCO_2 / Conventional CPET. Red line = bias, dotted line = limits of agreement.

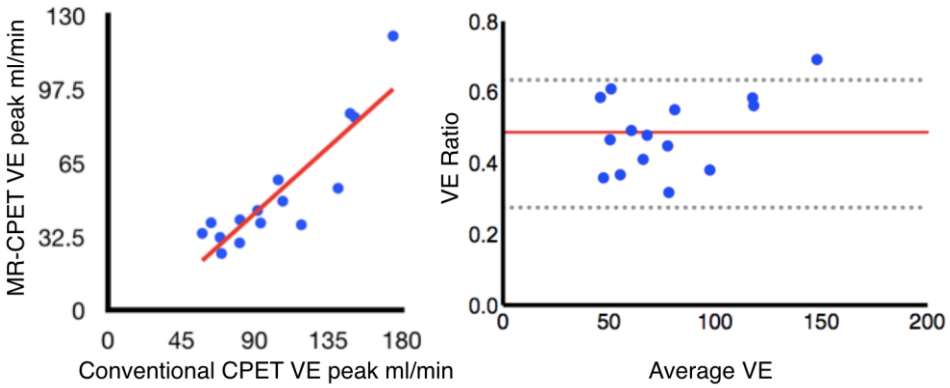

Figure 6.4 Scatter graph of peak VE measured during MR-CPET against conventional CPET. b) Ratio Bland-Altman analysis of peak VE as measured by conventional and MR-CPET. Ratio = VE / Conventional CPET. Red line = bias, dotted line = limits of agreement.

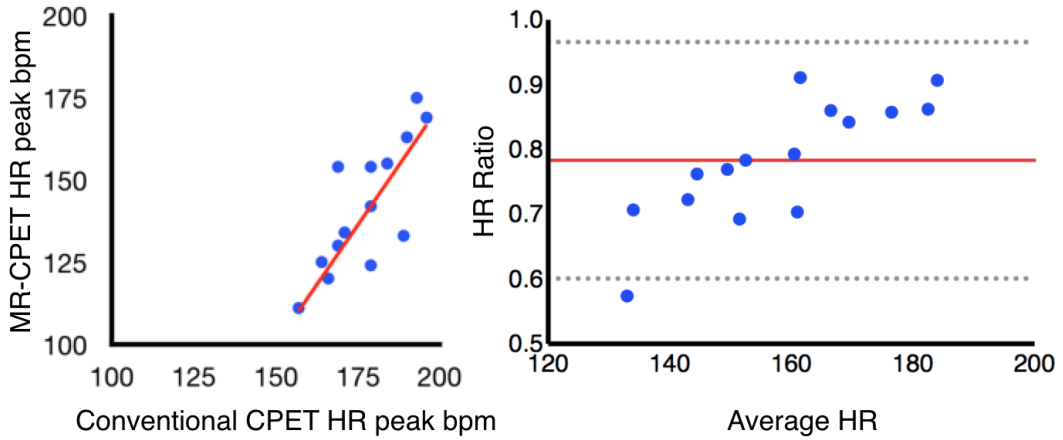

Figure 6.5 Scatter graph of peak HR measured during MR-CPET against conventional CPET. b) Ratio Bland-Altman analysis of peak HR as measured by conventional and MR-CPET. Ratio = HR / Conventional CPET. Red line = bias, dotted line = limits of agreement.

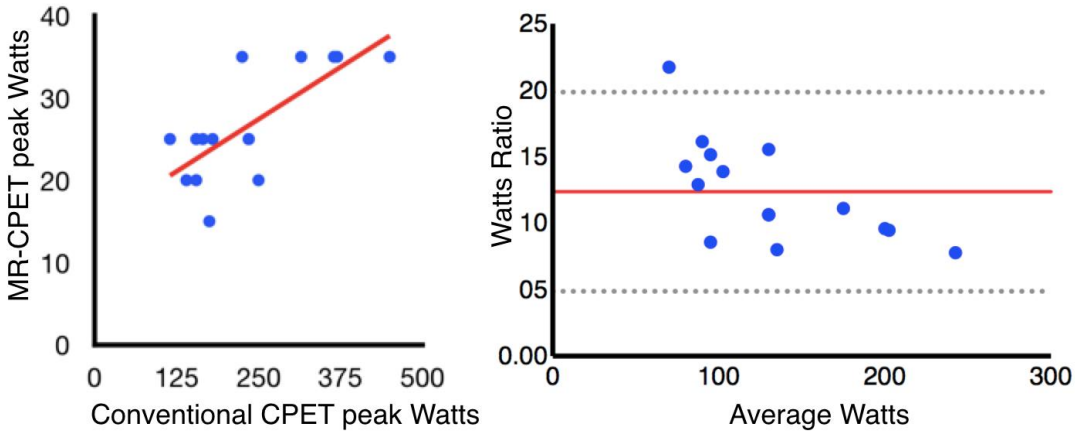

Figure 6.6 Scatter graph of peak Watts measured during MR-CPET against conventional CPET. b) Ratio Bland-Altman analysis of peak Watts as measured by conventional and MR-CPET. Ratio = Watts / Conventional CPET. Red line = bias, dotted line = limits of agreement.

Table 5 Established exercise metrics as measured with conventional and MR-CPET

	Conventional CPET	MR-CPET	*r*	p	Ratio bias
Peak VO_2 (l/min)	3.3±1.3	1.6 ±0.8	0.94	0	0.48 ±0.08
Peak VCO_2 (l/min)	3.6 ±1.5	1.6 ±0.9	0.87	0	0.45 ±0.10
VO_2 AT (l/min)	1.5 ±0.6	1.0 ±0.4	0.9	0	0.68± 0.13
Heart rate max (bpm)	176.9 ±11.7	139.0 ±22.4	0.76	0.001	0.78±0.09
V_E max (l/min)	103.5 ±36.2	51.5 ±26.5	0.88	0	0.58±0.18
Work (Watts)	235.33 ±98.5	25.7 ±5.9	0.66	0.007	0.12±0.04

6.6.4 MR-CPET findings

Values at rest and at peak VO_2 for VO_2, CO, SV, HR and a-vO_2 are shown in Table 5. The mean time to peak exercise was 4m 45s ± 1m 21s and the mean work rate achieved was 25.767 ± 5.9 Watts. The main findings were that VO_2, CO, HR and a-vO_2 significantly increased ($p<0.001$) during exercise, while across the whole population SV remained the same ($p=0.42$) (Figure 6.7). However, on multiple linear regression both increased HR ($b=0.76$, $p<0.001$) and SV ($b=0.67$, $p= 0.001$) contributed to the change in cardiac output. There was a large variation in peak VO_2 reflecting varying levels of fitness in the study population. Multiple linear regression demonstrated that both peak CO and a-vO_2 were independent predictors of peak VO_2 measured during both MR-CPET ($b=0.73$ and 0.38 respectively, $p<0.001$) and conventional CPET ($b=0.78$ and 0.28 respectively, $p<0.001$). Figure 6.8 shows VO_2, CO and a-vO_2 curves for one subject in the top quartile and one in the bottom quartile of peak VO_2. There was also moderate correlation between the amount of regular exercise performed and peak VO_2 ($r=0.73$ $p =0.002$), peak CO ($r=0.80$ $p<0.001$) and a trend for peak a-vO_2 ($r= 0.50$ $p= 0.058$).

Table 6 Values obtained during MR-CPET at rest and peak VO_2

	Resting	Peak	P Value
Heart Rate (bpm)	73.7 ±27.2	132.1 ±15.4	<0.001
Stroke Volume (ml/beat)	106.6 ±30.9	110.4 ±27.8	0.42
Cardiac Output (l/min)	7.6 ±4.7	14.4 ±1.7	<0.001
VO_2 (l/min)	0.3 ±0.8	1.6 ±0.8	<0.001
a-vO_2 mlO_2/ml blood	0.03 ±0.02	0.11 ±0.01	<0.001

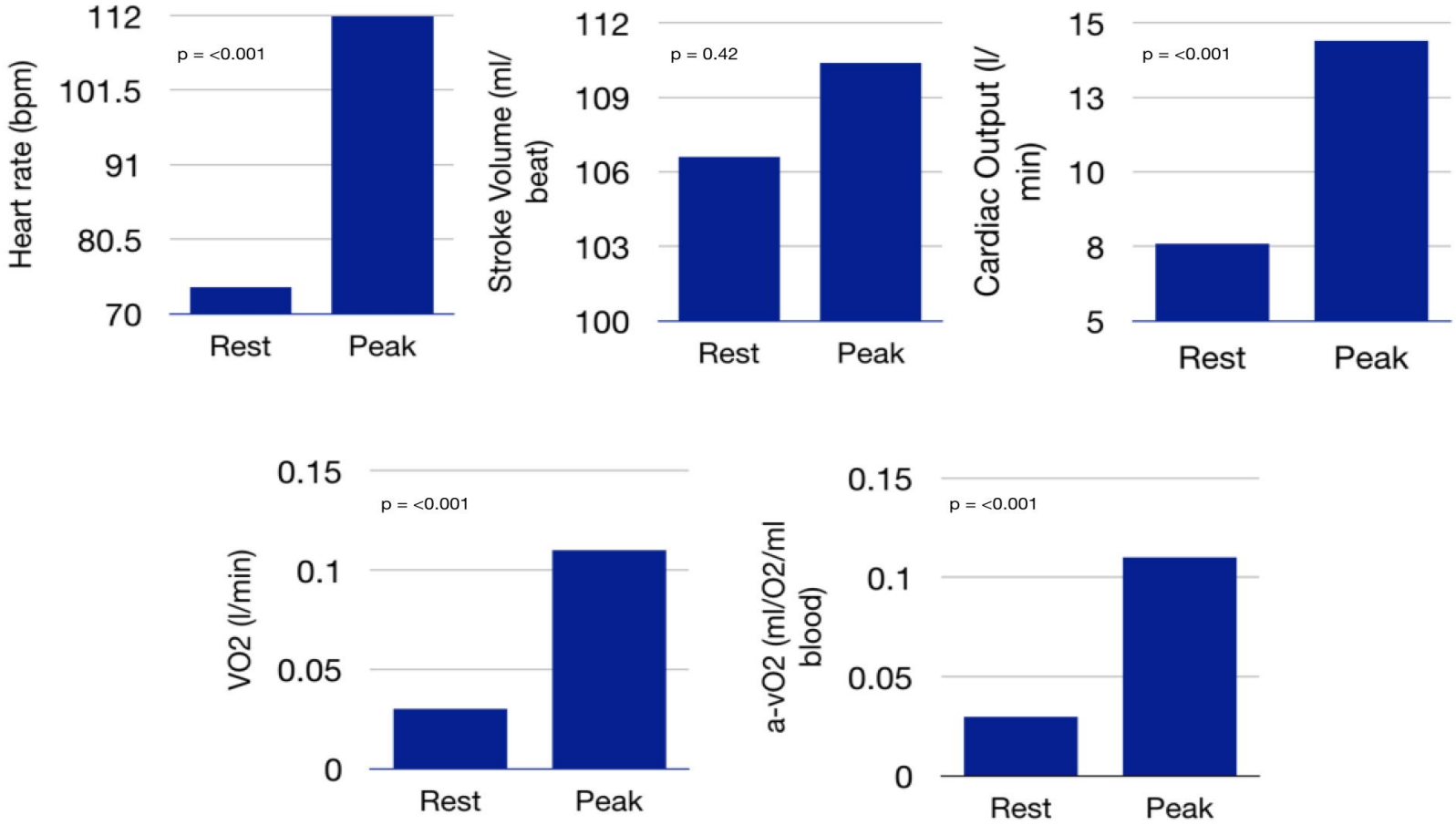

Figure 6.7 MR-CPET metrics at rest and peak exercise

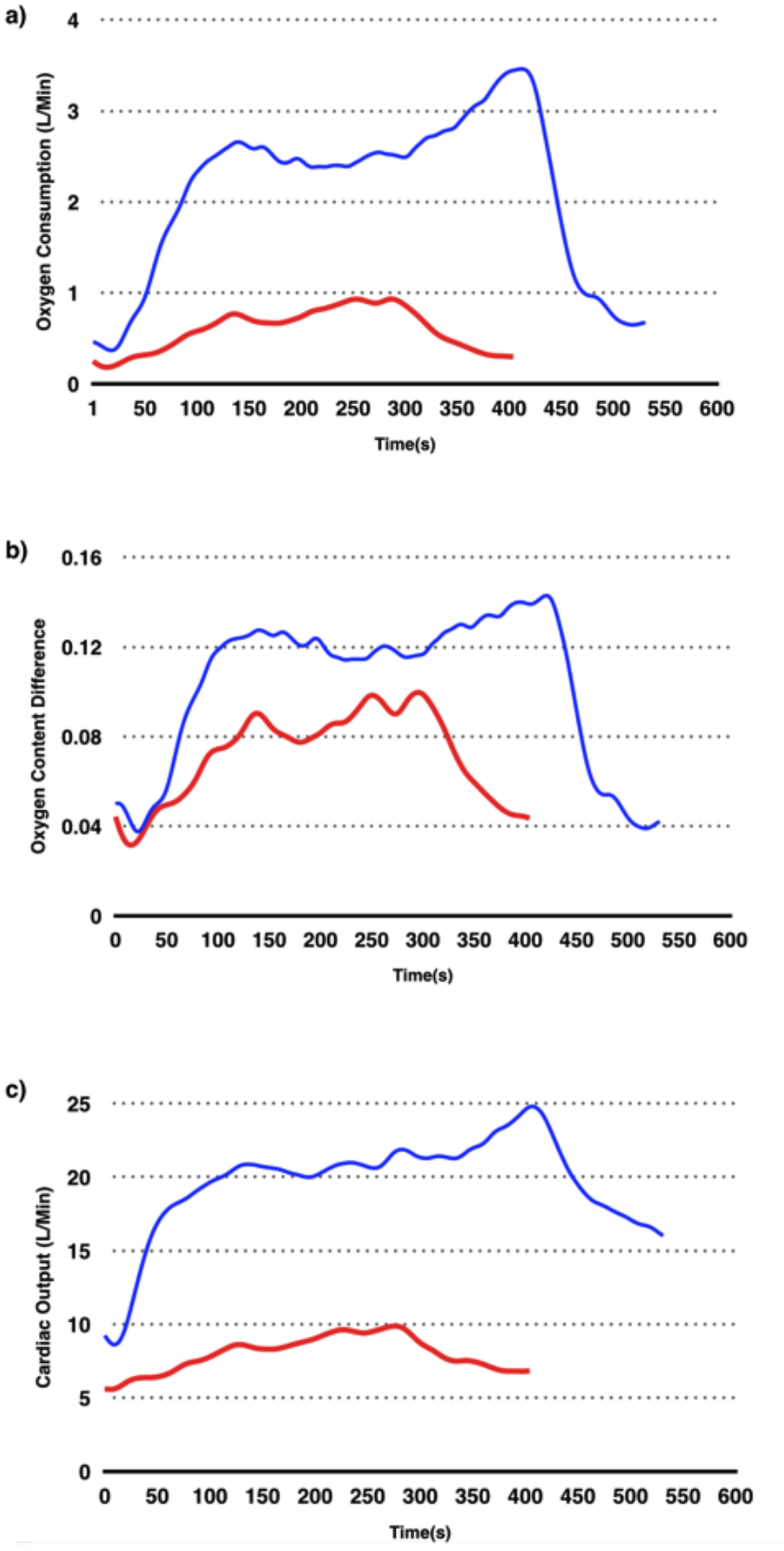

Figure 6.8 VO_2 a-vO_2 and CO curves from one subject in the top quartile of peak VO_2 (blue) and one subject in the bottom quartile (red)

6.7 Discussion

This study describes the first demonstration of MR-augmented cardiopulmonary exercise testing. Implementation of the technique described required modification of a commercial gas analyzer (ensuring MR compatibility) and a real-time PCMR sequence that allowed continuous assessment of CO. The main findings were: i) MR-CPET was feasible and well tolerated by subjects, ii) There was a good correlation between conventional CPET and MR-CPET measurement of established respiratory exercise metrics, and iii) Both peak CO and a-vO_2 measured during MR-CPET were independent predicators of peak VO_2.

In this study, we used a real-time PCMR technique that can be performed without cardiac gating or breath holding and was resistant to motion (162). Using this technique, we demonstrated that CO increased significantly during exercise, driven by both increased HR and SV. Interestingly, SV did not increase during exercise in population as a whole as has previously been seen in supine exercise(141). Instead, SV increased in fitter subjects and fell in less fit ones, explaining the CO relationship.

The strong correlation between standard metrics measured using conventional CPET (VO_2, VCO_2, HR, V_E) and using MR-CPET is an important finding that supports the further use of this technique. Peak VO_2 measurements acquired by MR-CPET using the up-down ergometer are sub-maximal. As discussed in chapter 2 maximal exercise testing is theoretically defined as a plateau in VO_2 despite increases in workload. Any test where this criterion is not achieved is considered sub-maximal. Although maximal testing is the gold standard in assessment of aerobic fitness in clinical practice most testing is terminated due to fatigue or musculoskeletal impairment before VO_2 plateaus. The maximal VO_2 achieved in these circumstances is correctly termed peak VO_2. To contextualize the potential clinical application of MR-CPET it is important to recognize that choice of conventional exercise test is pragmatic and determined by patient factors and the clinical question. The highest peak VO_2 values are typically measured with treadmill testing however for practical reasons including better stability, monitoring and control of workload cycle ergometry is preferred for clinical testing.

There are established precedents for the use of sub-maximal 'predictive' exercise testing in patient groups where maximal testing would be precluded CPET(163). The most well known sub-maximal exercise test is the modified Bruce treadmill protocol, designed to allow use in people with a lower functional capacity, it starts at a 'zero' stage (1.7mph and 0% gradient compared to a 1.7 mph at a 10% gradient in the original protocol(164)). Strong correlation has been reported between VO_{2max} predicted on submaximal testing and measured VO_{2max} both in health and disease(165). Sub-maximal exercise test data has an important prognostic role for example in adults with heart failure(166) and the Fontan circulation(167). Sub-maximal MR-CPET testing is therefore consistent with the spectrum of clinical exercise testing.

Simultaneous measurement of VO_2 and CO allowed calculation of a-vO_2, which is a proxy measure of tissue oxygen extraction (168).This is clinically relevant because (as described in chapter 1) both cardiac dysfunction and reduced peripheral tissue oxygen extraction are implicated in cardiac exercise intolerance. In this study, we were able to show that both peak CO and a-vO_2 were independent predictors of peak VO_2. This demonstrates that both increased cardiac function (CO) and tissue extraction (a-vO_2) are important components of 'fitness'. Biomarkers used to track exercise performance and recovery most commonly involve the measurement of proteins, electrolytes and metabolites in blood samples (169) but the range of emerging biomarkers in the field is broad including minimally invasive muscle biopsy and imaging biomarkers (170).The strong correlations between conventional and MR CPET suggest that MR-CPET has the potential to be a useful biomarker in cardiopulmonary disease.

In addition, we were able to show that (self-reported) exercise training resulted in increased VO_2 and CO, as well as a trend towards greater a-vO_2. Despite inherent limitations survey techniques are routinely used to assess physical activity levels (increasingly in conjunction with accelerometers) with acceptable reliability and validity (171). These findings suggest that MR-CPET may be able to assess the differential response to an intervention (for example exercise training). Thus MR-CPET may be suitable for more comprehensive assessment of baseline fitness (both

in disease and in healthy populations) as well as response to therapeutic interventions.

There are clearly significant practical challenges in implementing the MR-CPET approach described here that need to be addressed for it to be translated into a clinically useful technique. The MR scanner is an uncomfortable environment in which to perform exercise and this is particularly true when wearing a facemask. A contemporary meta-analysis suggests 1% to 2% of adult subjects experience claustrophobia when attempting MRI. The highest rates of scan termination for claustrophobia across all clinical MRI (including head and neck MRI) are for stress cardiac MRI (172). Claustrophobia is hypothesized to consist of two components, fear of constriction and fear of suffocation (173) MR-CPET clearly has several features that could exacerbate a claustrophobic reaction. In addition to the diameter of the scanner used (50cm) the subject's upper body was constrained by the body coil straps and lower limbs also restrained with Velcro straps. Although superior to potential alternatives the Hans Rudolf mask used is associated with claustrophobia when used in CPAP patients (174) and precludes the use of in-scanner entertainment systems that may aid success (175).

Based on the factors outlined above it would be reasonable to expect a high rate of failure due to claustrophobic reaction. Subjects did report slightly increased concern prior to, and discomfort during MR-CPET, compared to conventional CPET and one subject was unable to complete the MR-CPET due to claustrophobia. Nevertheless, the majority of subjects still rated MR-CPET within the clinically acceptable range, suggesting this technique would be feasible in patients. Factors that may have helped mitigate adverse reactions include a calm, relaxed scanning environment, clear explanation and demonstration of the equipment involved as well as written and verbal reassurance that the subject had full control over termination of testing.

One potential reason for lack of wider uptake of exercise MR (at the time of the study only 12 centres in the UK were maintaining the ergometer used here) is the comfort of commercially available ergometers. Following feedback from pilot MR-CPET testing additional padding was added to the leg support for all study

participants. Further improvements in patient experience may be achieved in the future by improved ergometer design along with the use of newer shorter length scanners.

Some subjects also found it difficult to master the up-down exercise technique on the MR-compatible ergometer, which may reduce the general applicability of MR-CPET in this form. It also raises the possibility that exercise performed within MR does not accurately reflect general exercise capacity (176). In fact, we did show that metrics such as peak VO_2 were significantly lower during MR-CPET. However, this is expected as only limited muscle groups are used during this type of exercise. Again, newer wider bore scanners allow the use of more familiar exercise techniques that could overcome the disadvantages described here. Additionally, the physiology of supine exercise is different from conventional upright exercise (141). Furthermore, there was excellent correlation between metrics measured conventionally and during MR-CPET. This is consistent with previous studies that showed good correlation but lower peak work rate and VO_2 assessed during cycle than treadmill testing(177) (178). As described in the literature review some groups have used MRI compatible treadmills adjacent to the MRI table in the context of cardiac stress MRI. A fundamental disadvantage to this interrupted approach is that exercise and imaging are not simultaneous (126). In a clinical setting post exercise imaging may have significantly reduced sensitivity and specificity with small differences in timing having a major impact on measurement of left ventricular function.

6.7.1 Limitations

The main limitation of this study was that supine exercise on an MR compatible ergometer is different to conventional upright exercise. This means that metrics are not directly comparable, although the good correlation suggests they do reflect the same physiology.

Successful exercise testing is dependent on the subject's understanding and motivation. All of the participants in this study worked in health or health related fields and as a group reported undertaking significantly more exercise than the UK average(179). The acceptability and successful performance of MR-CPET found

here may not be reflected when applied to a wider population. Another limitation from a clinical point of view is the lack of a continuous ECG. This is an ongoing problem with all MR exercise stress protocols and needs to be addressed before MR-CPET could be used clinically in ischaemic and arrhythmogenic patients.

A major challenge presented by this technique is how to manage the very large flow datasets generated (containing as many as 24000 frames). Although the process of image analysis is semi-automated (as discussed in chapter 5) visual inspection and manual correction is still required and this may take several hours. This is clearly not appropriate for use in a clinical setting and requires further improvement. The ergometer used in this work is heavy and could in the case of obese adults and adolescents exceed the recommended weight limit of the MRI table. A wide range of alternative commercial ergometers with more acceptable dimensions are however available (140,180,181) and could be used for MR-CPET.

6.7.2 Conclusion

This study demonstrates that MR-CPET using modified respiratory analysis equipment and real-time PCMR is possible and well tolerated in healthy adults. Using the technique it was possible to demonstrate the contribution of CO and tissue oxygen extraction to overall oxygen uptake. The results of this study support the ongoing use of this approach in studying exercise limitation.

Chapter 7 Application of MR-CPET in Healthy Children and Children with Right Heart Disease

7.1 Introduction

As described in the introduction/motivation to this work whilst highly prognostic conventional approaches to assessing exercise limitation do not comprehensively assess the contribution of the different factors involved. The MR-CPET approach is particularly appealing for use in children because invasive CPET is not possible in the majority of this group. Building on the experience gained in healthy adults this study implements MR-CPET in healthy children as well as children with right heart disease: repaired Tetralogy of Fallot and Pulmonary Arterial Hypertension.

The importance of the right ventricle in exercise is increasingly recognised(182). In healthy populations at rest the right ventricle performs less work to generate the same SV as the left ventricle because of the relatively lower afterload provided by the pulmonary vasculature. During exercise the relative increase in RV afterload may be proportionately greater than that to LV afterload resulting in greater RV wall stress. CMR is the established reference standard for imaging of the right ventricle in children, providing accurate and reproducible quantitative assessment(103). The complex geometry of the right ventricle makes CMR particularly useful in its non-invasive assessment as it does not rely on the geometric assumptions used in echocardiography (in addition to benefits of avoiding ionizing radiation and the risks of cardiac catheterization already stated, that are particularly pertinent to children). CMR has a proven role in assessing both clinical status and prognosis in paediatric pulmonary hypertension (183). Similarly CMR is central in determining the optimal timing of pulmonary valve replacement in patients with repaired ToF(184).

Conventional exercise testing also has an established role in children with PH and children with repaired ToF. European paediatric pulmonary vascular disease guidelines recommend serial 6MWT and from an appropriate age CPET in children with pulmonary hypertension(185). CPET is recommended to objectively assess exercise capacity as well as to monitor changes in exercise tolerance and response to treatment and to gauge prognosis. Relevant to the development of MR-CPET it is

only in more advanced disease with 6MWT distances of less than 300m that 6MWT distance correlates with peak VO_2 highlighting the potential role of more discriminative tests for use earlier in the course of disease(186). As described in the introductory chapter the evolving understanding of the mechanisms of treatment used in pulmonary hypertension also supports the need for new approaches to assessment. For example despite improved pulmonary haemodynamics impaired systemic oxygen extraction has been identified using invasive CPET in adults treated with Ambrisentan(187). The cause of this is not clear and the invasive methodology cannot be used to identify if the same findings are present in children.

Overall exercise tolerance in children and adolescents with repaired ToF is expected to be similar to healthy children, however later in life there is a decline in exercise capacity with reduced peak VO_2 and chronotropic insufficiency(56). In children and adolescents with repaired ToF self and parent reported quality of life is positively correlated with exercise capacity(188). This is important as other metrics used as markers of severity of disease such as pulmonary regurgitant fraction and RVEDV, although clearly clinically significant, do not demonstrate the same relationship(188). More discriminating tests may also be useful in understanding morbidity in this patient group. Early detection of abnormal RV physiology using pharmacological stress MRI has been proposed by a number of groups. Dobutamine stress MRI has been demonstrated to unmask diastolic dysfunction in young people with repaired ToF, differentiating patients with no dysfunction at rest and showing a strong correlation with exercise impairment (189). Dobutamine stress has also been used to demonstrate reduced contractile reserve (190,191) in these patients.

Studying these two patient groups has potential to provide insights into the physiology of a pressure (PAH) versus volume (ToF) loaded RV in exercise as well as into the emerging understanding of systemic causes of exercise intolerance in these patients. The hypothesis for this study was that MR-CPET would be feasible in children and able to explore patterns in cardiac output oxygen consumption and tissue oxygen extraction in response to exercise in children two distinct categories of right heart disease. Based on understanding of the systemic nature of pulmonary hypertension and of the physiologic response to exercise in repaired ToF it was

hypothesised that tissue oxygen extraction would be a limiting factor in PAH and reduced CO in ToF. Working towards a more integrated approach for clinical testing, this study also includes volumetric measurement at rest and peak exercise and measurement of the septal curvature ratio at rest and peak exercise. MR measurement of septal curvature ratio has been demonstrated to provide an accurate estimate of mean PA pressure as well as an ability to reflect acute changes in pulmonary haemodynamics(192).

7.2 Aims

The aims of this study were 1) to test the feasibility and tolerability of MR-CPET in healthy children and children with cardiopulmonary disease 2) to assess the differences in VO_2, CO and a-vO_2 between healthy children and children with right heart disease (PAH and ToF) 3) to assess volumetric and septal dynamic changes between rest and peak exercise.

7.3 Study Population

Thirty children divided into 3 groups were recruited into the study between February 2015 and February 2016. Group 1 (n=10; 6 female) were healthy paediatric controls recruited specifically for this study with no suspected or previous past medical history. Group 2 (n=10; 7 female) were children with a diagnosis of stable PAH with no recent changes in medication. Group 3 (n=10; 4 female) children had a primary diagnosis of ToF repaired in infancy with current pulmonary regurgitation.

General exclusion criteria were i) age <7 years (primarily due to the height requirement of the ergometer but also the relatively challenging protocol) ii) MR incompatible implant, iii) physical or intellectual disability that would preclude undertaking ergometry and iv) exercise induced collapse in the preceding 6 months v) previously documented desaturation on exercise, vi) non-trivial tricuspid regurgitation. Specific group 2 (PAH) exclusion criteria were: i) WHO functional class IV and ii) continuous intravenous therapy.

Control group subjects were recruited through local advertising and were screened to exclude volunteers with any medical co-morbidity, current medical treatment or

relevant family history. PAH patients were recruited via the national paediatric Pulmonary Hypertension service at Great Ormond Street Hospital. ToF group patients were recruited via general paediatric cardiology clinics also at Great Ormond Street Hospital.

7.4 Methods

7.4.1 Six Minute Walk Test

The methodology for this study was as described in the methods chapter with the addition that all participants completed a six-minute walk test following the American Thoracic Society guidelines(193), supervised by a single operator. The Six-minute walk test was included as a measure of functional status.

7.4.2 Exercise Protocol

The exercise protocol consisted of a 1-minute rest period followed by 2 minutes of unloaded exercise (Figure 7.1) and then a stepped workload protocol (increase of 2 Watts/minute for the first five minutes and subsequently 3 Watts/minute until exhaustion).

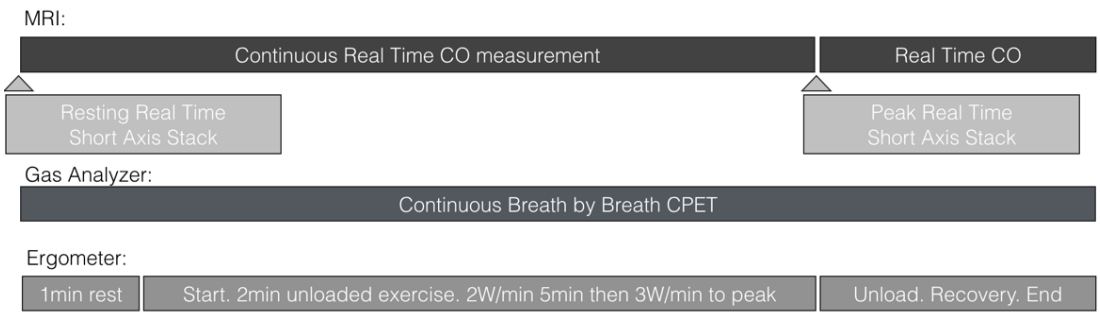

Figure 7.1 Paediatric Exercise Protocol

Ergometry was undertaken in hyperbolic mode and participants were verbally and visually encouraged to maintain revolutions per minute between 40 and 70, ensuring workload was independent of cadence. During the exercise protocol CO and VO_2 were continuously measured. As there was no prior experience of using the 'up-down' ergometer in paediatric populations this exercise protocol was based on pilot

testing in a small group of healthy children not included in the final study. Again the design was based on published data on the optimal duration for conventional exercise testing. At the point of exhaustion, resistance was reduced to zero and the subject was asked to exercise as hard as possible in order to maintain a high heart rate and prolong the exercise state. During this period, ventricular volumes (peak exercise) were assessed again (acquisition approximately 30 seconds).

7.4.3 Image analysis

PCMR exercise flow data processing and integration with VO_2 was performed as described in the general methods chapter. As the segmentation of flow data was only semi-automated requiring visual inspection and instances where the non-rigid registration algorithm failed required manual correction inter and intra observer variability was tested. Twenty cases were fully re-segmented both by the primary researcher and by a researcher experienced in segmenting conventional MRI data sets.

Ventricular volumetric assessment was performed using in-house plug-ins for the open-source software OsiriX (OsiriX Foundation, Geneva, Switzerland) End systolic and diastolic frames were identified by visual assessment. Segmentation was performed by tracing the endocardial border and excluding papillary muscles coarse trabeculae from the blood pool. Left ventricular (LV) and right ventricular (RV) end diastolic volume (EDV) and end systolic volume (ESV) were calculated using the slice summation method.

The stroke volume (SV) was the difference between these two values and ejection fraction (EF) was SV/EDV. As subjects with tricuspid regurgitation were excluded, it was possible to assess pulmonary regurgitation fraction (PRF) indirectly as: [(RVSV-LVSV)/RVSV)x100].

Septal curvature was measured from the short axis images at the mid-papillary level(192). As previously described raw curvature was taken as the inverse of the radius of the circle that was circumscribed by 3 points placed in the septum and propagated to all frames. The raw curvature was normalized using the lateral wall

curvature and the minimum septal curvature ratio was taken as the lowest or most negative value.

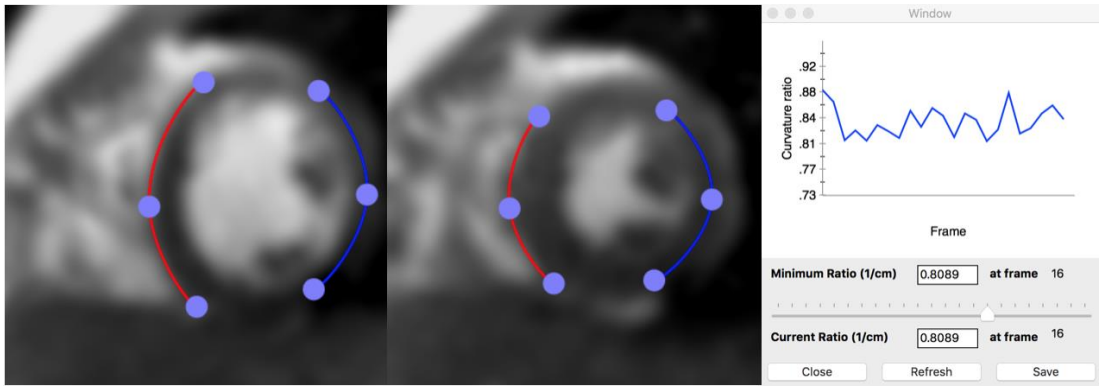

Figure 7.2 Calculation of septal curvature ratio: a circle circumscribed by 3 points placed in the septum (red line) and propagated throughout the cardiac cycle, normalized to the lateral wall (blue line). Results displayed for a normal subject.

7.5 Statistical Analysis

All statistical analysis was performed using StataSE 13.0 (StataCorp, College Station, USA). Data were examined for normality using the Shapiro-Wilk normality test and non-normally distributed data was transformed using a log transform to ensure normal distribution prior to analysis. Descriptive statistics were expressed as mean (±standard deviation) or geometric mean (±geometric standard deviation) where data was log transformed for skewness. Between group differences were assessed using one-way analysis of variance (ANOVA) with post-hoc Bonferroni corrected pairwise comparisons. Differences in absolute metrics with exercise in different groups were assessed using repeated measures ANOVA with main effects of disease type and exercise and an interaction term representing disease multiplied by exercise. Greenhouse-Geisser epsilon for all the repeated measures models was calculated to assess sphericity and in all cases it equaled 1. Post-hoc pairwise comparisons were performed for simple main effects with Bonferroni correction and these values are reported in the results when comparing groups. Inter and intra observer variability was tested using intraclass correlation coefficients. Likert scale data was compared using the Kruskal Wallis test and gender distribution compared using Fisher's exact test. A p-value <0.05 was considered statistically significant.

7.6 Results

7.6.1 Demographics

The mean age of the overall study population was 12.45±2.58 years with ToF patients being slightly older (p=0.03) than the PAH group (Table 7). There were no significant group differences in height, weight or body surface area (Table 7).

Table 7 Demographic Data.

Variable	Control	PAH	ToF	*P* Value
Male: female	4:6	3:7	6:4	0.53
Age, years	13±3	11±2.2	14±1.8	0.033
Height, cm*†	154±1.1	147±1.1	159±1.1	0.066
Weight, kg*	47±1.5	41±1.3	50±1.4	0.432
Body surface area, m^2†	1.5±0.38	1.3±0.17	1.5±0.29	0.145

PAH indicates pulmonary arterial hypertension; and ToF, tetralogy of Fallot.
* Log transformed (geometric mean).
† *W* test applied.

All PAH patients had idiopathic disease with 6/10 patients in functional class I and 4/10 patients in class II. Eight subjects had undergone right heart catheterization in the 2 years preceding the study (median time 9.1 months, range 6.4-17.9 months). The average mean pulmonary arterial pressure was 37.2±12.1 mmHg and pulmonary vascular resistance index was 9.6±5.0 $WU.m^2$. All patients were treated with either targeted mono or dual therapy; Bosentan: 9/10, Sildenafil: 8/10, Tadalafil: 2/10, Amlodipine: 6/10, Ambrisentan: 1/10 and inhaled Iloprost: 2/10**.** In the repaired ToF patients, 9/10 were functional class 1 and 1/10 functional class II. The median age of primary surgery was 0.78 years (range 0.4-1.7 years) and 7/10 had transannular patch placement during their primary repair. Secondary surgical or catheter right ventricular outflow tract interventions had not been performed in any patients.

There were no significant (p=0.71) differences in mean six-minute walk test distances between the control (444±1.1m), PAH (429±1.2) or ToF groups (449±1.1).

7.6.2 Feasibility and Acceptability

All recruited subjects successfully mastered the exercise technique and safely completed the MR-CPET protocol with no premature suspension of exercise. Cardiac output and VO_2 data was collected in all subjects allowing calculation of a-vO_2 in all cases.

All subjects exercised to exhaustion achieving a peak respiratory exchange ratio (RER = VCO_2/VO_2) ≥1.1. Healthy children achieved approximately 72% predicted heart rate, which was significantly higher than the PAH (62%, $p<0.001$) and ToF groups (56%, $p<0.001$). There were trends towards longer exercise duration and greater workload achieved in the control group compared to the PAH and ToF groups (Table 8).

Table 8 Exercise Capacity and Acceptability Data.

Variable	Control	PAH	ToF	*P* Value
Six-min walk test distance m*	452±1.1	432±1.2	449±1.1	0.718
MR-CPET duration min†	8.9±3	7.3±1.6	7±2.2	0.078
Peak work W*†	12.0±2	8.7±1.5	7.7±1.9	0.145
Peak work METS*	4.8±1.4	3.6±1.3	3.8±1.3	0.079
Percent predicted HR	72±8.2	62±9.6	56±8.1	<0.001
RER†	1.7±0.43	1.5±0.28	1.4±0.15	0.011
Satisfaction	4.4±0.7	4.3±0.48	4.6±0.52	0.45
Comfort*	3.5±1.3	3.5±1.3	3.8±1.2	0.82
Helplessness*	3.7±1.4	4±1.2	4.4±1.2	0.35

HR indicates heart rate; MR-CPET, magnetic resonance–augmented cardiopulmonary exercise testing; PAH, pulmonary arterial hypertension; RER, respiratory exchange ratio; and ToF, tetralogy of Fallot.
* Log transformed (geometric mean).
† *W* test applied.

There were no recorded complications (including documented arrhythmia) associated with exercise. All subjects reported clinically acceptable levels of satisfaction, comfort, worry and helplessness (Table 8, Figure 7.3). There were no significant differences in these measures between groups ($p>0.3$).

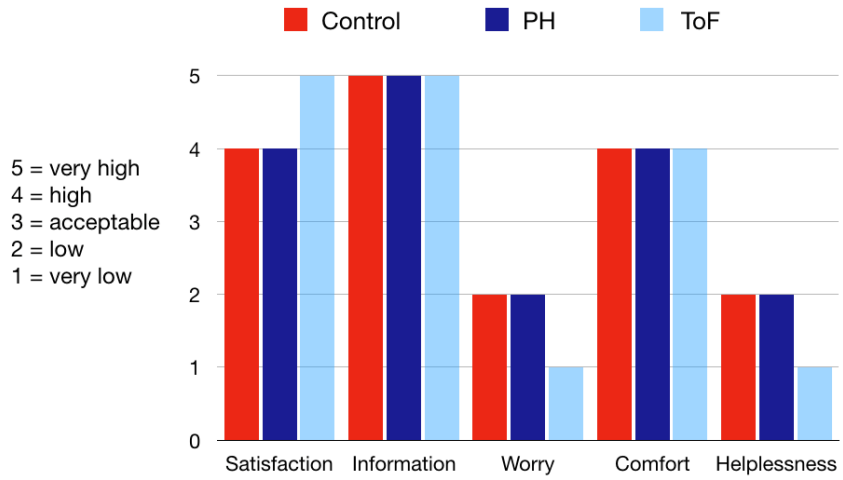

Figure 7.3 Acceptability survey responses by group (no significant difference in measures between groups)

7.6.3 MR CPET metrics – Rest and Exercise

At rest, there was no significant difference in VO_2 between the groups (Figure 7.4,Table 9). At peak exercise VO_2 increased 4.1±1.3x in controls, which was significantly greater than the increase in ToF (3.2±1.2x, p=0.04) and PAH (2.9±1.3x, p=0.01) patients. These differences resulted in peak VO_2 being lower in the PAH group (12.6±1.31 ml/kg/min, p=0.01) and trending towards lower in the ToF group (13.5±1.29 ml/kg/min, p=0.06) compared to controls (16.7±1.37 ml/kg/min). Resting CO was significantly (p<0.001) lower in ToF patients compared to controls and PAH patients (Figure 7.4,Table 9). In PAH patients augmentation of CO was non-significantly lower (1.3±1.3x) than in controls (1.6±1.3x, p=0.174) and peak CO only trended (p=0.1) towards being lower (Table 9). Augmentation of CO was greater in ToF patients (1.8±1.3x) than controls, but did not reach significance (p=0.217). Due to the lower baseline CO, peak CO was still significantly lower in ToF patients (5.3±1.2 vs. 6.6±1.2, p=0.003).

The ToF group had significantly higher a-vO_2 (4.7±1.2 mlO_2/100ml) at rest compared to the PAH (3.0±0.34 mlO_2/100ml, p=0.001) and control groups (3.1±0.76 mlO_2/100ml, p=0.003). There was no significant difference in a-vO_2 augmentation between controls (2.7±0.5x) and PAH patients (2.3±0.6x, p=0.18). Nevertheless, peak a-vO_2 was lower in the PAH patients (6.9±1.3 mlO_2/100ml vs. 8.4±1.4

mlO_2/100ml, p=0.005). Conversely, a-vO_2 augmentation was significantly lower in ToF patients (1.9±0.3x, p=0.001) compared to controls. However, due to the higher baseline value there was no significant difference (p=0.57) in peak a-vO_2 (Table 9).

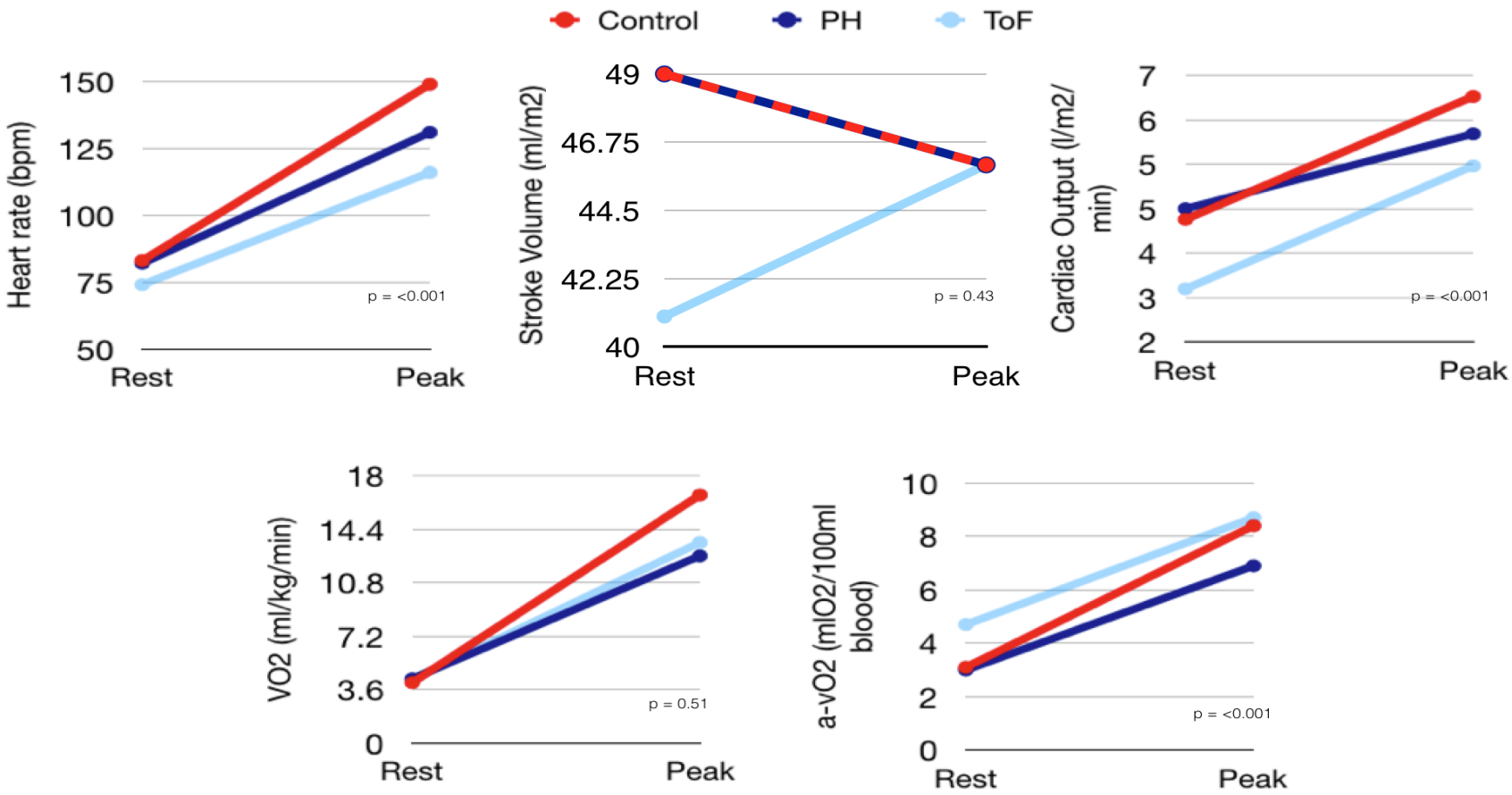

Figure 7.4 Changes in mean MR-CPET metrics between rest and peak exercise (p values for disease effect)

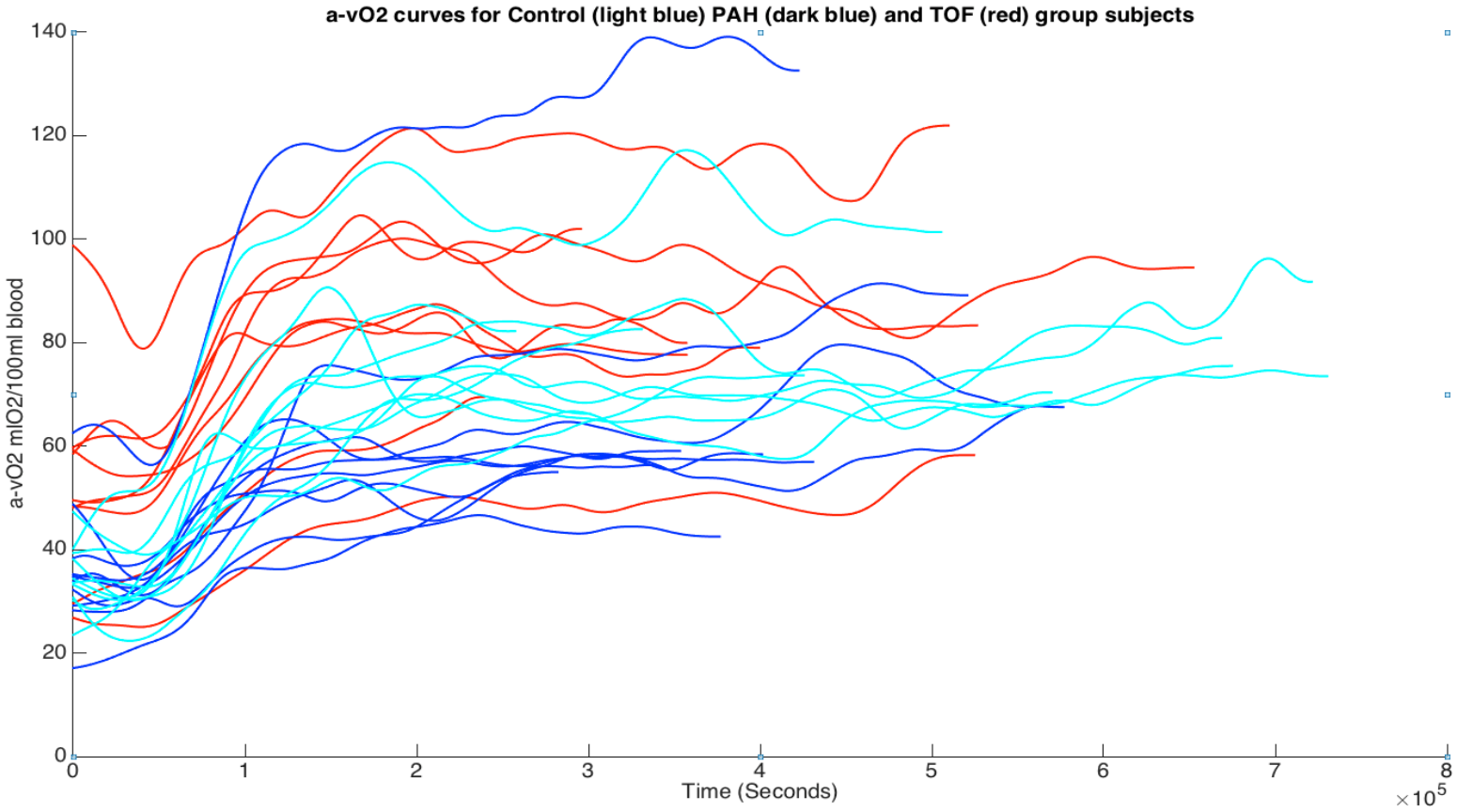

Figure 7.5 Combined a-vO_2 curves for all participants

Table 9 MR-CPET Derived Measures

Variable	Control		PAH		ToF		*P* Value		
	Rest	Peak	Rest	Peak	Rest	Peak	Disease Effect	Time Effect	Disease–Time Interaction
HR, bpm	83±17	149±18*	82±9.3	131±20*	74±12	116±17*	<0.001	<0.001	<0.001
SV, ml/m^2	49±11	46±8.2	49±5.9	46±6.3	41±8.4	46±5.4	0.43	0.75	<0.001
CO, l/m^2/min†	4.3±1.2	6.6±1.2*	4.5±1.1	5.9±1.1*	3±1.2	5.3±1.2*	<0.001	<0.001	0.0016
VO_2, ml/kg/min†	4.06±1.35	16.7±1.37*	4.32±1.18	12.6±1.31*	4.24±1.17	13.5±1.29*	0.51	<0.001	0.011
a-vO_2, mlO_2/100 mL blood	3.1±0.76	8.4±1.4*	3±0.34	6.9±1.3*	4.7±1.2	8.7±1.5*	<0.001	<0.001	0.013

a-vO_2 indicates arteriovenous oxygen content gradient; CO, cardiac output; HR, heart rate; SV, stroke volume; ToF, tetralogy of Fallot; and VO_2, oxygen uptake. *Significant difference rest to peak.

Table 10 Conventional MR Measures

Variable	Control		PAH		ToF		*P* Value		
	Rest	Peak	Rest	Peak	Rest	Peak	Disease Effect	Time Effect	Disease–Time Interaction
RVEDV, mL/m²	77±16	68±13*	83±9.2	71±9.1*	95±16	86±14*	<0.001	<0.001	0.6
RVESV, mL/m²†	29±1.3	20±1.6*	34±1.3	28±1.3*	39±1.3	30±1.5*	0.041	<0.001	0.44
RVSV, mL/m²	47±11	45±9.5	48±6.7	46±6.9	55±7.8	54±7.1	0.045	0.095	0.9
RVEF, %	62±5	67±12	58±7.8	66±9.8*	58±6	63±8.6	0.59	<0.001	0.67
LVEDV, mL/m²	67±13	59±9.6*	68±7.4	61±8.1*	63±5.2	64±6.2	0.87	<0.001	0.011
LVESV, mL/m²†	18±1.3	11±2*	20±1.2	14±1.4*	19±1.3	17±1.3	0.18	<0.001	0.14
LVSV, mL/m²	48±9.9	47±7.2	48±6.7	47±7	43±6.1	46±5.5	0.55	0.59	0.024
LVEF, %	72±5.5	80±11*	70±4.4	77±7.3*	68±7.1	73±5.9	0.17	<0.001	0.54
PRF, %	0.48±1.0	0.29±0.89	1.11±1.47	0.14±0.43	30.24±8.03	16.3±5.79*	<0.001	<0.001	<0.001
Septal curvature ratio†	0.84±0.05	0.82±0.08	0.15±0.42	-0.44±0.53	0.85±0.13	0.86±0.071	<0.001	<0.001	<0.001

EDV indicates end-diastolic volume; EF, ejection fraction; ESV, end-systolic volume; LV, left ventricle; mPAP, estimated mean pulmonary arterial pressure; PAH, pulmonary arterial hypertension; PRF, pulmonary regurgitant fraction; RV, right ventricle; SV, stroke volume; and ToF, tetralogy of Fallot.* Significant difference rest to peak.† Log transformed (geometric mean).

7.6.4 Ventricular volumes – Rest and Exercise

Resting RVEDV, RVESV and RVSV were higher in the ToF group compared to controls (p<0.03). In all groups, RVEDV and RVESV decreased significantly by a similar amount with exercise (

Table 13,Figure 7.6). RVEF increased during exercise in all groups but only reached significance in the PAH group (p=0.01).

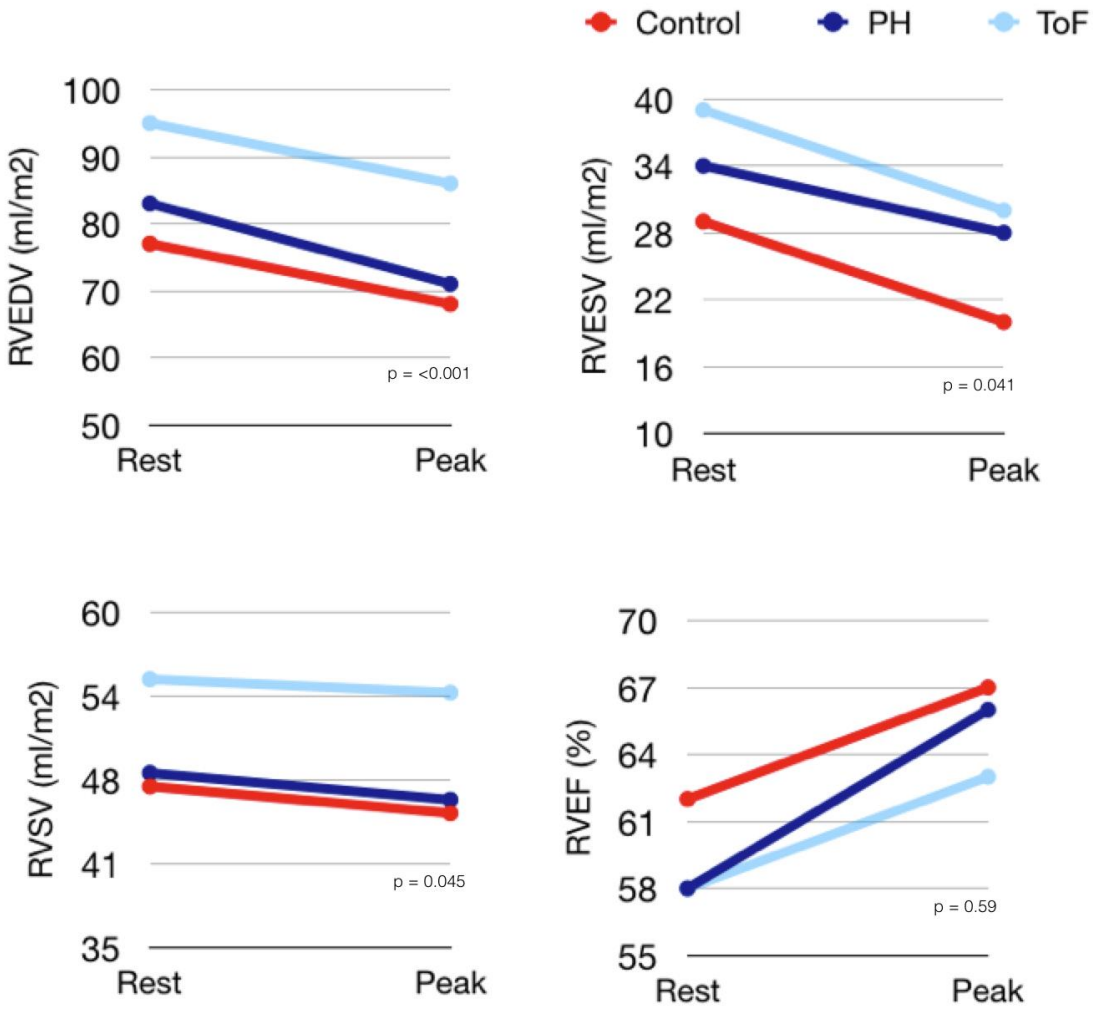

Figure 7.6 Conventional MRI RV metrics at rest and peak exercise (p values for disease effect)

At peak exercise, LVEDV fell significantly in controls (p=0.004) and PAH patients (p=0.006) but not in ToF patients. LVESV also fell at peak exercise but only reached

significance in the control (p=0.002) and PAH groups (p=0.013). LVSV only increased significantly during exercise in the ToF group (p=0.035). In all groups, LVEF was significantly higher at peak exercise.

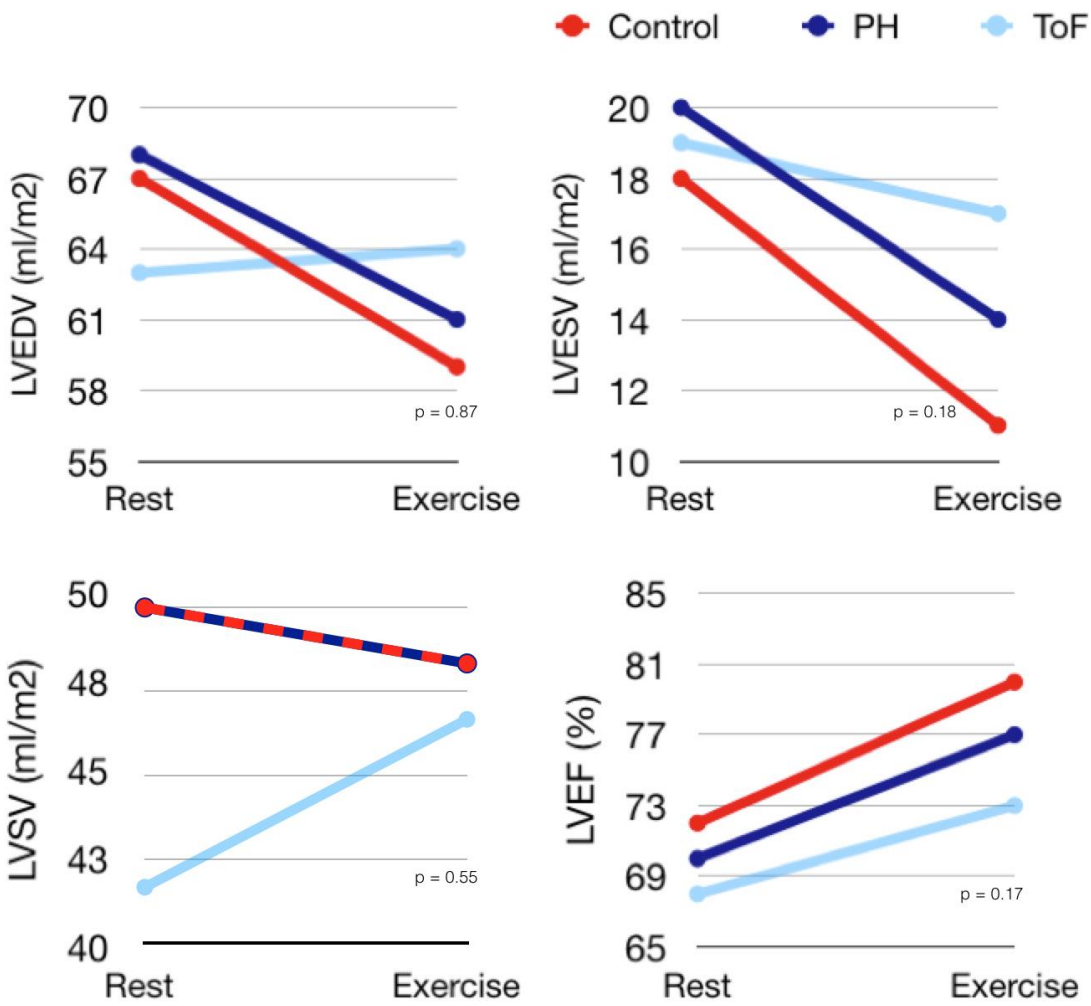

Figure 7.7 Conventional MRI LV metrics at rest and peak exercise (p values for disease effect)

7.6.5 Other metrics – Rest and Exercise

Non-trivial PR was only present in the ToF group and at peak exercise. PRF fell significantly in this group (p<0.001). Abnormal septal curvature was only present at rest in the PAH group (Table 9) with significant worsening during exercise (p<0.001). This corresponds to an estimated mean PA pressure (mPAP) of 30±0.4mmHg at rest, rising to 55±0.53mmHg at peak exercise.

7.6.6 Intra and Inter-observer reliability

As expected there was good intraobserver reliability in real time CO data (ICC 0.995, 95% CI 0.98–0.999 p<0.001). There was also good interobserver reliability (ICC 0.996, 95% CI 0.983–0.999 p<0.001).

7.7 Discussion

This study demonstrates MR-CPET is feasible and well tolerated in healthy children and children with cardiovascular disease. The main findings of this study are i) MR-CPET is safe in healthy children and those with right heart disease, ii) peak VO_2 is reduced in paediatric PAH and ToF patients and iii) PAH and ToF patients have different peak values and patterns of augmentation of CO and a-vO_2 compared to controls.

7.7.1 MR CPET findings

In this study, we recruited relatively well patients in whom there was no significant difference in 6MWT distance compared to controls. Nevertheless, PAH patients had reduced peak VO_2 and ToF patients had a trend towards lower peak VO_2. This is in keeping with previous studies in relatively well patients(53,194) and demonstrates the sensitivity of conventional CPET for assessing mild exercise intolerance.

Using MR-CPET, we were also able to demonstrate significant differences between the groups that were not apparent based on VO_2 alone. For example, PAH patients had a slightly blunted CO response to exercise and a trend towards lower peak CO. On the other hand, ToF patients had reduced resting and peak CO despite a slightly amplified CO response to exercise. The findings in the PAH patients were not surprising, but the findings in ToF group were unexpected and therefore warrant further explanation. Conventionally CO is believed to be preserved in ToF patients until late in the disease. Therefore the findings of this study may simply be an artefact of non-representative sampling. There are some CMR studies however that suggest CO is lower in paediatric ToF patients in comparison to healthy children (assessed in a separate study but by the same group)(195,196). These studies would appear to strengthen the validity of the resting findings in this study. Studies of a

larger patient population would be required to corroborate this further. The slightly better augmentation of CO in ToF patients is the result of increased effective RVSV due to a fall in PR (197). However, peak CO is still lower in ToF patients (due to the lower baseline value) and this could have important consequences for exercise tolerance. Right ventricular dysfunction as a driver of adverse biventricular interaction is increasingly recognised (198)and is a potential explanation for the reduced resting and peak CO seen in this study. Left ventricular systolic dysfunction is observed in around 20% of adults with repaired ToF (199) and has also been shown in asymptomatic children and adults with repaired ToF (200). The mechanisms behind adverse ventricular-ventricular interactions remain incompletely understood. Tissue phase mapping has recently been used to demonstrate abnormalities of LV mechanics in young adults with repaired ToF preserved global LV function and could be integrated into a future study.

MR-CPET data also allows evaluation of differences in tissue oxygen extraction as assessed by a-vO_2. The results of this study demonstrate a blunted response to exercise in PAH patients, resulting in a lower peak tissue oxygen extraction. Similar findings have been demonstrated in adults with PAH using iCPET(201), but the underlying cause is unclear. Biopsy studies have demonstrated skeletal muscle abnormalities in animal and human models of PAH including reduced capillary density(202), changes in ratio of muscle fiber type(203) and alterations in mitochondrial function(204). Such changes could be the cause of reduced peak tissue oxygen extraction in these patients. Tissue oxygen extraction could also be affected by the vasodilator therapy, which was universal in the PAH group. Possible mechanisms for this include intramuscular shunting and direct effects on muscle/mitochondrial physiology. Therefore, it would by useful to evaluate tissue oxygen extraction on a vasodilator naïve population in a future study.

Children with repaired ToF also had abnormal patterns of tissue oxygen extraction. The higher resting a-vO_2 in ToF patients may simply be due to mathematical coupling between a CO and VO_2, although it may have physiological relevance. The ToF patients also had a significantly blunted increase in a-vO_2, although they

reached a similar peak to controls. Further investigation is required to determine if and how these abnormalities impact on exercise tolerance.

The results of this study demonstrate the potential of MR-CPET in allowing incremental improvement in understanding the mechanism of exercise dysfunction. Specifically, it provides insight not available through the independent measurement of CO and VO_2. Similar data is also available using iCPET, which has the added benefit of providing simultaneous assessment of pulmonary artery pressure. This is pertinent in PAH patients because exercise induced increase in pulmonary artery pressure may be a useful clinical biomarker(205). Unfortunately as discussed in chapter 2 performing iCPET is challenging in all patient groups and especially in children, as general anesthesia is usually required to perform cardiac catheterization. Consequently, MR-CPET may be useful as a substitute in populations where an invasive approach is not appropriate.

7.7.2 Additional exercise MRI findings

There is limited published experience of exercise cardiac MRI volumetric assessment in children (either in health or disease). In addition to the data specific to MR-CPET, the methodology described here allows investigation of changes in ventricular function between rest and exercise and therefore provides new insight.

Most studies in adults undergoing exercise MRI show falls in both RV EDV and ESV but only LV ESV in response to exercise. In this study both LV and RV EDV and ESV fell significantly with exercise in healthy children. These findings are consistent with a large study of healthy children undergoing supine cycle echocardiography(206). In children with repaired ToF RVEDV and RVESV fell in response to exercise. This is consistent with a study of adults with repaired ToF undergoing dobutamine stress MRI. This study identified two distinct groups of response to high dose dobutamine, a ‘normal’ response, also seen in healthy adults of reduced RVEDV and RVESV with no change in SV as seen in the paediatric ToF population here. There was also a ‘non responder’ group that exhibited unchanged RVESV representing systolic dysfunction(191).

The finding of a fall in RESV in response to exercise in children with PAH contrasts with a study of adults with PAH who were unable to decrease their RVESV in response to exercise(207).

One important finding that has not been previously described is worsening septal curvature in PAH during exercise. It has been shown that septal curvature (measured using MR) correlates strongly with resting mPAP in children with PAH(208). The results of this study suggest that mPAP increases significantly during exercise in this group. This is consistent with invasive studies in adults(205), but has not been shown in children due to the restrictions to performing exercise catheterization in this age group. The ability to non-invasively assess pulmonary hemodynamics during exercise has several potential clinical uses. These include unmasking borderline PAH patients, assessing exercise induced pulmonary hypertension and investigating the causes of unexplained exercise intolerance.

7.7.3 Feasibility and Safety

In this study, all tests were completed safely with no arrhythmia or exercise induced complications. This is not surprising as conventional CPET has been shown to be safe in the patient groups studied(45,53). Additionally we chose only to study children in functional class I and II. However, full 12-lead ECG monitoring is not readily available in MR and this does prevent the use of MR-CPET in patients with significant risk of ischemia or arrhythmia. Unlike in the adult validation study (209) in which ECGs were non-interpretable it was possible to obtain a continuous ECG during exercise in children. A potential reason for the superior quality of the ECG signal in children is less upper body movement during exercise and consequently less motion artefact. An alternative possible reason is improved positioning of leads and coils with accumulated experience. For MR-CPET to become a useful clinical tool it is vital that a universal and robust solution to monitoring electrical activity is developed. Notably, unlike the adult population in the validation study, all of the children who volunteered for this study were able to master the exercise technique and none reported experiencing claustrophobia. Data on anxiety and claustrophobia in children undergoing MRI is relatively limited but suggests that it is generally well tolerated in paediatric populations (210) but that loud noises the need to stay still and

confined space all contribute to anxiety(211). Whilst overall measures of acceptability and satisfaction for MR-CPET were good across the groups studied it is important to consider potential self-selection bias amongst volunteers. Exercise MRI is intrinsically demanding and further improvements to the user experience could increase its potential for clinical use.

7.7.4 Limitations

A major limitation in the interpretation of this study is that although the subjects exercised until exhaustion with satisfactory RERs, the exercise performed was sub-maximal. As discussed in chapter 5 we used an up-down ergometer that requires a kicking, rather than rotary motion due to the difficulty of performing cycling within the confines of a 60cm scanner bore. A disadvantage is that this type of motion uses fewer muscle groups than cycling, partially explaining the significantly lower power output achieved in this study compared to studies using conventional CPET.

Supine exercise cannot be directly compared to conventional CPET and this must be taken into consideration when interpreting the results. Peak VO_2 and SV augmentation are consistently found to be lower at peak supine exercise compared to upright exercise in both adults and children(178),(27),(155,212). Nevertheless, a good correlation between peak VO_2 obtained during MR-CPET and conventional CPET was found in the validation study (described in chapter 6) supporting the use of peak VO_2 measured during MR-CPET as a marker of exercise capacity.

Another possible cause of these findings is abnormal pulmonary reserve, which was not formally tested in all three of these studies. It is known that these patient groups do exhibit abnormalities in lung function(213) and therefore, it would be important to evaluate this in the future.

As discussed in chapter 6, although steps were made to optimise the post-processing of the very large flow data sets, segmentation of a full data set remains time consuming. An alternative approach, examining only resting and peak exercise data is described in the following chapter.

7.7.5 Conclusions

This proof of concept study demonstrates the innovative use of an integrated MR-CPET approach both in healthy children and children with cardiac disease. Using this novel non-invasive methodology, it was possible to show significant differences in the exercise responses in the patient groups studied. The technique is potentially of wider utility in cardiovascular disease, particularly when symptoms are induced or exacerbated by exercise.

Chapter 8 Application of MR-CPET in Adults with the Fontan Circulation

8.1 Introduction

The Fontan circulation is the final stage of surgery for patients where a univentricular circulation is necessary(214). Despite improvements in long term outcome(215) it remains a palliative procedure with expected deterioration in cardiac function over time and known impairment of exercise capacity. There is considerable variation in the functional status of young adults with the Fontan Circulation(56,216). Exercise limitation is recognised to be multifactorial in Fontan patients(217). The primary determinants of reduced exercise capacity in this group are thought to be cardiac (chronotropic incompetence and limited ability to augment SV). Respiratory abnormalities include reduced V_E and increased ventilatory inefficiency. There is also evidence of skeletal muscle impairment in this group. Not only do Fontan patients have a lower muscle mass than healthy peers but there may also be reduced regional blood flow to exercising muscle(218), endothelial dysfunction(219) and abnormal oxygen uptake(16). Skeletal muscle deficit in these patients is associated with reduced exercise capacity(220). Recent findings of the largest longitudinal study of children and young adults with the Fontan circulation (followed for more than a decade) demonstrate that impaired exercise performance is associated with worse functional status and importantly that alongside ventricular function, functional status is a predictor of cardiac transplantation or death(221).

Previous studies of the impact of muscle mass have used alternative measures of skeletal muscle (for example dual energy x-ray absorptiometry(16,220)) however MR is a reference standard technique for the quantification of skeletal muscle(222) Studies of both aerobic and combined aerobic and resistance exercise rehabilitation in patients with the Fontan circulation have shown small but significant improvements in capacity following training(223).

Better understanding of the determinants of exercise capacity in adults with the Fontan circulation is important as exercise limitation is a cause of poor quality of life in these patients and because such knowledge could help target exercise intervention

which may improve both functional capacity and quality of life(224,225). Invasive CPET has the potential to further define the relative contribution of factors limiting exercise in this group however a non invasive MR-CPET approach may be more acceptable to patients.

8.2 Aims

The aims of this study were 1) to assess the differences in VO_2, CO and a-vO_2 between healthy adults and adults with Fontan circulation 2) to assess conventional volumetric measures at rest and peak exercise as well as distribution of blood flow in these two groups 3) to assess the contribution of sarcopenia to exercise limitation.

8.3 Study population

Thirteen adults with Fontan Circulation (11 male, 2 female) and thirteen age matched healthy controls (11 male, 2 female) were recruited between June 2016 and January 2018. Exclusion criteria were i) age <16 years ii) arrhythmia iii) MR incompatible implant iv) intellectual disability or physical disability that would preclude exercise v) pregnancy.

Patients with Fontan circulation were recruited via paediatric cardiology transition clinics at Great Ormond Street Hospital and with the support of the Grown-up congenital heart disease (GUCH) clinical nurse specialist team at St. Bartholomew's Hospital Heart Centre. Control group subjects were recruited through local advertising and were screened to exclude volunteers with any medical co-morbidity, current medical treatment or relevant family history.

8.4 Methods

The methodology for this study was as described in the methods chapter with the addition of measurement of above knee leg muscle volume as well as volumetric and descending aortic flow measurement at rest and peak exercise.

8.4.1 Leg muscle volume

As described above the role of skeletal muscle (particularly lower limb skeletal muscle) in Fontan patients' exercise limitation is increasingly recognized. Other CMR studies in this area have typically not used MRI to quantify skeletal muscle. We used the T_2* - IDEAL (Iterative Decomposition of water and fat with Echo Asymmetry and Least squares estimation) algorithm to perform muscle quantification. We acquired six echoes at different TE's (3.47, 5.01, 6.55, 8.09, 9.63, 11.17) to create four sets of images from a single acquisition; water only, fat only, in-phase, and out-of-phase (Figure 8.1) and used the water only images to quantify muscle.

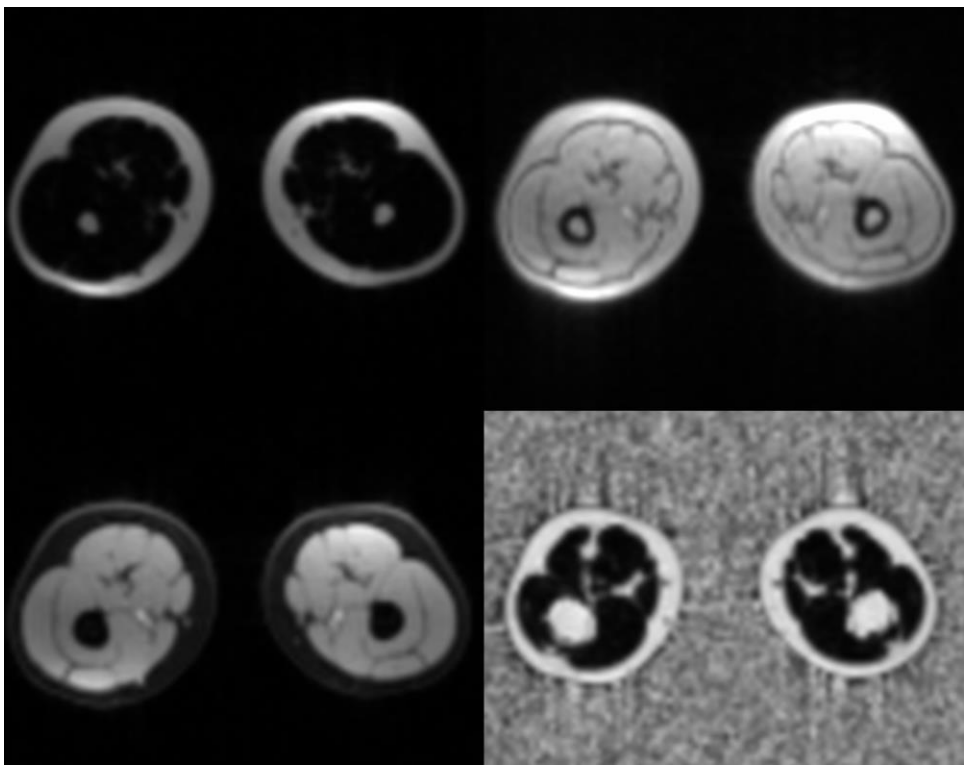

Figure 8.1 Fat only, water only, in phase and out of phase images.

This approach has been demonstrated to have a good signal to noise ratio and image sharpness with homogeneity of fat suppression as well as the advantage of a short acquisition time(226). A further benefit is that because IDEAL is a single acquisition

technique, the in phase and out of phase images are inherently registered, leading to faster interpretation and higher diagnostic confidence.

In this study we acquired IDEAL data prior to MR-CPET, using two-phase array coils placed around the subjects legs covering the iliac crests and knees. The following parameters were used: field of view 600mm matrix 114x112, voxel size 3.1x3.1x10, TR 27 (TE –opposed opposite phases), flip angle =12°, slice thickness=10mm.

8.4.2 Descending Aortic Flow

Rest and peak exercise descending aorta flow was measured at the level of the diaphragm using same UNFOLDed-SENSE spiral PCMR sequence both at rest and at peak exercise. The following parameters were used: field of view=450mm, matrix=160x160, voxel size=2.8x2.8x7mm. TR=5.92/1.9, flip angle =20, VENC = 200cm/s, temporal resolution= 35ms. Descending aortic flow measurement was included to determine any difference in distribution of blood flow with exercise (potentially associated with systemic to pulmonary collateral vessels) between Fontan and control patients.

As in the previous study ventricular volumes were assessed at rest and peak exercise by obtaining a short axis stack using a previously validated real-time radial k-t SENSE steady-state free precession sequence. The parameters used were as follows: field of view =320 mm, matrix=128×128, voxel size 2.5×2.5×8, TR/TE=2.4/1.17 ms, flip angle =47°, *R*=8, and temporal resolution =36 ms.

8.4.3 Exercise Protocol

The same standardised MR-CPET exercise protocol as that implemented with adult volunteers in the validation study was used with the addition of resting and peak exercise acquisition of descending aorta flow and volumetric assessment.

The exercise protocol consisted of one minute rest followed by 2 minutes unloaded cycling then a 1 Watt increase every 20 seconds for the next 5 minutes and subsequent 2 Watt increase every 30 seconds to exhaustion. At the point of

exhaustion, resistance was reduced to zero and the subject was asked to exercise as hard as possible in order to maintain a high heart rate and prolong the exercise state. During this period, ventricular volumes and descending aortic flow (peak exercise) were assessed again (acquisition less than 60 seconds).

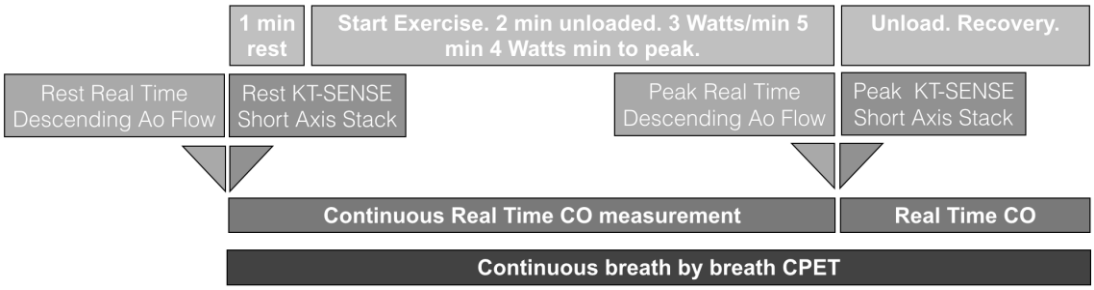

Figure 8.2 MR-CPET protocol

As described in the methodology chapter continuous real-time flow data and breath-by-breath CPET data acquisition was performed from rest through to peak exercise.

8.4.4 Monitoring

Peripheral oxygen saturation was monitored continuously using a MRI compatible monitoring system (Datex-Ohmeda MRI Monitor, Datex-Ohmeda, Helsinki, Finland) Participants were asked to rate exertion on the Borg scale of perceived exertion(227) prior to starting exercise and on completing exercise. This scale used in conventional exercise testing runs from 6 to 20. A Borg score of 12 and above is consistent with moderate intensity exertion. As per previous studies ECG was continuously monitored using the Siemens magnetic resonance imaging vectorcardiogram (Siemens Medical Solutions, Erlangen, Germany).

8.4.5 Image analysis

All images were processed using plug-ins for the open-source software OsiriX (OsiriX Foundation, Geneva, Switzerland).

In order to calculate leg muscle volume from the IDEAL acquisition, we extracted contiguous “water-only” slices. Leg muscles between the level of the greater

trochanter of the femur and the patella were segmented using the Osirix Grow Region 3D segmentation tool. Using this tool a 'seed point' is selected and upper and an upper and lower limit threshold for pixel inclusion set. The region of interest is then 'grown' within these parameters before visual inspection and manual correction. Finally, slice summation was used to provide a final volume (Figure 8.3).

Figure 8.3 Stages of leg muscle segmentation

Flow data was processed using the same in-house Osirix plugin as previously described. With the objective of developing a study protocol that was more readily translatable to the clinical environment shorter sections of flow data relating to rest and peak exercise were interrogated. Magnitude images corresponding to the first 30 seconds of rest and 30 seconds at peak exercise were segmented using a registration-based segmentation algorithm with manual operator correction. The resultant raw flow curves and VO_2 data were further analysed using Matlab (Matlab 2012). The flow curves were automatically split into separate heartbeats as previously described (data supplement) and the stroke volume (SV) was calculated by integration. The heart rate (HR) and SV data were combined to calculate CO (HR x SV). Arterio-venous oxygen content gradient (a-vO_2) was then calculated as VO_2/CO.

For ventricular volumetric assessment, end systolic and diastolic frames were identified by visual assessment. Manual segmentation allowed measurement of left ventricular (LV) end diastolic volume (EDV) and end systolic volume (ESV) in the

control group and univentricular EDV and ESV in the Fontan group. The stroke volume (SV) was the difference between these two values and ejection fraction (EF) was SV/EDV.

8.4.6 Statistical Analysis

All statistical analysis was performed using StataSE 13.0 (StataCorp, College Station, USA). Descriptive statistics are expressed as mean (95% CI) or mean (±SD). Likert and Borg scale data was compared using the Kruskal Wallis test. A p-value <0.05 was considered statistically significant.

8.5 Results

8.5.1 Demographics

The mean age of the Fontan group was 22 years (18-27 years) and the mean age of control group was 23.5 years (17-25 years), there was no significant difference between groups (p=0.52). There was no significant difference in height, weight or BSA between groups. Above knee leg muscle volume was however significantly lower in the Fontan group. No significant difference in reported hours of exercise undertaken per week reported by the two groups (Table 11).

Table 11 Demographic, Anthropometric and Exercise Data.

Variable	Control Group	Fontan Group	P value
Male: Female	11: 2	11: 2	
Age, years*	21 (17- 25)	22 (18-27)	0.516
Height, cm	176 (171-181)	172 (167-177)	0.254
Weight, kg	70 (62-78)	67 (59-76)	0.615
BSA, m^2	1.9 (1.7-2)	1.8 (1.7-1.9)	0.418
Muscle volume cm^3	9800 (8700-11000)	8200 (7100-9200)	0.030
Muscle volume cm^3 / height cm	56 (50-61)	47 (42-53)	0.032
Exercise hours / week*	3.8 (2.3-6.4)	3 (2-4.6)	0.454

* Log transformed (geometric mean).

In the Fontan group the mean age of surgery was 7.6 (±6.6) years. The mean time since surgery was 15.5 (± 5.4) years. 4/13 had intracardiac Fontan Circulations with

the remaining 9/13 being extracardiac. 7/13 were on aspirin, 2/10 warfarin, 1/13 on enalapril, 2/13 on lisinopril and 1/10 on bisoprolol. The underlying diagnosis was tricuspid atresia and pulmonary atresia or stenosis in 5/13, congenitally corrected transposition of the great arteries with VSD or ASD and VSD and pulmonary atresia or stenosis in 4/13 and right atrial isomerism common atrioventricular valve, double outlet right ventricle and pulmonary stenosis in 2/13, tricuspid atresia with transposition of the great arteries and hypoplastic aortic arch in 1/13 and mitral and aortic stenosis and hypoplastic aortic arch in 1/13. All subjects exercised to exhaustion achieving a peak respiratory exchange ratio (RER = VCO_2/VO_2) $\geq$1.1.

There was no significant difference in the perceived effort associated with MR-CPET between groups; mean Borg rating 12.77 (11.43-14.11) in the Fontan group compared to 13.46 (11.96-14.96) in the control group p=0.37. However, the maximal work rate achieved was significantly higher in the control group than the Fontan group: 24 (19-29) Watts vs. 12 (8.4-15) Watts. There were no adverse events or complications (including documented arrhythmia during exercise) associated with MR-CPET in either group.

There were no significant differences in any of the measures of acceptability (satisfaction (p=0.48), information (p=0.45), comfort (p=0.23), perceived helplessness (p=0.5) and worry (p=0.33) between groups.

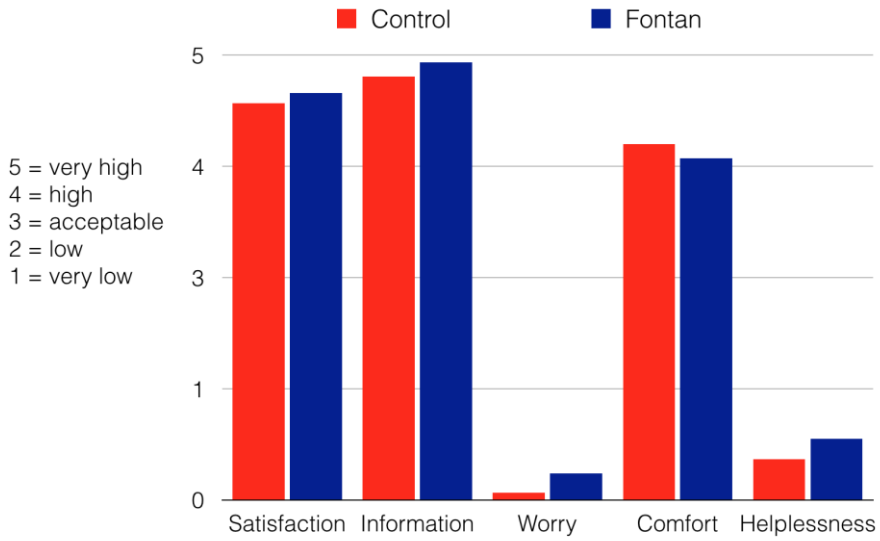

Figure 8.4 Acceptability measures (no significant differences in all measures between groups)

8.5.2 MR CPET metrics – Rest and Exercise

There was no significant difference in resting VO_2 between groups. At peak exercise VO_2 was significantly lower in the Fontan group than controls: 11 (±3.1) ml/kg/minute vs. 18 (±3.9) ml/kg/minute. There was no significant difference in resting heart rate between the two groups. Peak heart rate was however significantly higher in the control group at 141 bpm (±120) v. 104 bpm (±14) (p=<0.001). Stroke volume was not significantly different between groups either at rest or at peak exercise. CO was not significantly different at rest, but driven by heart rate peak CO was significantly higher in the control group at 6.7 l/m^2/min (±1.3) compared to 4.6 l/m^2/min (±1.4) in the Fontan group (p= 0.001). Although peak a-vO_2 was lower in the Fontan group this was not significant despite the significant differences in peak CO and VO_2.

Table 12 MR-CPET Derived Measures

Variable	Control		Fontan		*P* Value		
	Rest	Peak	Rest	Peak	Disease Effect	Time Effect	Disease–Time Interaction
HR, bpm	83 ± 18	141 ± 20*	77 ± 14	104 ± 14*	0.001	<0.001	<0.001
SV, ml/m^2	49 ± 12	48 ± 8.5	43 ± 11	45 ± 12	0.250	0.940	0.360
CO, l/m^2/min	4.1 ± 1.4	6.7 ± 1.3*	3.4 ± 1.2	4.6 ± 1.4*	0.007	<0.001	0.012
VO_2, ml/kg/min	3.9 ± 0.8	18 ± 3.9*	3.4 ± 1.1	11 ± 3.1*	<0.001	<0.001	<0.001
VCO_2 Ml/kg/min	3.9 ± 1.2	19 ± 1.3*	3.3 ± 1.3	11 ± 1.3*	<0.001	<0.001	0.001
A-vO_2, mlO_2/100 mL blood	3.7 ± 1.4	9.8 ± 1.3*	3.8 ± 1.6	8.7 ± 1.4*	0.750	<0.001	0.180
V_E,	10000 ± 1600	40000 ± 8900*	9800 ± 2500	27000 ± 8500*	0.002	<0.001	<0.001
RR,	17 ± 5.6	36 ± 9.3*	19 ± 5	32 ± 8.9*	0.640	<0.001	0.031
SaO2, %	99 ± 1	95 ± 1	95 ± 1	89± 1.1*	<0.001	<0.001	0.170

a-vO_2 indicates arteriovenous oxygen content gradient; CO, cardiac output; HR, heart rate; SV, stroke volume; VE, minute ventilation; VO_2, oxygen uptake. * Significant difference rest to peak.

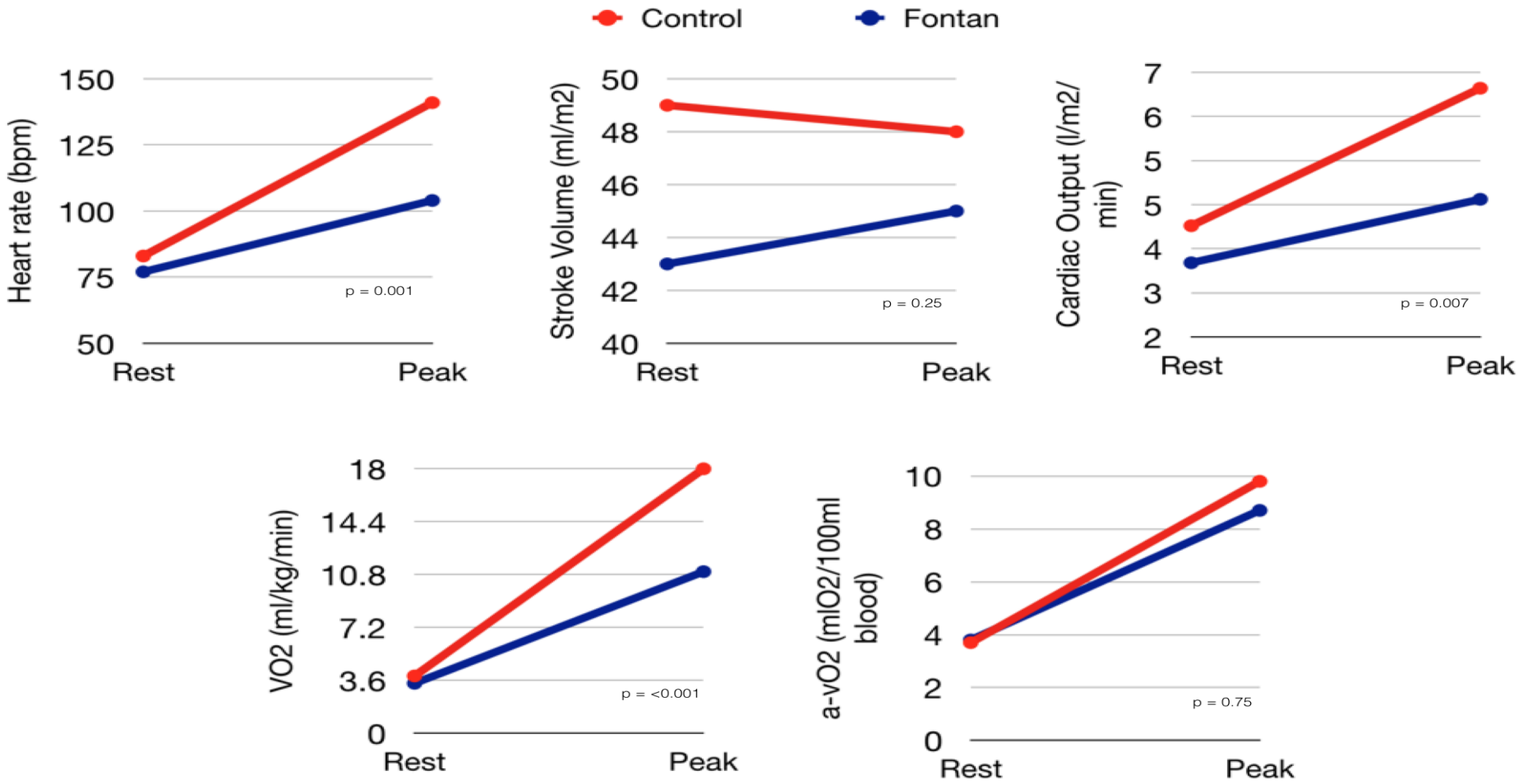

Figure 8.5 Change in MR-CPET derived measures between rest and peak exercise.

8.5.3 Ventricular volumes – Rest and Exercise

Both resting and peak ejection fraction were significantly higher in the control group (65% (±4.5) vs. 56% (±7.3) ($p = 0.002$) at rest, 71% (±6.3) vs. 60% (±8.6) ($p=0.001$) at peak exercise. This was due to a lower ESV at peak exercise in the control group (20 (±7.9) vs. 30 (±9.5) ($p=0.010$). ESV was lower in the Fontan group at rest but this was not significant ($p=0.067$). As expected there was a strong correlation between SV values obtained by both methods at rest ($r = 0.98$, $p = 0.000$) and at exercise $r = 0.96$, $p = 0.000$). Correlation was less strong between CO measured using the two approaches at rest ($r = 0.37$, $p = 0.062$) and at exercise $r = 0.54$, $p = 0.005$) (this in part will relate to differences in measured heart rate).

Percent of CO in the descending aorta increased to a similar extent in both the Fontan and control groups. This reflects increased blood flow to the lower limbs during exercise. There was no significant difference in change between the two groups indicating no significant aorto-pulmonary shunting in the Fontan group. The correlation coefficient between rest-to peak change in ascending and descending aortic cardiac output was not strong ($r = 0.45$, $p = 0.023$).

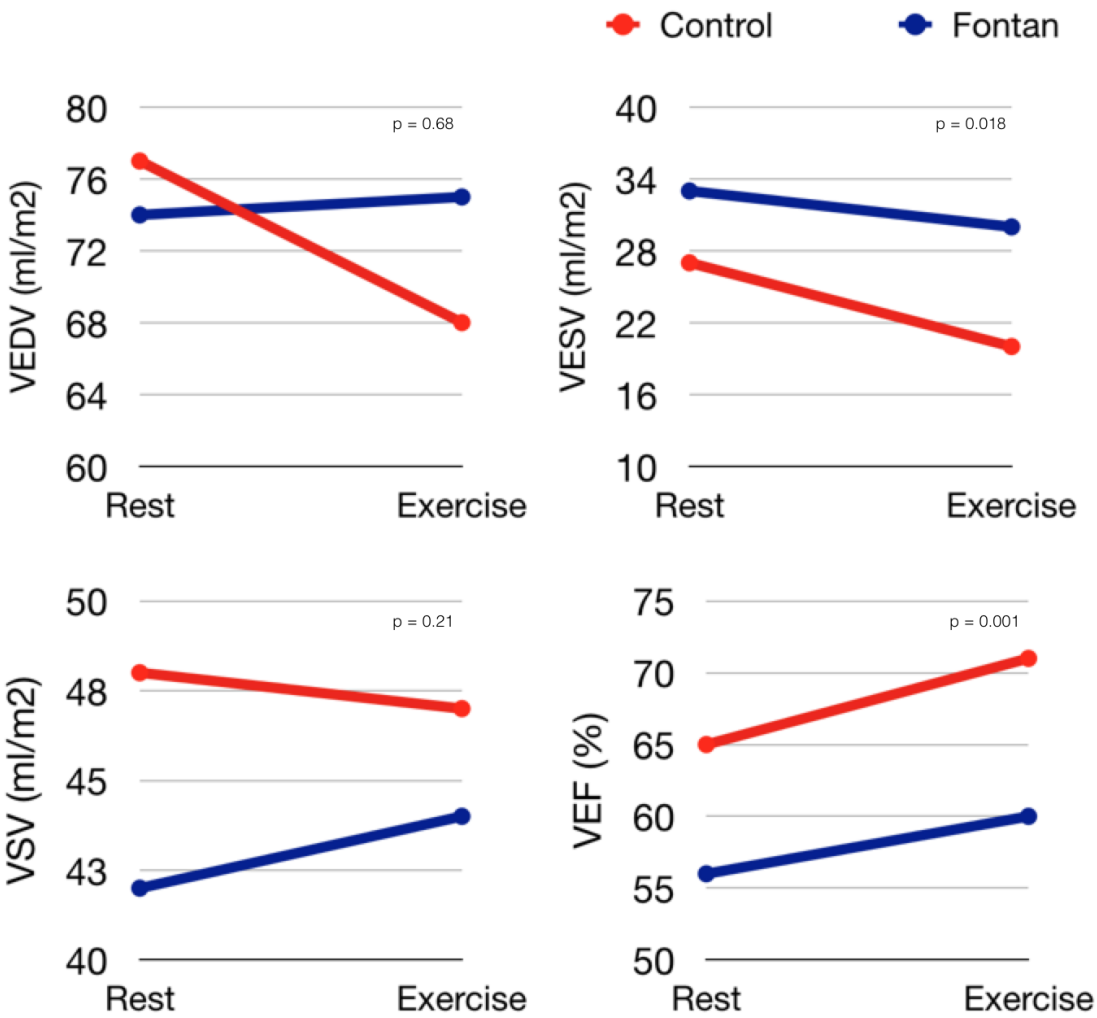

Figure 8.6 Change in conventional MR derived measures between rest and peak exercise.

Table 13 Conventional MR Measures

Variable	Control		Fontan		*P* Value		
	Rest	Peak	Rest	Peak	Disease Effect	Time Effect	Disease–Time Interaction
VEDV, mL/m^2	77 ± 18	68 ± 15*	74 ± 12	75 ± 17	0.680	0.083	0.022
VESV, mL/m^2	27 ± 7.4	20 ± 7.9*	33 ± 7.2	30 ± 9.5	0.018	<0.001	0.068
VSV, mL/m^2	48 ± 1.3	47 ± 1.2	42 ± 1.2	44 ± 1.3	0.210	0.750	0.230
EF, %	65 ± 4.5	71 ± 6.3*	56 ± 7.3	60 ± 8.6	0.001	<0.001	0.380
Percent CO desc. Aorta	21 ± 7.4	32 ± 11*	26 ± 11	29 ± 14	0.830	0.002	0.035

EDV indicates end-diastolic volume; ESV, end-systolic volume; SV, stroke volume; EF, ejection fraction; CO, cardiac output. * Significant difference rest to peak.

8.5.4 Muscle volume

Both absolute muscle volume and muscle volume indexed for height were significantly lower in the Fontan group (p=0.030 and p=0.032 respectively). In the control group there was a positive correlation between indexed above knee leg muscle volume and both resting VO_2 (r=0.74, p=0.004) and peak VO_2 (r=0.63, p=0.020). There was also a positive correlation between muscle volume and both resting CO (r=0.6, p=0.032) and peak CO (r=0.74, p=0.004). There was no correlation between indexed muscle volume and a-vO_2. As expected in healthy volunteers there was a positive correlation between muscle volume and LVEDV (at rest: r=0.65, p=0.017, at peak: r=0.68 p=0.011). There was also a significant positive correlation with LVESV at rest (r=0.81, p=0.001) and LVSV at peak exercise (r=0.79, p=0.001). In Fontan patients there were no significant correlations between above knee leg muscle volume and MR-CPET or conventional CMR measures either at rest or at peak exercise.

Table 14 Correlations between muscle volume and MR / MR-CPET metrics

	Control				Fontan			
	Rest		Peak		Rest		Peak	
Variable	***r***	**P value**	***r***	**P value**	***r***	**P value**	***r***	**P value**
VO_2, ml/min	0.74	0.004	0.63	0.020	0.24	0.429	0.37	0.209
CO, l/min	0.60	0.032	0.74	0.004	0.33	0.265	0.32	0.280
a-vO_2, mlO_2/100 mL blood	0.11	0.716	0.06	0.856	0.17	0.580	0.27	0.375
VEDV, mL/m²	0.65	0.017	0.68	0.011	-0.33	0.272	0.07	0.823
VESV, mL/m²	0.81	0.001	0.49	0.091	0.06	0.853	0.27	0.369
VSV, mL/m²	0.48	0.099	0.79	0.001	-0.19	0.528	-0.14	0.657

VO_2 indicates oxygen uptake; CO, cardiac output; a-vO_2 arteriovenous oxygen content gradient; VEDV, left or univentricular end-diastolic volume; VESV, left or univentricular end-systolic volume; VSV, left or univentricular stroke volume.

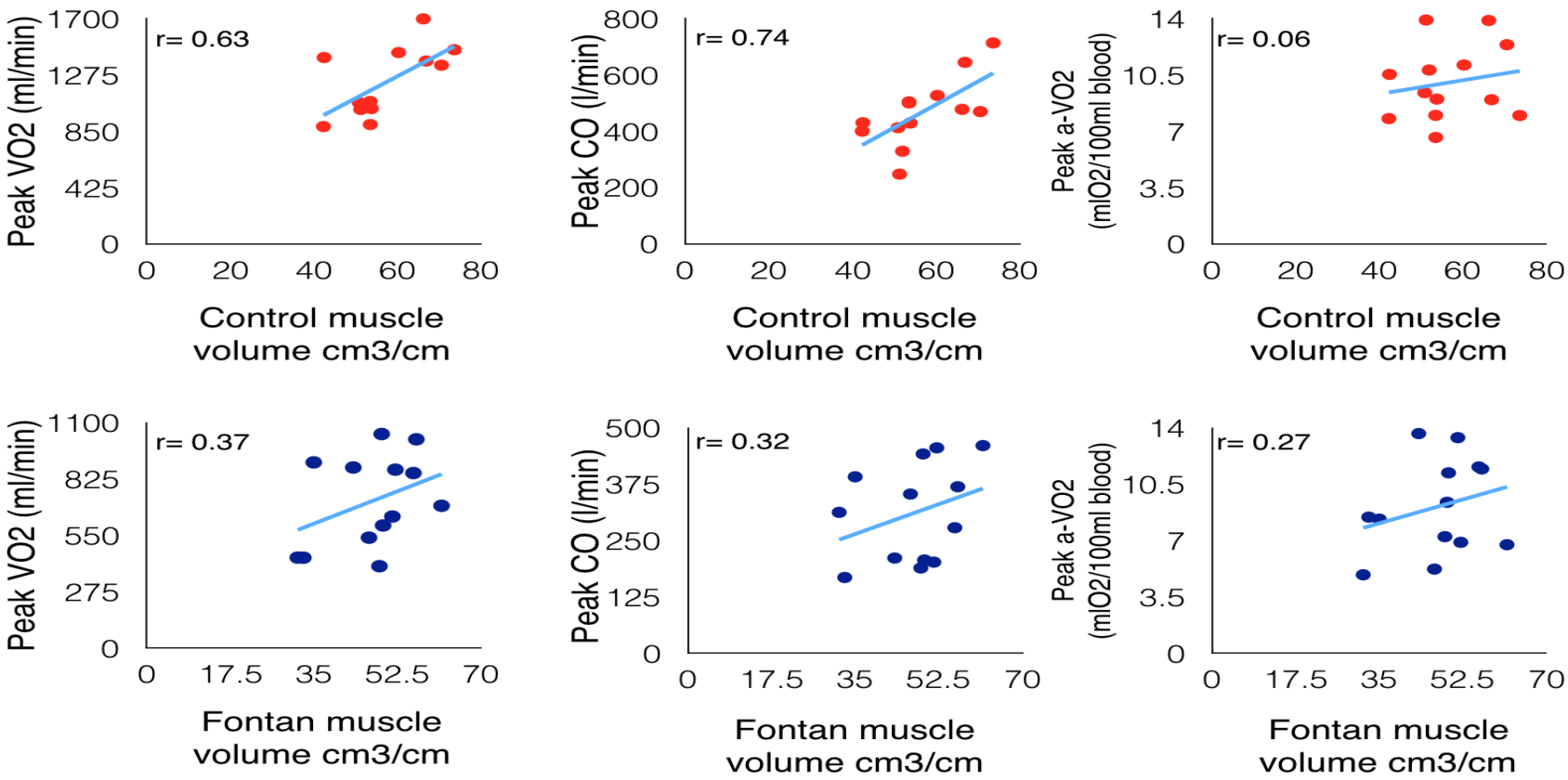

Figure 8.7 Correlation between MR-CPET derived measures and volume.

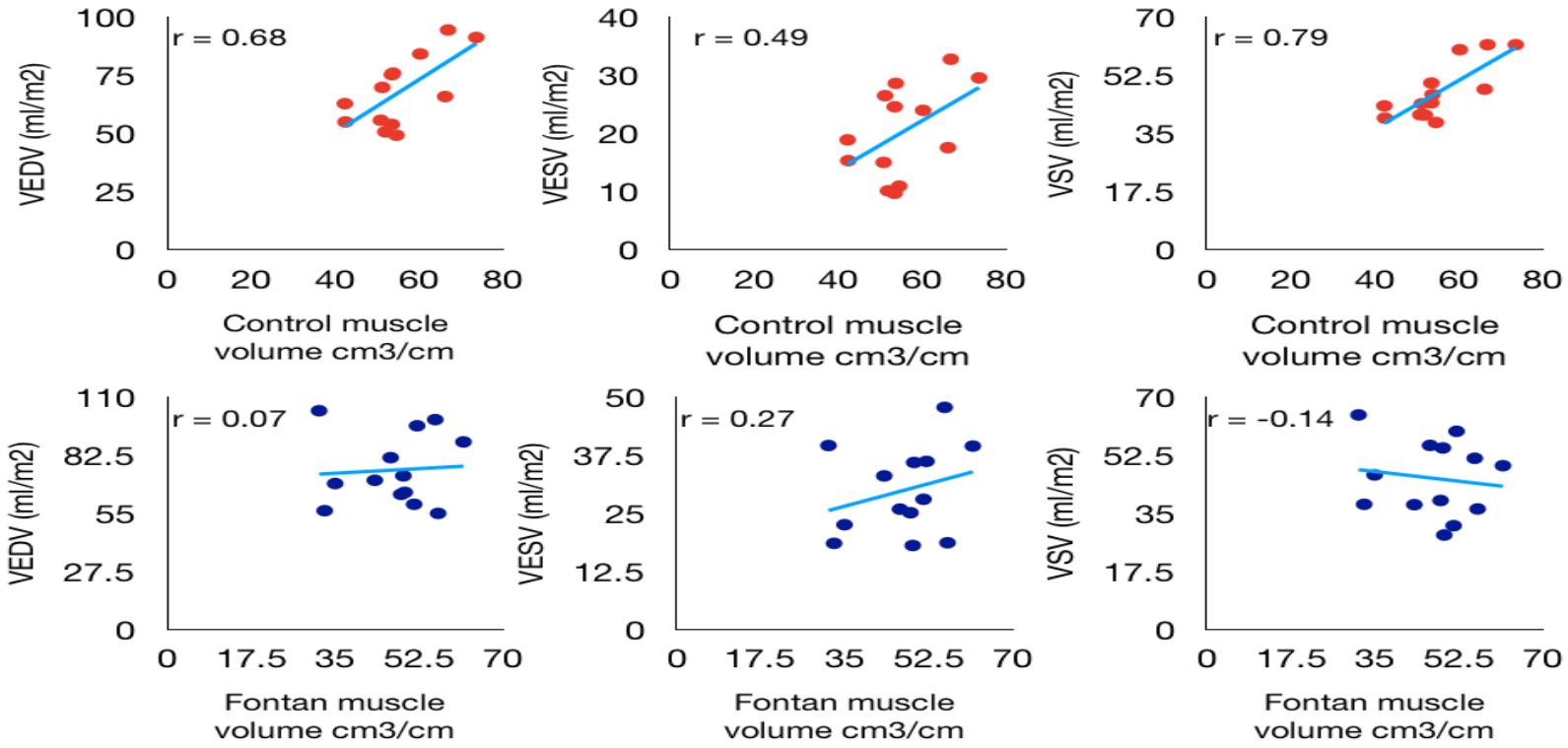

Figure 8.8 Correlation between conventional MRI derived measures and muscle volume.

8.6 Discussion

The main findings of this study are i) MR-CPET can be performed safely in selected adults with the Fontan Circulation ii) Adults with Fontan circulation have chronotropic incompetence with a resulting failure to augment CO iii) Although tissue oxygen extraction in the Fontan group was lower this difference was not significant.

Results of this study are consistent with known features of exercise intolerance in adults with the Fontan circulation. Aerobic capacity in this patient group is believed to be largely dependent on inability to increase CO. This lack of cardiac reserve is related to known chronotropic incompetence. Studies using conventional CPET have consistently demonstrated reduced peak heart rate(216) reflecting the results seen in this study. Although findings are not new in themselves the ability to demonstrate them simultaneously and non-invasively using MRI is novel.

Patients with the Fontan circulation have previously been shown to have impaired SV augmentation to exercise. In this study there was no significant difference in SV at peak exercise. Supine exercise is known to differ significantly from upright exercise. Previous MR studies have shown minimal augmentation of SV with moderate intensity supine exercise in healthy controls(141) and this was also the finding in the validation study for this technique. This limitation is in common with most current exercise imaging but does not negate its implications as real-world exercise and therefore exercise limitation occurs predominantly in an upright position. A further feature of patients with Fontan circulation that was not demonstrated in this study was a higher resting heart rate (related to impaired parasympathetic nervous activity(228)); a possible explanation for this is that subjects in the Fontan group are more habituated to the hospital environment including the MRI scanner and were therefore less anxious than controls.

Although lower in the Fontan group, this study did not demonstrate a significant difference in a-vO_2. This may be type II error relating to the sample size or heterogeneity of the population studied.

Above knee muscle volume was significantly lower in the Fontan group. This is in keeping with findings of previous studies using alternative approaches to measuring muscle mass(220). Unlike in previous studies(16,220) the correlation seen between peak VO_2 and muscle volume in healthy volunteers was not reproduced in the Fontan group. This is unexpected and could relate to a number of factors including the sample size and relatively heterogeneous population. Similarly the expected positive correlation between muscle volume and stroke volume seen in the control group and previously demonstrated in Fontan patients was not reproduced. Of note there was no significant difference in reported hours of exercise between the two groups with Fontan patients reporting between 2 and 4.6 hours exercise a week. The lack of clear difference between patients and the control group may relate to a relatively active patient population following current advice to exercise regularly.

One patient in the Fontan group was on a beta-blocker however they were not an outlier for heart rate at rest, peak exercise or for change in heart rate (all values within one standard deviation of the mean) and was therefore included in all statistical analysis. Three patients were on angiotensin converting enzyme (ACE) inhibitors. As the overall numbers in this study are small sub-group analysis would not be justified. This group of drugs are used in Fontan patients with the intention of improving haemodymics through reduction in systemic vascular resistance. Short term studies have not demonstrated any benefit in terms of exercise capacity in Fontan patients treated with enalapril(229). Despite the lack of evidence ACE inhibitors continue to be used in Fontan patients and additional benefit of a larger study allowing subgroup analysis would be valuable.

8.6.1 Limitations

The patient group studied here was carefully selected as for the purposes of research, and it would not be appropriate to attempt this technique in more severely impaired higher risk patients without proven clinical benefit. Despite recruiting from a large centre with a high level of participation from potential candidates, relatively few patients met the inclusion criteria. Arrhythmia is an important cause of morbidity and exercise limitation in this group of patients, that increases over time (at 12 years post surgery a third of patients are treated for arrhythmia(221)). However as only the

3 lead MRI vectorgram was available in the study, patients with known arrhythmia were excluded. The underlying diagnoses of the study population are heterogeneous and there are therefore likely to be significant haemodynamic differences, for example between patients with intra and extra cardiac conduits. A larger sample size would allow for investigation of differences relating to underlying pathology and type of surgery as well as to age and gender.

Respiratory variation and the effects of exercise on pulmonary blood flow are not fully investigated here, developments in MR technology for example ultrafast 4D flow in combination with the MR-CPET approach could help answer these questions.

A further limitation of this study is the lack of blood pressure monitoring during exercise. Blood pressure monitoring was not added to monitoring included in the study protocol as it was felt that this might seem overwhelming to volunteers (already wearing a mask, ECG monitoring, pulse oximeter and pulse gating). Patients with the Fontan circulation are known to have impaired blood pressure response to exercise and this would be an important consideration in future work (blood pressure monitoring has been successfully added to a study currently underway in children).

Finally, an important criticism of this study design is that conventional exercise testing was not included. Six minute walk testing could have been included in the study protocol without adding significant burden to volunteers however it is not a good discriminator in this situation as it has at best moderate correlation with peak VO_2 in young adults without significant functional limitation(230). Conventional exercise testing would have provided more information on the characteristics of the patient group and may have helped explain lack of difference between Fontan patients and healthy controls. For valid conventional CPET results MR-CPET could not be performed on the same day, for pragmatic reasons recruiting patients able to attend for both tests on consecutive dates was not attempted.

8.7 Conclusions

Non-invasively assessing exercise capacity in adult patients with the Fontan Circulation using MR-CPET was able to provide a detailed assessment of the response to exercise demonstrating impaired ability to augment CO and a lower peak VO_2. As expected in healthy patients peak VO_2 and CO were correlated with muscle volume but in Fontan patients this was not the case. This suggests that muscle mass alone does not explain impairment at the level of skeletal muscle (and therefore highlights the need for improved understanding of the potential determinants of aerobic capacity such as capillary density capillary to fibre ratio and endothelial function).

This patient group has known functional limitation that deteriorates over time. It is also a growing population with an estimated 50-70,000 adult patients, expected to double in the next 20 years(231). Developing a better understanding of the causes of exercise limitation in this group is a priority given the association between functional capacity and both quality of life and survival in this group. MR-CPET in conjunction with MR skeletal muscle assessment has the potential to help interpret the causes of exercise limitation and response to treatment in patients with the Fontan circulation.

Chapter 9 Discussion

9.1 Introduction

Exercise limitation is a central feature of cardiopulmonary disease, contributes significantly to disease morbidity and has prognostic value across a range of conditions(2,57). Despite symptoms typically occurring or worsening with exercise, most cardiac imaging is done at rest and therefore does not demonstrate the acute effects of exercise. Pharmacological stressors have an established role in cardiac imaging but have significant disadvantages and are not a true substitute for exercise(107). Increasingly the multisystem nature of exercise limitation is recognised and demands novel techniques to comprehensively assess it (10,11). The work described in this thesis set out to develop a new MR augmented CPET approach for the non-invasive assessment of exercise physiology and to apply it in patient groups. In order to implement MR-CPET it was necessary to apply innovative real-time MR sequences and to find solutions to the processing of the very large data sets not found in routine practice.

The development and validation of MR-CPET is described in chapter 6. Working with commercial manufactures we were able to inexpensively modify a conventional CPET system for safe use in the MR environment. Real time PCMR data was simultaneously acquired with conventional CPET data and the results integrated to produce a more comprehensive exercise data set. It was possible to demonstrate a close correlation between variables obtained using conventional CPET and MR-CPET, validating the use of this technique. It was also possible to calculate a-vO_2 through exercise and to show that this was an independent predictor of VO_2. Importantly for the potential translation of MR-CPET into clinical practice it was well tolerated by healthy adult volunteers paving the way for use in paediatric and disease populations.

In Chapter 7 the application of MR-CPET in three paediatric populations is described. MR-CPET was feasible and well tolerated in children. Building on the protocol used in the validation study real time short axis stacks were acquired at rest and peak exercise providing anatomical and functional data. Distinct characteristic

patterns of haemodynamic, functional and metabolic responses to exercise are described between the three groups. Consistent with conventional CPET findings (56,213) peak VO_2 was found to be lower in PAH patients and there was a trend towards lower peak VO_2 in repaired ToF. MR-CPET was able to demonstrate reduced a-vO_2 in PAH patients. This is congruent with the findings of invasive CPET in adults(232). Other exercise changes in haemodynamics not previously demonstrated in children using MRI were also found, including a fall in pulmonary regurgitant fraction in the ToF group and a worsening in the septal curvature ratio in the PAH group. Fall in pulmonary regurgitant fraction during exercise has been previously demonstrated (233). Primarily this is a function of increased heart rate resulting in decrease in diastole with less time for regurgitation to occur. Altered diastolic function has also been proposed as a contributory factor (233,234). Septal curvature is known to correlate strongly with mean PA pressures(208). The finding of worsening septal curvature in children with PAH is consistent with invasive findings in adults with PAH and points to a potential indication for exercise MRI in investigating exercise intolerance unmasking undiagnosed PH and exercise PH.

In Chapter 8 MR-CPET is applied in a group of young adults with the Fontan Circulation. Importantly in this group of patients with a high burden of arrhythmia, it was possible to safely perform exercise with continuous ECG monitoring in all patients in this group. Although this was a selected group of patients who were relatively 'well' with similar reported hours of exercise per week to healthy controls, a significantly lower maximal work rate was achieved. As expected peak VO_2 was significantly lower in the Fontan group. The finding that peak CO was lower in the Fontan group, primarily due to chronotropic incompetence was also consistent with previous studies(216). Despite these differences a-vO2 was not significantly different between Fontan patients and controls. As patients selected for this study were in a high functional class and exercised regularly, there may be no difference between the two groups. Alternatively, the lack of difference may be a result of sampling error or be related to self-selection bias. Increasing the sample size and widening inclusion criteria would help determine the reason for lack of significant difference.

The methodology was further developed with the addition of upper leg skeletal muscle quantification in an attempt to address the role of sarcopenia in tissue oxygen extraction. As expected, absolute and indexed muscle volume was lower in the Fontan group. In healthy controls there were positive correlations between muscle volume and peak exercise CO, stroke volume and VO_2, however these findings were not reproduced in the Fontan Group. This divergence from the normal relationship seen in healthy controls is unexpected and may point to more complex multisystem interactions in this group.

9.2 Technical considerations

The MR-CPET methodology described here relies on real time imaging techniques in relation to which concerns over reduced image quality and robustness have been expressed. Real-time MR techniques have however been extensively tested against conventional gated MR with good agreement (235). In addition, a recent study has demonstrated good agreement between SV assessed using real-time MR volumes and the direct Fick method during exercise (143). These findings support real-time MR as a valid method of evaluating physiology during exercise. Furthermore, recent innovations in real-time MR post-processing such as pseudo-cardiac and respiratory gating (143) and improved automated flow (156) and ventricular segmentation (236) may also improve reproducibility.

A major challenge of this work was the need to continuously measure flow in order to guarantee acquisition of data at peak exercise. The resultant data consisted of up to 24,000 frames of flow images, representing a significant reconstruction and post-processing problem. We used an online GPU reconstruction system (155) to ensure that data was available in a clinically meaningful time. Currently there are no commercial software solutions that can handle this amount of data and consequently we had to use an in-house post-processing tool. Even using this optimized system, data analysis was time consuming and could take several hours with operator adjustments. One method of reducing total processing time is to only segment the data at rest and around the point of exhaustion as described in chapter 8. This can take as little as 30 minutes and the reduced time makes MR-CPET more feasible in the clinical environment. Reducing the amount of image segmentation might also

enable data to be more easily processed on commercial software. This is vital as the inability to process data using validated and quality controlled software is a major limitation of this technique and an impediment to dissemination. One disadvantage of only processing a portion of the data is that the 'shape' of the full VO_2, CO and a-vO_2 curves may be clinically important. Exploring the shape of these curves is an important area for future research.

We used a standard clinical CPET system that was made MR compatible by a simple and inexpensive modification to the umbilicus. Other studies have made similar modifications (with removal of ferromagnetic parts) to commercially available gas analysis systems to make them MR compatible (128). Importantly even though these modifications resulted in increased dead space, there was no significant measurement difference compared to an unmodified system. Another possible solution is to adapt the fully MR-compatible gas analysis systems for monitoring of patients under general anesthesia. These systems are not validated for exercise, but do suggest a future direction for development.

9.3 Limitations

Clearly no laboratory test can ever fully reproduce the range of activity that occurs in daily life (particularly in young children) and MR-CPET shares this limitation with other laboratory exercise tests. An important limitation of this work is the heterogeneity in SV response to exercise in healthy volunteers across the three studies. In the validation study there was no increase in SV in the population as a whole, whereas healthy children SV did increase due to a significant fall in LVSV. There was also a significant fall in LVESV in healthy adult volunteers in the Fontan study.

A recent meta-analysis of 16 exercise MRI studies (15 supine, 1 near scanner upright ergometer) published between 2001 and 2018 (with a combined total of 226 healthy subjects) concluded that increase in cardiac output with exercise was primarily due to increase in heart rate with a smaller contribution of increase in SV. Increase in SV with exercise was driven by a fall in ESV with no change in EDV in supine exercise. Overall the authors conclude that supine exercise as currently performed in the MRI

scanner may not recruit sufficient muscle groups to provide the challenge needed do drive significant changes in SV(28). However they do site multiple examples that suggest intensity dependent reductions in ESV (142-144).This could help explain inconsistency in SV response in healthy controls seen in this work.

An important alternative explanation is the effect of inadequate temporal resolution on the accuracy of real time imaging at the high heart rates present in exercise. The k-t SENSE sequence used here has a temporal resolution of 35 ms. At a heart rate of 150 beats per minute approximately 11 phases per cycle are captured. This is the minimum considered to provide accurate volumetric assessment with a systematic under estimation when fewer phases are acquired(237). Whilst the temporal resolution of the real-time sequence used in this study is superior to other published work in the field a valid criticism is that true end systole and end diastole may have been missed.

An aim of this study was to develop a non-invasive technique suitable for use in children. Invasive MR-CPET would not be viable in children, however in adult populations combining MR-CPET and cardiac catheterization using radial and internal jugular or antecubital pulmonary artery catheters would be possible and allow the direct measurement of pulmonary arterial pressure and pulmonary capillary wedge pressure, helping to validate the non-invasive MR-CPET measures. Potentially this could be done using MR guided catheterization and avoid the use of ionizing radiation(238). Performing muscle biopsy would be counter to the goals of developing a non-invasive technique and was therefore not included in the study design but would provide useful information about cell surface area and microcirculation. As part of an extended non-invasive assessment MR spectroscopy could usefully be combined with MR-CPET. Low signal to noise ratio and poor spatial resolution was initially a limitation of this technique however with improvements in MR spectroscopy coils and use of higher strength magnetic fields this has significantly improved(239). MR spectroscopy is increasingly used for studies of muscle metabolism related to exercise(240). The technique has predominantly been used during isometric exercise(241,242), although a recent study has demonstrated measurement of ^{31}P with a temporal resolution of 8 seconds during

moderate steady state exercise(243). Combining MR spectroscopy with simultaneous VO2 measurement in the MR scanner could provide important information on the dynamics of oxygen uptake at a cellular level, believed to be central to determining the duration of tolerance of high intensity exercise(244).

As this work describes a novel technique an inherent limitation is that there are not established reference values for MR-CPET. Reassuringly there is consistency in MR-CPET specific findings between the three studies. Whilst there are exercise MRI studies in healthy adults, a lack of previous exercise MRI studies in children means that directly comparable normal values do not exist for paediatric patients. Interpreting conventional CPET in children and adolescents is more complex than in adults because of changes related to growth and pubertal stage (245). Although there was good matching for age and sex these are important potential sources of error in interpreting MR-CPET and could only be fully addressed by much larger studies of healthy volunteers. Test-retest reproducibility was not studied either as part of the validation study or in patient populations and is a major limitation of this work. This was primarily for pragmatic reasons. Cardiopulmonary exercise testing cannot be accurately repeated on the same day, but for meaningful test-retest reproducibility data should be repeated in a short time period (days) to avoid the effects of changes in conditioning. Ideally, three separate tests are needed as there is some learned effect between the first and second test(36). Unfortunately the resources for this level of testing were not available. Conditions of the ethical approval for testing in paediatric patients did not allow for multiple visits.

By necessity the patient populations studied here are small, recruiting from relatively small populations. Because of the lack of previous experience of the safety MR-CPET we only sought to recruit patients with mild functional limitation (functional class I-II) and excluded patients with known risk factors for exercise related events (arrhythmia, recent syncope). Although testing patients with moderate or severe functional limitation (functional class III-IV) may have elicited clearer differences from healthy patients it could be argued that testing patients who are symptomatic at rest (class IV) is less clinically relevant as they have already exhausted their functional reserve. Despite the constraints on recruitment there was a high level of

uptake from potential volunteers across the studies, for example the PAH group represents 10/13 of the eligible children in the UK and Ireland during the recruitment period.

The practical challenges of performing MR-CPET even in children and adults without functional impairment are not insignificant. Although MR-CPET was found to be clinically acceptable throughout the studies, it was significantly less comfortable and more concerning than conventional CPET to healthy adults in the validation study and these factors should be addressed in future work. The use of supine cycle Ergometry in larger bore scanners has the potential to improve comfort and reduce concern. We were able to obtain ECG monitoring during exercise in all of our patient groups but this still suboptimal and requires further improvements for clinical use. Additional information could be leveraged using further monitoring (for example with MR compatible NIRS), however the benefits of additional monitoring have to be weighed against their impact on overall acceptability to patients. Only 1 of the 73 volunteers reported in these studies experienced claustrophobia that precluded testing, however it is unclear how this experience with motivated volunteers would translate to unselected patient populations.

9.4 Implications for Clinical Practice

Together, the findings of these three studies illustrate the potential of exercise MRI to reveal physiology that is not apparent at rest. MR-CPET was safe and well tolerated in the populations studied. The finding of strong correlation between conventional and MR-CPET derived metrics in the validation study supports wider experimentation using this technique. MR-CPET elicited distinct profiles of physiological response to exercise in the three groups of patients studied. If reproducible characteristic patterns were to be established, these could facilitate diagnosis and help to guide therapy.

In its current form MR-CPET cannot replace conventional upright exercise testing but it is possible to envisage circumstances where (if proven to have diagnostic or prognostic value) it would be an appropriate alternative investigation, for example following the initiation of treatment of PAH or for determining the causes of

unexplained exercise limitation. The experience of invasive CPET in adults has demonstrated that use of the technique has the potential to reduce the time to diagnosis as well as avoiding repeated inconclusive tests, saving expense to the health system as well as time and inconvenience for patients(65) and this could also be the case for MR-CPET.

High spatial and temporal resolution real time sequences equivalent to the sequences used here are not currently universally accessible at centres performing CMR, although availability is expanding. Alternative approaches involve performing exercise until a steady state is reached and then performing imaging over a longer period are possible and have been described in other MRI studies (without VO_2 measurement) as well as in exercise echocardiography (with VO_2 measurement). Although potentially useful, exercise with a continuous increment to exhaustion provides more insight into peak performance physiological reserve and is therefore preferable in the longer term.

9.5 Implications for Research

As exercise intolerance is common to a broad spectrum of disease, potential applications of MR-CPET are wide ranging. Registered trials using similar methodologies include work in patients with cystic fibrosis and in breast cancer patients after chemotherapy. In our department a proof of concept study using MR-CPET in adults with sickle cell disease demonstrated exercise intolerance secondary to impaired peripheral oxygen extraction (246) and we are applying the same approach in a larger cohort of children with sickle cell disease, a population with poorly understood exercise intolerance.

There is also potential benefit from this kind of approach in therapeutic trials both in interpreting the mechanism of action of drugs and tracking response to treatment. Similarly, whilst studies of exercise intervention in cardiopulmonary disease have shown the ability of rehabilitation to improve functional capacity (13,247), the mechanisms behind improvement are not fully understood and could be clarified using MR-CPET.

9.6 Future Work

As discussed in chapter 8 some of the findings in the Fontan population studied were unexpected particularly the lack of significant difference in a-vO_2.

This may be due to an inadequate sample size as well as the relatively well patient cohort selected which is unlikely to accurately represent Fontan patients of this age group as a whole. Having demonstrated the safety of MR-CPET n selected patients it would be justifiable to judiciously expand the inclusion criteria and recruit larger numbers of patients. Invasive cardiopulmonary exercise testing has proven to be useful in patients with unexplained exercise intolerance both in identifying patients with inadequate pre load and in identifying exercise induced pulmonary hypertension(65). Patients with the Fontan circulation have by definition limited pre-load and this is believed to be the major determinant of CO (248). MR-CPET is an attractive technique to study this group in exercise further because of its non-invasive nature and lack of use of ionising radiation in a group of patients who may undergo multiple catheterisations. Developments in real time 4D PCMR with high temporal resolution allowing flow measurement in multiple vessels (249) could help definitively determine exercise physiology in this group.

Another group of patients where this methodology may be of interest is heart transplant recipients. A recent systematic review of exercise studies in paediatric heart transplant patients found significantly decreased peak VO_2 (57-73 percent predicted VO_2) in this population(250). Importantly in this population although depressed at rest, echocardiographic measures of left ventricular function in exercise were found to be comparable to healthy controls. A range of factors including immunosuppression, graft dysfunction and deconditioning have been implicated. MR-CPET offers a potential non-invasive approach not only to determine the causes of exercise intolerance in this group but also to assess response to reconditioning.

Beyond primarily cardiac and pulmonary disease MR-CPET has a potential role in understanding disease where there is secondary cardiac-respiratory dysfunction in

addition to skeletal muscle dysfunction. An important example is sickle cell disease where there is a significant morbidity associated with poorly understood exercise intolerance. Our group studied 14 adult patients with homozygous sickle cell disease and 14 matched controls using the same MR-CPET methodology described in this work. This study found a significantly lower peak VO_2 in sickle cell patients with linear regression analysis demonstrating reduced tissue oxygen extraction as the primary determinant(251).

9.7 Outlook

MR-CPET is unlikely to become a routine clinical investigation in the next 5 years. The outlook for the uptake of MR-CPET in is dependent on increased availability of vendor supplied real time sequences, use of wider bore scanners and improvements in technology such as improved MRI ECG monitoring and the development of less cumbersome ergometers. If with larger, longer-term studies MR-CPET is proven to have diagnostic and prognostic value the demand for this kind of integrated assessment is potentially considerable.

9.8 Conclusions

MR-CPET has been demonstrated to be safe, feasible and well tolerated in a range of patient populations with cardiopulmonary disease in a clinical research setting. Reflecting the novelty of the technique there remain areas that require further development, particularly the patient experience and data post-processing. Despite the limitations described MR-CPET has the potential to reveal physiology not demonstrated using conventional imaging or exercise testing. For the technique to become relevant to routine clinical practice its acceptability, diagnostic and prognostic role need to be tested across a range of conditions and settings.

References

1. Brubaker PH, Kitzman DW. Chronotropic incompetence: causes, consequences, and management. Circulation. 2011 Mar;123(9):1010–20.

2. Cahalin LP, Chase P, Arena R, Myers J, Bensimhon D, Peberdy MA, et al. A meta-analysis of the prognostic significance of cardiopulmonary exercise testing in patients with heart failure. Heart Fail Rev. 2013 Jan;18(1):79–94.

3. Baker JS, McCormick MC, Robergs RA. Interaction among Skeletal Muscle Metabolic Energy Systems during Intense Exercise. J Nutr Metab. Hindawi; 2010;2010(1):905612–3.

4. Guazzi M, Bandera F, Ozemek C, Systrom D, Arena R. Cardiopulmonary Exercise Testing: What Is its Value? Journal of the American College of Cardiology. 2017 Sep 26;70(13):1618–36.

5. di Prampero PE. An analysis of the factors limiting maximal oxygen consumption in healthy subjects. Chest. 1992 May;101(5 Suppl):188S–191S.

6. Coats A. The "Muscle Hypothesis" of Chronic Heart Failure. Journal of Molecular and Cellular Cardiology. 1996 Nov;28(11):2255–62.

7. Georgiadou P, Adamopoulos S. Skeletal Muscle Abnormalities in Chronic Heart Failure. Current Heart Failure Reports. Current Science Inc; 2012 Mar 21;9(2):128–32.

8. Zizola C, Schulze PC. Metabolic and structural impairment of skeletal muscle in heart failure. Heart Fail Rev. Springer US; 2013 Sep;18(5):623–30.

9. Ponikowski P, Voors AA, Anker SD, Bueno H, Cleland JGF, Coats AJS, et al. 2016 ESC Guidelines for the diagnosis and treatment of acute and chronic heart failure. European Journal of Heart Failure. 2016 May 20;18(8):891–975.

10. Mathew J, Redington A. Cardioskeletal Myopathies in Congenital Heart Diseases. In: Cardioskeletal Myopathies in Children and Young Adults. Elsevier; 2017. pp. 347–57.

11. Panagiotou M, Peacock AJ, Johnson MK. Respiratory and limb muscle dysfunction in pulmonary arterial hypertension: a role for exercise training? Pulmonary Circulation. 2015 Jul 23;:000–0.

12. Tran DL, Lau EMT, Celermajer DS, Davis GM, Cordina R. Pathophysiology of exercise intolerance in pulmonary arterial hypertension. Respirology. 2018 Feb;23(2):148–59.

13. Mereles D, Ehlken N, Kreuscher S, Ghofrani S, Hoeper MM, Halank M, et al. Exercise and Respiratory Training Improve Exercise Capacity and Quality of Life in Patients With Severe Chronic Pulmonary Hypertension. Circulation. 2006 Oct 3;114(14):1482–9.

14. Inuzuka R, Diller G-P, Borgia F, Benson L, Tay ELW, Alonso-Gonzalez R, et al. Comprehensive use of cardiopulmonary exercise testing identifies adults with congenital heart disease at increased mortality risk in the medium term. Circulation. American Heart Association, Inc; 2012 Jan 17;125(2):250–9.

15. Sandberg C, Thilén U, Wadell K, Johansson B. Adults with complex congenital heart disease have impaired skeletal muscle function and reduced confidence in performing exercise training. Eur J Prev Cardiol. SAGE PublicationsSage UK: London, England; 2014 Nov 14;22(12):1523–30.

16. Cordina R, O'Meagher S, Gould H, Rae C, Kemp G, Pasco JA, et al. Skeletal muscle abnormalities and exercise capacity in adults with a Fontan circulation. Heart. 2013 Oct;99(20):1530–4.

17. Duppen N, Takken T, Hopman MTE, Harkel ten ADJ, Dulfer K, Utens EMWJ, et al. Systematic review of the effects of physical exercise training programmes in children and young adults with congenital heart disease. Int J Cardiol. 2013 Oct 3;168(3):1779–87.

18. Novaković M, Prokšelj K, Rajkovič U, Vižintin Cuderman T, Janša Trontelj K, Fras Z, et al. Exercise training in adults with repaired tetralogy of Fallot: A randomized controlled pilot study of continuous versus interval training. Int J Cardiol. 2018 Mar;255:37–44.

19. Berry NC, Manyoo A, Oldham WM, Stephens TE, Goldstein RH, Waxman AB, et al. Protocol for exercise hemodynamic assessment: performing an invasive cardiopulmonary exercise test in clinical practice. Pulmonary Circulation. University of Chicago PressChicago, IL; 2015 Dec;5(4):610–8.

20. Fagard R, Conway J. Measurement of cardiac output: Fick principle using catheterization. European Heart Journal. 1990 Dec;11 Suppl I:1–5.

21. Bulthuis Y, Drossaers-Bakker W, Oosterveld F, van der Palen J, van de Laar M. Arm crank ergometer is reliable and valid for measuring aerobic capacity during submaximal exercise. J Strength Cond Res. Journal of Strength and Conditioning Research; 2010 Oct;24(10):2809–15.

22. Kimura Y, Yeater RA, Martin RB. Simulated swimming: a useful tool for evaluation the VO2 max of swimmers in the laboratory. Br J Sports Med. BMJ Publishing Group; 1990 Sep;24(3):201–6.

23. Hermansen L, Saltin B. Oxygen uptake during maximal treadmill and bicycle exercise. J Appl Physiol. 1969 Jan;26(1):31–7.

24. Stenberg J, Astrand PO, Ekblom B, Royce J, Saltin B. Hemodynamic response to work with different muscle groups, sitting and supine. J Appl Physiol. 1967 Jan;22(1):61–70.

25. Poliner LR, Dehmer GJ, Lewis SE, Parkey RW, Blomqvist CG, Willerson JT. Left ventricular performance in normal subjects: a comparison of the responses to exercise in the upright and supine positions. Circulation. 1980 Sep;62(3):528–34.

26. Egana M, Green S. Effect of body tilt on calf muscle performance and blood flow in humans. J Appl Physiol (1985). 2005 Jun;98(6):2249–58.

27. May LJ, Punn R, Olson I, Kazmucha JA, Liu MY, Chin C. Supine Cycling in Pediatric Exercise Testing: Disparity in Performance Measures. Pediatr Cardiol. 2013 Nov 20;35(4):705–10.

28. Beaudry RI, Samuel TJ, Wang J, Tucker WJ, Haykowsky MJ, Nelson MD. Exercise cardiac magnetic resonance imaging: a feasibility study and meta-analysis. Am J Physiol Regul Integr Comp Physiol. 2018 Oct 1;315(4):R638–45.

29. Teixeira AL, Daher M, Souza MC, Ramos PS, Fisher JP, Vianna LC. Sympathetically mediated cardiac responses to isolated muscle metaboreflex activation following exercise are modulated by body position in humans. Am J Physiol Heart Circ Physiol. 2018 Mar 1;314(3):H593–H602.

30. Egana M, Green S, Garrigan EJ, Warmington S. Effect of posture on high-intensity constant-load cycling performance in men and women. Eur J Appl Physiol. 2006 Jan;96(1):1–9.

31. Convertino VA, Goldwater DJ, Sandler H. Oxygen uptake kinetics of constant-load work: upright vs. supine exercise. Aviat Space Environ Med. 1984 Jun;55(6):501–6.

32. Egana M, Smith S, Green S. Revisiting the effect of posture on high-intensity constant-load cycling performance in men and women. Eur J Appl Physiol. 2007 Mar;99(5):495–501.

33. Bonzheim SC, Franklin BA, DeWitt C, Marks C, Goslin B, Jarski R, et al. Physiologic responses to recumbent versus upright cycle ergometry, and implications for exercise prescription in patients with coronary artery disease. Am J Cardiol. 1992 Jan 1;69(1):40–4.

34. Reddy YNV, Olson TP, Obokata M, Melenovsky V, Borlaug BA. Hemodynamic Correlates and Diagnostic Role of Cardiopulmonary Exercise Testing in Heart Failure With Preserved Ejection Fraction. JACC: Heart Failure. 2018 Aug;6(8):665–75.

35. Walsh-Riddle M, Blumenthal JA. Cardiovascular responses during upright and semi-recumbent cycle ergometry testing. Medicine &

Science in Sports & Exercise. 1989 Oct;21(5):581–5.

36. ATS/ACCP Statement on Cardiopulmonary Exercise Testing. Am J Respir Crit Care Med. 2003 Jan 15;167(2):211–77.

37. Mauritz KA, Moore RB. State of Understanding of Nafion. Chemical Reviews. 2004 Oct;104(10):4535–86.

38. Takken T, Blank AC, Hulzebos EH, van Brussel M, Groen WG, Helders PJ. Cardiopulmonary exercise testing in congenital heart disease: (contra)indications and interpretation. Neth Heart J. Springer; 2009 Oct;17(10):385–92.

39. Beltz NM, Gibson AL, Janot JM, Kravitz L, Mermier CM, Dalleck LC. Graded Exercise Testing Protocols for the Determination of VO2max: Historical Perspectives, Progress, and Future Considerations. J Sports Med (Hindawi Publ Corp). Hindawi; 2016;2016(1):3968393–12.

40. Myers J, Bellin D. Ramp exercise protocols for clinical and cardiopulmonary exercise testing. Sports Med. 2000 Jul;30(1):23–9.

41. Armstrong N, Welsman J, Winsley R. Is peak VO2 a maximal index of children's aerobic fitness? Int J Sports Med. 1996 Jul;17(5):356–9.

42. Barron A, Dhutia N, Mayet J, Hughes AD, Francis DP, Wensel R. Test-retest repeatability of cardiopulmonary exercise test variables in patients with cardiac or respiratory disease. Eur J Prev Cardiol. 2014 Apr;21(4):445–53.

43. Whipp BJ, Higgenbotham MB, Cobb FC. Estimating exercise stroke volume from asymptotic oxygen pulse in humans. J Appl Physiol (1985). American Physiological SocietyBethesda, MD; 1996 Dec;81(6):2674–9.

44. Oliveira RB, Myers J, Araújo CGS de. Long-term stability of the oxygen pulse curve during maximal exercise. Clinics (Sao Paulo). Hospital das Clinicas da Faculdade de Medicina da Universidade de Sao Paulo; 2011;66(2):203–9.

45. Rhodes J, Tikkanen AU, Jenkins KJ. Exercise Testing and Training in Children With Congenital Heart Disease. Circulation. Lippincott Williams & Wilkins; 2010 Nov 9;122(19):1957–67.

46. Khrisanapant W, Promsrisuk T, Pasurivong O, Boonsawat W, Patjanasoontorn B, Benjapornlert P. Influence of age, weight and height on oxygen pulse during maximal exercise. European Respiratory Journal. European Respiratory Society; 2016 Sep 1;48(suppl 60):PA2282.

47. Perim RR, Signorelli GR, Myers J, Arena R, Araújo CGS de. The slope of the oxygen pulse curve does not depend on the maximal heart rate in

elite soccer players. Clinics. Faculdade de Medicina / USP; 2011;66(5):829–35.

48. Bansal M, Fiutem JJ, Hill JA, O'Riordan MA, Zahka KG. Oxygen pulse kinetics in Fontan patients during treadmill ramp protocol cardiopulmonary exercise testing. Pediatr Cardiol. Springer-Verlag; 2012 Dec;33(8):1301–6.

49. Wallace AG, Sarnoff SJ. Effects of Cardiac Sympathetic Nerve Stimulation on Conduction in the Heart. Circulation Research. American Heart Association, Inc; 1964 Jan;14(1):86–92.

50. Balady GJ, Arena R, Sietsema K, Myers J, Coke L, Fletcher GF, et al. Clinician's Guide to cardiopulmonary exercise testing in adults: a scientific statement from the American Heart Association. Vol. 122, Circulation. Lippincott Williams & Wilkins; 2010. pp. 191–225.

51. Blais S, Berbari J, Counil F-P, Dallaire F. A Systematic Review of Reference Values in Pediatric Cardiopulmonary Exercise Testing. Pediatr Cardiol. Springer US; 2015 Jun 3;36(8):1553–64.

52. Paap D, Takken T. Reference values for cardiopulmonary exercise testing in healthy adults: a systematic review. Expert Review of Cardiovascular Therapy. 2014 Dec;12(12):1439–53.

53. Abumehdi MR, Wardle AJ, Nazzal R, Charalampopoulos A, Schulze-Neick I, Derrick G, et al. Feasibility and safety of cardiopulmonary exercise testing in children with pulmonary hypertension. Cardiol Young. 2015 Sep;26(6):1144–50.

54. Nadruz W, West E, Sengeløv M, Santos M, Groarke JD, Forman DE, et al. Prognostic Value of Cardiopulmonary Exercise Testing in Heart Failure With Reduced, Midrange, and Preserved Ejection Fraction. J Am Heart Assoc. 2017 Oct 31;6(11):e006000.

55. Poggio R, Arazi HC, Giorgi M, Miriuka SG. Prediction of severe cardiovascular events by VE/VCO2 slope versus peak VO2 in systolic heart failure: a meta-analysis of the published literature. Am Heart J. 2010 Dec;160(6):1004–14.

56. Kempny A, Dimopoulos K, Uebing A, Moceri P, Swan L, Gatzoulis MA, et al. Reference values for exercise limitations among adults with congenital heart disease. Relation to activities of daily life--single centre experience and review of published data. European Heart Journal. 2012 Jun;33(11):1386–96.

57. Dallaire F, Wald RM, Marelli A. The Role of Cardiopulmonary Exercise Testing for Decision Making in Patients with Repaired Tetralogy of Fallot. Pediatr Cardiol. 5 ed. Springer US; 2017 Aug;38(6):1097–105.

58. Egbe AC, Driscoll DJ, Khan AR, Said SS, Akintoye E, Berganza FM, et

al. Cardiopulmonary exercise test in adults with prior Fontan operation: The prognostic value of serial testing. Int J Cardiol. 2017 May 15;235:6–10.

59. Wax D, Garofano R, Barst RJ. Effects of Long-term Infusion of Prostacyclin on Exercise Performance in Patients With Primary Pulmonary Hypertension. Chest. 1999 Oct;116(4):914–20.

60. Wensel R, Opitz CF, Ewert R, Bruch L, Kleber FX. Effects of iloprost inhalation on exercise capacity and ventilatory efficiency in patients with primary pulmonary hypertension. Circulation. American Heart Association, Inc; 2000 May 23;101(20):2388–92.

61. Groepenhoff H, Vonk-Noordegraaf A, van de Veerdonk MC, Boonstra A, Westerhof N, Bogaard HJ. Prognostic Relevance of Changes in Exercise Test Variables in Pulmonary Arterial Hypertension. Kuwana M, editor. PLoS One. Public Library of Science; 2013 Sep 5;8(9):e72013.

62. Deboeck G, Scoditti C, Huez S, Vachiéry J-L, Lamotte M, Sharples L, et al. Exercise testing to predict outcome in idiopathic versusassociated pulmonary arterial hypertension. European Respiratory Journal. 2012 Nov 30;40(6):1410–9.

63. Rausch CM, Taylor AL, Ross H, Sillau S, Ivy DD. Ventilatory efficiency slope correlates with functional capacity, outcomes, and disease severity in pediatric patients with pulmonary hypertension. Int J Cardiol. 2013 Nov;169(6):445–8.

64. Maron BA, Cockrill BA, Waxman AB, Systrom DM. The invasive cardiopulmonary exercise test. Circulation. 2013 Mar;127(10):1157–64.

65. Huang W, Resch S, Oliveira RK, Cockrill BA, Systrom DM, Waxman AB. Invasive cardiopulmonary exercise testing in the evaluation of unexplained dyspnea: Insights from a multidisciplinary dyspnea center. Eur J Prev Cardiol. 5 ed. 2017 Jul;24(11):1190–9.

66. Lancellotti P, Pellikka PA, Budts W, Chaudhry FA, Donal E, Dulgheru R, et al. The Clinical Use of Stress Echocardiography in Non-Ischaemic Heart Disease: Recommendations from the European Association of Cardiovascular Imaging and the American Society of Echocardiography. J Am Soc Echocardiogr. 2017 Feb;30(2):101–38.

67. Sicari R, Nihoyannopoulos P, Evangelista A, Kasprzak J, Lancellotti P, Poldermans D, et al. Stress echocardiography expert consensus statement: European Association of Echocardiography (EAE) (a registered branch of the ESC). 2008. pp. 415–37.

68. Charloux A, Lonsdorfer-Wolf E, Richard R, Lampert E, Oswald-Mammosser M, Mettauer B, et al. A new impedance cardiograph device for the non-invasive evaluation of cardiac output at rest and during

exercise: comparison with the “direct” Fick method. Eur J Appl Physiol. Springer-Verlag; 2000 Jul 24;82(4):313–20.

69. Welsman J, Bywater K, Farr C, Welford D, Armstrong N. Reliability of peak VO2 and maximal cardiac output assessed using thoracic bioimpedance in children. Eur J Appl Physiol. Springer-Verlag; 2005 May 26;94(3):228–34.

70. Rowland T, Whatley Blum J. Cardiac dynamics during upright cycle exercise in boys. American Journal of Human Biology. John Wiley & Sons, Ltd; 2000;12(6):749–57.

71. Nottin S, Vinet A, Lecoq A-M, Guenon P, Obert P. Test-Retest Reproducibility of Submaximal and Maximal Cardiac Output by Doppler Echocardiography and CO 2-Rebreathing in Prepubertal Children. Pediatr Exerc Sci. 2001 Aug;13(3):214–24.

72. Panagiotou M, Vogiatzis I, Jayasekera G, Louvaris Z, Mackenzie A, Mcglinchey N, et al. Validation of impedance cardiography in pulmonary arterial hypertension. Clin Physiol Funct Imaging. 2018 Mar;38(2):254–60.

73. Legendre A, Bonnet D, Bosquet L. Reliability of Peak Exercise Stroke Volume Assessment by Impedance Cardiography in Patients with Residual Right Outflow Tract Lesions After Congenital Heart Disease Repair. Pediatr Cardiol. 2nd ed. Springer US; 2018 Jan;39(1):45–50.

74. Jakovljevic DG, Trenell MI, MacGowan GA. Bioimpedance and bioreactance methods for monitoring cardiac output. Best Practice & Research Clinical Anaesthesiology. Elsevier Ltd; 2014 Dec;28(4):381–94.

75. Jones TW, Houghton D, Cassidy S, MacGowan GA, Trenell MI, Jakovljevic DG. Bioreactance is a reliable method for estimating cardiac output at rest and during exercise. Br J Anaesth. 2015 Sep;115(3):386–91.

76. Myers J, Gujja P, Neelagaru S, Burkhoff D. Cardiac output and cardiopulmonary responses to exercise in heart failure: application of a new bio-reactance device. J Card Fail. 2007 Oct;13(8):629–36.

77. Gama de Abreu M, Winkler T, Pahlitzsch T, Weismann D, Albrecht DM. Performance of the partial CO2 rebreathing technique under different hemodynamic and ventilation/perfusion matching conditions. Crit Care Med. 2003 Feb;31(2):543–51.

78. Ohlsson J, Wranne B. Non-invasive assessment of cardiac output and stroke volume in patients during exercise. European Journal of Applied Physiology and Occupational Physiology. 7 ed. Springer-Verlag; 1986 Sep;55(5):538–44.

79. Hassan M, Wagdy K, Kharabish A, Elguindy A, Nabil A, Philip P, et al. Inert Gas Rebreathing for Non-Invasive Quantification of Cardiac Output: Validation Against Cardiac Catheterization and Magnetic Resonance Imaging. J Card Fail. 2016 Aug;22(8):S52.

80. Saur J, Trinkmann F, Doesch C, Weissmann J, Hamm K, Schoenberg SO, et al. Non-Invasive Measurement of Cardiac Output during Atrial Fibrillation: Comparison between Cardiac Magnetic Resonance Imaging and Inert Gas Rebreathing. Cardiology. 2010;115(3):212–6.

81. Peyton PJ, Thompson B. Agreement of an Inert Gas Rebreathing Device with Thermodilution and the Direct Oxygen Fick Method in Measurement of Pulmonary Blood Flow. Journal of Clinical Monitoring and Computing. 4 ed. Kluwer Academic Publishers; 2004 Dec;18(5-6):373–8.

82. Marma AK, Opotowsky AR, Fromm BS, Ubeda-Tikkanen A, Porras D, Rhodes J. Noninvasive cardiac output estimation by inert gas rebreathing in pediatric and congenital heart disease. Am Heart J. 2016 Apr;174:80–8.

83. Agostoni P, Vignati C, Gentile P, Boiti C, Farina S, Salvioni E, et al. Reference Values for Peak Exercise Cardiac Output in Healthy Individuals. Chest. 2017 Jun;151(6):1329–37.

84. Cattadori G, Schmid J-P, Agostoni P. Noninvasive Measurement of Cardiac Output During Exercise by Inert Gas Rebreathing Technique. Heart Failure Clinics. 2009 Apr;5(2):209–15.

85. Bogert LWJ, Wesseling KH, Schraa O, Van Lieshout EJ, de Mol BAJM, van Goudoever J, et al. Pulse contour cardiac output derived from non-invasive arterial pressure in cardiovascular disease. Anaesthesia. Blackwell Publishing Ltd; 2010 Nov;65(11):1119–25.

86. Bartels SA, Stok WJ, Bezemer R, Boksem RJ, van Goudoever J, Cherpanath TGV, et al. Noninvasive cardiac output monitoring during exercise testing: Nexfin pulse contour analysis compared to an inert gas rebreathing method and respired gas analysis. Journal of Clinical Monitoring and Computing. Springer Netherlands; 2011 Oct;25(5):315–21.

87. Scott AD, Keegan J, Firmin DN. Motion in Cardiovascular MR Imaging. Radiology. Radiological Society of North America; 2009 Feb;250(2):331–51.

88. Usman M, Ruijsink B, Nazir MS, Cruz G, Prieto C. Free breathing whole-heart 3D CINE MRI with self-gated Cartesian trajectory. Magn Reson Imaging. 2017 May;38:129–37.

89. Nayak KS, Nielsen J-F, Bernstein MA, Markl M, D Gatehouse P, M Botnar R, et al. Cardiovascular magnetic resonance phase contrast

imaging. Journal of Cardiovascular Magnetic Resonance. BioMed Central; 2015 Aug 9;17(1):776.

90. Srichai MB, Lim RP, Wong S, Lee VS. Cardiovascular applications of phase-contrast MRI. AJR Am J Roentgenol. American Roentgen Ray Society; 2009 Mar;192(3):662–75.

91. Lotz J, Meier C, Leppert A, Galanski M. Cardiovascular Flow Measurement with Phase-Contrast MR Imaging: Basic Facts and Implementation. RadioGraphics. Radiological Society of North America; 2002 May;22(3):651–71.

92. Powell AJ, Maier SE, Chung T, Geva T. Phase-velocity cine magnetic resonance imaging measurement of pulsatile blood flow in children and young adults: in vitro and in vivo validation. Pediatr Cardiol. 2000 Mar;21(2):104–10.

93. Beerbaum P, Körperich H, Barth P, Esdorn H, Gieseke J, Meyer H. Noninvasive quantification of left-to-right shunt in pediatric patients: phase-contrast cine magnetic resonance imaging compared with invasive oximetry. Circulation. 2001 May 22;103(20):2476–82.

94. Greil G, Geva T, Maier SE, Powell AJ. Effect of acquisition parameters on the accuracy of velocity encoded cine magnetic resonance imaging blood flow measurements. J Magn Reson Imaging. 2002 Jan;15(1):47–54.

95. Kilner PJ, Gatehouse PD, Firmin DN. Flow measurement by magnetic resonance: a unique asset worth optimising. J Cardiovasc Magn Reson. 2007;9(4):723–8.

96. Valsangiacomo Buechel ER, Grosse-Wortmann L, Fratz S, Eichhorn J, Sarikouch S, Greil GF, et al. Indications for cardiovascular magnetic resonance in children with congenital and acquired heart disease: an expert consensus paper of the Imaging Working Group of the AEPC and the Cardiovascular Magnetic Resonance Section of the EACVI. Cardiol Young. Cambridge University Press; 2015 Jun;25(5):819–38.

97. Nayak KS, Hu BS. The future of real-time cardiac magnetic resonance imaging. Current Cardiology Reports. Current Medicine Group; 2005 Jan;7(1):45–51.

98. Nayak KS, Pauly JM, Kerr AB, Hu BS, Nishimura DG. Real-time color flow MRI. Magn Reson Med. 2000 Feb;43(2):251–8.

99. Klein C, Schalla S, Schnackenburg B, Bornstedt A, Fleck E, Nagel E. Magnetic resonance flow measurements in real time: comparison with a standard gradient-echo technique. J Magn Reson Imaging. 2001 Sep;14(3):306–10.

100. Körperich H, Gieseke J, Barth P, Hoogeveen R, Esdorn H, Peterschröder

A, et al. Flow volume and shunt quantification in pediatric congenital heart disease by real-time magnetic resonance velocity mapping: a validation study. Circulation. American Heart Association, Inc; 2004 Apr 27;109(16):1987–93.

101. Nezafat R, Kellman P, Derbyshire JA, McVeigh ER. Real-time blood flow imaging using autocalibrated spiral sensitivity encoding. Magn Reson Med. Wiley-Blackwell; 2005 Dec;54(6):1557–61.

102. Steeden JA, Atkinson D, Taylor AM, Muthurangu V. Assessing vascular response to exercise using a combination of real-time spiral phase contrast MR and noninvasive blood pressure measurements. J Magn Reson Imaging. Wiley Subscription Services, Inc., A Wiley Company; 2010 Apr;31(4):997–1003.

103. Geva T. Is MRI the preferred method for evaluating right ventricular size and function in patients with congenital heart disease?: MRI is the preferred method for evaluating right ventricular size and function in patients with congenital heart disease. Circ Cardiovasc Imaging. American Heart Association, Inc; 2014 Jan;7(1):190–7.

104. Kawel-Boehm N, Maceira A, Valsangiacomo-Buechel ER, Vogel-Claussen J, Turkbey EB, Williams R, et al. Normal values for cardiovascular magnetic resonance in adults and children. Journal of Cardiovascular Magnetic Resonance. 3rd ed. BioMed Central; 2015 Apr 18;17(1):29.

105. Muthurangu V, Lurz P, Critchely JD, Deanfield JE, Taylor AM, Hansen MS. Real-time assessment of right and left ventricular volumes and function in patients with congenital heart disease by using high spatiotemporal resolution radial k-t SENSE. Radiology. 2008 Sep;248(3):782–91.

106. Lurz P, Muthurangu V, Schievano S, Nordmeyer J, Bonhoeffer P, Taylor AM, et al. Feasibility and reproducibility of biventricular volumetric assessment of cardiac function during exercise using real-time radial k-t SENSE magnetic resonance imaging. J Magn Reson Imaging. Wiley Subscription Services, Inc., A Wiley Company; 2009 May;29(5):1062–70.

107. Wolk MJ, Bailey SR, Doherty JU, Douglas PS, Hendel RC, Kramer CM, et al. ACCF/AHA/ASE/ASNC/HFSA/HRS/SCAI/SCCT/SCMR/STS 2013 Multimodality Appropriate Use Criteria for the Detection and Risk Assessment of Stable Ischemic Heart Disease: A Report of the American College of Cardiology Foundation Appropriate Use Criteria Task Force, American Heart Association, American Society of Echocardiography, American Society of Nuclear Cardiology, Heart Failure Society of America, Heart Rhythm Society, Society for Cardiovascular Angiography and Interventions, Society of Cardiovascular Computed

Tomography, Society for Cardiovascular Magnetic Resonance, and Society of Thoracic Surgeons. Journal of the American College of Cardiology. Elsevier; 2014 Feb 4;63(4):380–406.

108. Siontis GC, Mavridis D, Greenwood JP, Coles B, Nikolakopoulou A, Jüni P, et al. Outcomes of non-invasive diagnostic modalities for the detection of coronary artery disease: network meta-analysis of diagnostic randomised controlled trials. BMJ. BMJ Publishing Group; 2018 Feb 21;360:k504.

109. Gargiulo P, Dellegrottaglie S, Bruzzese D, Savarese G, Scala O, Ruggiero D, et al. The prognostic value of normal stress cardiac magnetic resonance in patients with known or suspected coronary artery disease: a meta-analysis. Circ Cardiovasc Imaging. American Heart Association, Inc; 2013 Jul;6(4):574–82.

110. Pontone G, Andreini D, Guaricci AI, Rota C, Guglielmo M, Mushtaq S, et al. The STRATEGY Study (Stress Cardiac Magnetic Resonance Versus Computed Tomography Coronary Angiography for the Management of Symptomatic Revascularized Patients): Resources and Outcomes Impact. Circ Cardiovasc Imaging. American Heart Association, Inc; 2016 Oct;9(10):e005171.

111. Chotenimitkhun R, Hundley WG. Pharmacological stress cardiovascular magnetic resonance. Postgrad Med. 2011 May;123(3):162–70.

112. Rang HP, Dale MM, Ritter JM, Flower RJ, Henderson G. Purines. In: Rang & Dale's Pharmacology. Elsevier; 2012. pp. 204–7.

113. Marwick TH. Adenosine echocardiography in the diagnosis of coronary artery disease. European Heart Journal. 1997 Jun 2;18(suppl D):31–6.

114. Nagel E, Lorenz C, Baer F, Hundley WG, Wilke N, Neubauer S, et al. Stress Cardiovascular Magnetic Resonance: Consensus Panel Report. Journal of Cardiovascular Magnetic Resonance. 2001 Oct 31;3(3):267–81.

115. Anna Mitręga K, Stankiewicz M, Krzeminski TF. Positive Inotropic Drugs and Drugs Used in Dysrhythmias. Side Effects of Drugs Annual. Elsevier; 2014 Jan 1;36:257–65.

116. Charoenpanichkit C, Hundley WG. The 20 year evolution of dobutamine stress cardiovascular magnetic resonance. Journal of Cardiovascular Magnetic Resonance. BioMed Central; 2010 Oct 26;12(1):59.

117. Monmeneu Menadas JV, Lopez-Lereu MP, Estornell Erill J, Garcia Gonzalez P, Igual Muñoz B, Maceira Gonzalez A. Pharmacological stress cardiovascular magnetic resonance: feasibility and safety in a large multicentre prospective registry. Eur Heart J Cardiovasc Imaging. 2016 Mar;17(3):308–15.

118. Ntsinjana HN, Hughes ML, Taylor AM. The Role of Cardiovascular Magnetic Resonance in Pediatric Congenital Heart Disease. Journal of Cardiovascular Magnetic Resonance. BioMed Central; 2011;13(1):51.

119. Ntsinjana H, Tann O, Hughes M, Schievano S, Muthurangu V, Taylor A. Role of adenosine stress perfusion CMR in guiding clinical decision making in pediatric and congenital cardiology: a single pediatric center experience. Journal of Cardiovascular Magnetic Resonance. BioMed Central; 2014 Jan 1;16(1):P128.

120. Knobelsdorff-Brenkenhoff von F, Dieringer MA, Fuchs K, Hezel F, Niendorf T, Schulz-Menger J. Isometric handgrip exercise during cardiovascular magnetic resonance imaging: set-up and cardiovascular effects. J Magn Reson Imaging. Wiley Subscription Services, Inc., A Wiley Company; 2013 Jun;37(6):1342–50.

121. Mortensen KH, Jones A, Steeden JA, Taylor AM, Muthurangu V. Isometric stress in cardiovascular magnetic resonance-a simple and easily replicable method of assessing cardiovascular differences not apparent at rest. Eur Radiol. Springer Berlin Heidelberg; 2016 Apr;26(4):1009–17.

122. Alegret JM, Beltran-Debon R, Franco L, Rubio F, Ligero C, Palazon O, et al. Effect of isometric exercise on aortic regurgitation assessed by cardiovascular magnetic resonance. European Heart Journal. 2013 Sep 3;34(suppl 1):1908–8.

123. Hays AG, Iantorno M, Schär M, Mukherjee M, Stuber M, Gerstenblith G, et al. Local coronary wall eccentricity and endothelial function are closely related in patients with atherosclerotic coronary artery disease. Journal of Cardiovascular Magnetic Resonance. BioMed Central; 2017 Jul 6;19(1):51.

124. Rerkpattanapipat P, Gandhi SK, Darty SN, Williams RT, Davis AD, Mazur W, et al. Feasibility to detect severe coronary artery stenoses with upright treadmill exercise magnetic resonance imaging. Am J Cardiol. 2003 Sep 1;92(5):603–6.

125. Jekic M, Foster EL, Ballinger MR, Raman SV, Simonetti OP. Cardiac function and myocardial perfusion immediately following maximal treadmill exercise inside the MRI room. Journal of Cardiovascular Magnetic Resonance. BioMed Central; 2008 Jan 15;10(1):3.

126. Foster EL, Arnold JW, Jekic M, Bender JA, Balasubramanian V, Thavendiranathan P, et al. MR-compatible treadmill for exercise stress cardiac magnetic resonance imaging. Magn Reson Med. 2012 Mar;67(3):880–9.

127. Nandi PS, Spodick DH. Recovery from exercise at varying work loads. Time course of responses of heart rate and systolic intervals. Br Heart J. BMJ Group; 1977 Sep;39(9):958–66.

128. Lafountain RA, da Silveira JS, Varghese J, Mihai G, Scandling D, Craft J, et al. Cardiopulmonary exercise testing in the MRI environment. Physiological Measurement. IOP Publishing; 2016 Apr 1;37(4):N11–N25.

129. Schaefer S, Peshock RM, Parkey RW, Willerson JT. A new device for exercise MR imaging. AJR Am J Roentgenol. American Roentgen Ray Society; 1986 Dec;147(6):1289–90.

130. Cheng CP, Schwandt DF, Topp EL, Anderson JH, Herfkens RJ, Taylor CA. Dynamic exercise imaging with an MR-compatible stationary cycle within the general electric open magnet. Magn Reson Med. Wiley Subscription Services, Inc., A Wiley Company; 2003 Mar;49(3):581–5.

131. Cheng CP, Herfkens RJ, Lightner AL, Taylor CA, Feinstein JA. Blood flow conditions in the proximal pulmonary arteries and vena cavae: healthy children during upright cycling exercise. Am J Physiol Heart Circ Physiol. American Physiological Society; 2004 Aug;287(2):H921–6.

132. Mohiaddin RH, Gatehouse PD, Firmin DN. Exercise-related changes in aortic flow measured with spiral echo-planar MR velocity mapping. J Magn Reson Imaging. 1995 Mar;5(2):159–63.

133. Niezen RA, Doornbos J, van der Wall EE, de Roos A. Measurement of aortic and pulmonary flow with MRI at rest and during physical exercise. J Comput Assist Tomogr. 1998 Mar;22(2):194–201.

134. Weber TF, Tengg-Kobligk von H, Kopp-Schneider A, Ley-Zaporozhan J, Kauczor H-U, Ley S. High-resolution phase-contrast MRI of aortic and pulmonary blood flow during rest and physical exercise using a MRI compatible bicycle ergometer. Eur J Radiol. 2011 Oct;80(1):103–8.

135. Pieles GE, Szantho G, Rodrigues JCL, Lawton CB, Stuart AG, Bucciarelli-Ducci C, et al. Adaptations of aortic and pulmonary artery flow parameters measured by phase-contrast magnetic resonance angiography during supine aerobic exercise. Eur J Appl Physiol. Springer Berlin Heidelberg; 2014 May;114(5):1013–23.

136. Forouzan O, Flink E, Warczytowa J, Thate N, Hanske A, Lee T, et al. Low Cost Magnetic Resonance Imaging-Compatible Stepper Exercise Device for Use in Cardiac Stress Tests. J Med Device. 2014 Dec;8(4):0450021–8.

137. Heiberg J, Asschenfeldt B, Maagaard M, Ringgaard S. Dynamic bicycle exercise to assess cardiac output at multiple exercise levels during magnetic resonance imaging. Clinical Imaging. 2017 Nov;46:102–7.

138. Wei Z, Whitehead KK, Khiabani RH, Tree M, Tang E, Paridon SM, et al. Respiratory Effects on Fontan Circulation During Rest and Exercise Using Real-Time Cardiac Magnetic Resonance Imaging. Ann Thorac

Surg. 2016 May;101(5):1818–25.

139. Roest AA, Kunz P, Lamb HJ, Helbing WA, van der Wall EE, de Roos A. Biventricular response to supine physical exercise in young adults assessed with ultrafast magnetic resonance imaging. Am J Cardiol. 2001 Mar 1;87(5):601–5.

140. Gusso S, Salvador C, Hofman P, Cutfield W, Baldi JC, Taberner A, et al. Design and testing of an MRI-compatible cycle ergometer for non-invasive cardiac assessments during exercise. Biomed Eng Online. 2012;11:13.

141. Steding-Ehrenborg K, Jablonowski R, Arvidsson PM, Carlsson M, Saltin B, Arheden H. Moderate intensity supine exercise causes decreased cardiac volumes and increased outer volume variations: a cardiovascular magnetic resonance study. J Cardiovasc Magn Reson. 2013;15:96.

142. Le T-T, Bryant JA, Ting AE, Ho PY, Su B, Teo RCC, et al. Assessing exercise cardiac reserve using real-time cardiovascular magnetic resonance. Journal of Cardiovascular Magnetic Resonance. Journal of Cardiovascular Magnetic Resonance; 2017 Jan 13;:1–10.

143. La Gerche A, Claessen G, Van de Bruaene A, Pattyn N, Van Cleemput J, Gewillig M, et al. Cardiac MRI A New Gold Standard for Ventricular Volume Quantification During High-Intensity Exercise. Circ Cardiovasc Imaging. Lippincott Williams & Wilkins; 2013 Mar 1;6(2):329–38.

144. Claessen G, Claus P, Delcroix M, Bogaert J, La Gerche A, Heidbuchel H. Interaction between respiration and right versus left ventricular volumes at rest and during exercise: a real-time cardiac magnetic resonance study. Am J Physiol Heart Circ Physiol. 2014 Mar;306(6):H816–24.

145. Claessen G, La Gerche A, Wielandts J-Y, Bogaert J, Van Cleemput J, Wuyts W, et al. Exercise pathophysiology and sildenafil effects in chronic thromboembolic pulmonary hypertension. Heart. BMJ Publishing Group Ltd and British Cardiovascular Society; 2015 Apr;101(8):637–44.

146. Van de Bruaene A, La Gerche A, Claessen G, De Meester P, Devroe S, Gillijns H, et al. Sildenafil improves exercise hemodynamics in Fontan patients. Circ Cardiovasc Imaging. American Heart Association, Inc; 2014 Mar;7(2):265–73.

147. Caterini JE, Elzibak AH, St Michel EJ, McCrindle BW, Redington AN, Thompson S, et al. Characterizing blood oxygen level-dependent (BOLD) response following in-magnet quadriceps exercise. MAGMA. Springer Berlin Heidelberg; 2015 Jun;28(3):271–8.

148. Muller MD, Li Z, Sica CT, Luck JC, Gao Z, Blaha CA, et al. Muscle

oxygenation during dynamic plantar flexion exercise: combining BOLD MRI with traditional physiological measurements. Physiol Rep. 2016 Oct;4(20):e13004.

149. Hall ET, Sá RC, Holverda S, Arai TJ, Dubowitz DJ, Theilmann RJ, et al. The effect of supine exercise on the distribution of regional pulmonary blood flow measured using proton MRI. J Appl Physiol (1985). American Physiological Society Bethesda, MD; 2014 Feb 15;116(4):451–61.

150. Wells GD, Wilkes DL, Schneiderman JE, Rayner T, Elmi M, Selvadurai H, et al. Skeletal Muscle Metabolism in Cystic Fibrosis and Primary Ciliary Dyskinesia. Pediatric Research. Nature Publishing Group; 2011 Jan;69(1):40–5.

151. Ellwein L, Samyn MM, Danduran M, Schindler-Ivens S, Liebham S, LaDisa JF. Toward translating near-infrared spectroscopy oxygen saturation data for the non-invasive prediction of spatial and temporal hemodynamics during exercise. Biomechanics and Modeling in Mechanobiology. 2nd ed. Springer Berlin Heidelberg; 2016 Jul 4;16(1):75–96.

152. Mathewson KW, Haykowsky MJ, Thompson RB. Feasibility and reproducibility of measurement of whole muscle blood flow, oxygen extraction, and VO 2with dynamic exercise using MRI. Magn Reson Med. 2014 Dec 22;74(6):1640–51.

153. MHRA MAHPRA, 2015. Safety guidelines for magnetic resonance imaging equipment in clinical use [Internet]. Medicines and Healthcare Products …

. Available from: https://assets.publishing.service.gov.uk/government/uploads/system/uploads/attachment_data/file/476931/MRI_guidance_2015_-_4-02d1.pdf

154. Dill T. Contraindications to magnetic resonance imaging: non-invasive imaging. Heart. 2008 Jul;94(7):943–8.

155. Kowalik GT, Steeden JA, Pandya B, Odille F, Atkinson D, Taylor A, et al. Real-time flow with fast GPU reconstruction for continuous assessment of cardiac output. J Magn Reson Imaging. 2012 Dec;36(6):1477–82.

156. Odille F, Steeden JA, Muthurangu V, Atkinson D. Automatic segmentation propagation of the aorta in real-time phase contrast MRI using nonrigid registration. J Magn Reson Imaging. 2011 Jan;33(1):232–8.

157. Sekhon M, Cartwright M, Francis JJ. Acceptability of healthcare interventions: an overview of reviews and development of a theoretical framework. BMC Health Serv Res. BioMed Central; 2017 Jan

26;17(1):88.

158. Schonenberger E, Schnapauff D, Teige F, Laule M, Hamm B, Dewey M. Patient acceptance of noninvasive and invasive coronary angiography. PLoS One. Public Library of Science; 2007;2(2):e246.

159. Albouaini K, Egred M, Alahmar A, Wright DJ. Cardiopulmonary exercise testing and its application. Postgrad Med J. The Fellowship of Postgraduate Medicine; 2007 Nov;83(985):675–82.

160. Beaver WL, Wasserman K, Whipp BJ. A new method for detecting anaerobic threshold by gas exchange. J Appl Physiol (1985). 1986 Jun;60(6):2020–7.

161. Bland JM, Altman DG. Measuring agreement in method comparison studies. Statistical Methods in Medical Research. Sage PublicationsSage CA: Thousand Oaks, CA; 2016 Jul 2;8(2):135–60.

162. Kowalik GT, Knight DS, Steeden JA, Tann O, Odille F, Atkinson D, et al. Assessment of cardiac time intervals using high temporal resolution real-time spiral phase contrast with UNFOLDed-SENSE. Magn Reson Med. 2015 Feb;73(2):749–56.

163. Noonan V, Dean E. Submaximal Exercise Testing: Clinical Application and Interpretation. Phys Ther. Oxford University Press; 2000 Aug 1;80(8):782–807.

164. Bruce RA, Kusumi F, Hosmer D. Maximal oxygen intake and nomographic assessment of functional aerobic impairment in cardiovascular disease. Am Heart J. 1973 Apr;85(4):546–62.

165. Foster C, Jackson AS, Pollock ML, Taylor MM, Hare J, Sennett SM, et al. Generalized equations for predicting functional capacity from treadmill performance. Am Heart J. 1984 Jun;107(6):1229–34.

166. Woods PR, Bailey KR, Wood CM, Johnson BD. Submaximal exercise gas exchange is an important prognostic tool to predict adverse outcomes in heart failure. European Journal of Heart Failure. Wiley-Blackwell; 2011 Mar;13(3):303–10.

167. Chen C-A, Chen S-Y, Chiu H-H, Wang J-K, Chang C-I, Chiu I-S, et al. Prognostic value of submaximal exercise data for cardiac morbidity in Fontan patients. Medicine & Science in Sports & Exercise. 2014 Jan;46(1):10–5.

168. De Cort SC, Innes JA, Barstow TJ, Guz A. Cardiac output, oxygen consumption and arteriovenous oxygen difference following a sudden rise in exercise level in humans. J Physiol. 1991 Sep;441:501–12.

169. Lee EC, Fragala MS, Kavouras SA, Queen RM, Pryor JL, Casa DJ. Biomarkers in Sports and Exercise: Tracking Health, Performance, and

Recovery in Athletes. J Strength Cond Res. 2017 Oct;31(10):2920–37.

170. Institute of Medicine. Monitoring Metabolic Status: Predicting Decrements in Physiological and Cognitive Performance. Washington, DC: The National Academies Press; 2004.

171. Helmerhorst HJ, Brage S, Warren J, Besson H, Ekelund U. A systematic review of reliability and objective criterion-related validity of physical activity questionnaires. International Journal of Behavioral Nutrition and Physical Activity. BioMed Central; 2012;9(1):103.

172. Munn Z, Moola S, Lisy K, Riitano D, Murphy F. Claustrophobia in magnetic resonance imaging: A systematic review and meta-analysis. Radiography. 2015 May;21(2):e59–e63.

173. Harris LM, Robinson J, Menzies RG. Evidence for fear of restriction and fear of suffocation as components of claustrophobia. Behaviour Research and Therapy. 1999 Feb;37(2):155–9.

174. Edmonds JC, Yang H, King TS, Sawyer DA, Rizzo A, Sawyer AM. Claustrophobic tendencies and continuous positive airway pressure therapy non-adherence in adults with obstructive sleep apnea. Heart & Lung: The Journal of Acute and Critical Care. 2015 Mar;44(2):100–6.

175. Olsen ØE. MRI: How to perform a pediatric scan. Acta Radiologica. SAGE PublicationsSage UK: London, England; 2013 Nov;54(9):991–7.

176. Denis R, Perrey S. Influence of posture on pulmonary o2 uptake kinetics, muscle deoxygenation and myolectrical activity during heavy-intensity exercise. J Sports Sci Med. 2006;5(2):254–65.

177. Astrand PO. Measurement of maximal aerobic capacity. Can Med Assoc J. 1967 Mar;96(12):732–5.

178. Koga S, Shiojiri T, Shibasaki M, Kondo N, Fukuba Y, Barstow TJ. Kinetics of oxygen uptake during supine and upright heavy exercise. J Appl Physiol (1985). 1999 Jul;87(1):253–60.

179. NHS Health Survey For England 2016 [Internet]. [cited 2018 Apr 22]. Available from: http://healthsurvey.hscic.gov.uk/support-guidance/public-health/health-survey-for-england-2016.aspx

180. Jeneson JAL, Schmitz JPJ, Hilbers PAJ, Nicolay K. An MR-compatible bicycle ergometer for in-magnet whole-body human exercise testing. Magn Reson Med. Wiley Subscription Services, Inc., A Wiley Company; 2010 Jan;63(1):257–61.

181. Pesta D, Paschke V, Hoppel F, Kobel C, Kremser C, Esterhammer R, et al. Different metabolic responses during incremental exercise assessed by localized 31P MRS in sprint and endurance athletes and untrained individuals. Int J Sports Med. © Georg Thieme Verlag KG; 2013

Aug;34(8):669–75.

182. La Gerche A, Roberts T, Claessen G. The response of the pulmonary circulation and right ventricle to exercise: exercise-induced right ventricular dysfunction and structural remodeling in endurance athletes (2013 Grover Conference series). Pulmonary Circulation. 2014 Sep;4(3):407–16.

183. Moledina S, Pandya B, Bartsota M, Mortensen KH, McMillan M, Quyam S, et al. Prognostic significance of cardiac magnetic resonance imaging in children with pulmonary hypertension. Circ Cardiovasc Imaging. Lippincott Williams & Wilkins; 2013 May 1;6(3):407–14.

184. Geva T. Repaired tetralogy of Fallot: the roles of cardiovascular magnetic resonance in evaluating pathophysiology and for pulmonary valve replacement decision support. Journal of Cardiovascular Magnetic Resonance. BioMed Central; 2011;13(1):9.

185. Lammers AE, Apitz C, Zartner P, Hager A, Dubowy K-O, Hansmann G. Diagnostics, monitoring and outpatient care in children with suspected pulmonary hypertension/paediatric pulmonary hypertensive vascular disease. Expert consensus statement on the diagnosis and treatment of paediatric pulmonary hypertension. The European Paediatric Pulmonary Vascular Disease Network, endorsed by ISHLT and DGPK. Heart. BMJ Publishing Group Ltd and British Cardiovascular Society; 2016 May;102 Suppl 2(Suppl 2):ii1–13.

186. Lammers AE, Diller GP, Odendaal D, Tailor S, Derrick G, Haworth SG. Comparison of 6-min walk test distance and cardiopulmonary exercise test performance in children with pulmonary hypertension. Archives of Disease in Childhood. 2011 Jan 12;96(2):141–7.

187. Faria-Urbina M, Oliveira RKF, Segrera SA, Lawler L, Waxman AB, Systrom DM. Impaired systemic oxygen extraction in treated exercise pulmonary hypertension: a new engine in an old car? Pulmonary Circulation. SAGE PublicationsSage UK: London, England; 2018 Jan;8(1):2045893218755325.

188. Kwon EN, Mussatto K, Simpson PM, Brosig C, Nugent M, Samyn MM. Children and adolescents with repaired tetralogy of fallot report quality of life similar to healthy peers. Congenit Heart Dis. Wiley/Blackwell (10.1111); 2011 Jan;6(1):18–27.

189. van den Berg J, Wielopolski PA, Meijboom FJ, Witsenburg M, Bogers AJJC, Pattynama PMT, et al. Diastolic Function in Repaired Tetralogy of Fallot at Rest and during Stress: Assessment with MR Imaging. Radiology. Radiological Society of North America; 2007 Apr 1;243(1):212–9.

190. Valverde I, Parish V, Tzifa A, Head C, Sarikouch S, Greil G, et al. Cardiovascular MR dobutamine stress in adult tetralogy of Fallot:

disparity between CMR volumetry and flow for cardiovascular function. J Magn Reson Imaging. Wiley-Blackwell; 2011 Jun;33(6):1341–50.

191. Parish V, Valverde I, Kutty S, Head C, Qureshi SA, Sarikouch S, et al. Dobutamine stress MRI in repaired tetralogy of Fallot with chronic pulmonary regurgitation: a comparison with healthy volunteers. Int J Cardiol. 2013 Jun 5;166(1):96–105.

192. Real-Time Magnetic Resonance Assessment of Septal Curvature Accurately Tracks Acute Hemodynamic Changes in Pediatric Pulmonary Hypertension. Circ Cardiovasc Imaging. Lippincott Williams & Wilkins; 2014 Jul 1;7(4):706–13.

193. ATS Committee on Proficiency Standards for Clinical Pulmonary Function Laboratories. ATS statement: guidelines for the six-minute walk test. Vol. 166, American Journal of Respiratory and Critical Care Medicine. 2002. pp. 111–7.

194. Mahle WT, McBride MG, Paridon SM. Exercise performance in tetralogy of Fallot: the impact of primary complete repair in infancy. Pediatr Cardiol. Springer-Verlag; 2002 Mar;23(2):224–9.

195. Sarikouch S, Koerperich H, Dubowy K-O, Boethig D, Boettler P, Mir TS, et al. Impact of gender and age on cardiovascular function late after repair of tetralogy of Fallot: percentiles based on cardiac magnetic resonance. Circ Cardiovasc Imaging. Lippincott Williams & Wilkins; 2011 Nov;4(6):703–11.

196. Sarikouch S, Peters B, Gutberlet M, Leismann B, Kelter-Kloepping A, Koerperich H, et al. Sex-specific pediatric percentiles for ventricular size and mass as reference values for cardiac MRI: assessment by steady-state free-precession and phase-contrast MRI flow. Circ Cardiovasc Imaging. Lippincott Williams & Wilkins; 2010 Jan;3(1):65–76.

197. Lurz P, Muthurangu V, Schuler PK, Giardini A, Schievano S, Nordmeyer J, et al. Impact of reduction in right ventricular pressure and/or volume overload by percutaneous pulmonary valve implantation on biventricular response to exercise: an exercise stress real-time CMR study. European Heart Journal. 2012 Oct 1;33(19):2434–41.

198. Redington AN. Low cardiac output due to acute right ventricular dysfunction and cardiopulmonary interactions in congenital heart disease (2013 Grover Conference series). Pulmonary Circulation. SAGE PublicationsSage UK: London, England; 2014 Jun;4(2):191–9.

199. Broberg CS, Aboulhosn J, Mongeon F-P, Kay J, Valente AM, Khairy P, et al. Prevalence of left ventricular systolic dysfunction in adults with repaired tetralogy of fallot. Am J Cardiol. 2011 Apr 15;107(8):1215–20.

200. Fernandes FP, Manlhiot C, Roche SL, Grosse-Wortmann L, Slorach C,

McCrindle BW, et al. Impaired left ventricular myocardial mechanics and their relation to pulmonary regurgitation, right ventricular enlargement and exercise capacity in asymptomatic children after repair of tetralogy of Fallot. J Am Soc Echocardiogr. 2012 May;25(5):494–503.

201. Tolle J, Waxman A, Systrom D. Impaired systemic oxygen extraction at maximum exercise in pulmonary hypertension. Medicine & Science in Sports & Exercise. 2008 Jan;40(1):3–8.

202. Potus F, Malenfant S, Graydon C, Mainguy V, Tremblay È, Breuils-Bonnet S, et al. Impaired angiogenesis and peripheral muscle microcirculation loss contribute to exercise intolerance in pulmonary arterial hypertension. Am J Respir Crit Care Med. American Thoracic Society; 2014 Aug 1;190(3):318–28.

203. Batt J, Shadly Ahmed S, Correa J, Bain A, Granton J. Skeletal Muscle Dysfunction in Idiopathic Pulmonary Arterial Hypertension. Am J Respir Cell Mol Biol. 2013 Aug 23;:130823100749008–13.

204. Enache I, Charles A-L, Bouitbir J, Favret F, Zoll J, Metzger D, et al. Skeletal muscle mitochondrial dysfunction precedes right ventricular impairment in experimental pulmonary hypertension. Mol Cell Biochem. Springer US; 2013 Jan;373(1-2):161–70.

205. Tolle JJ, Waxman AB, Van Horn TL, Pappagianopoulos PP, Systrom DM. Exercise-Induced Pulmonary Arterial Hypertension. Circulation. Lippincott Williams & Wilkins; 2008 Nov 18;118(21):2183–9.

206. Punn R, Obayashi DY, Olson I, Kazmucha JA, DePucci A, Hurley MP, et al. Supine Exercise Echocardiographic Measures of Systolic and Diastolic Function in Children. Journal of the American Society of Echocardiography. 2012 Jul;25(7):773–81.

207. Lin ACW, Strugnell WE, Seale H, Schmitt B, Schmidt M, O'Rourke R, et al. Exercise cardiac MRI-derived right ventriculo-arterial coupling ratio detects early right ventricular maladaptation in PAH. Eur Respir J. 2016 Dec;48(6):1797–800.

208. Pandya B, Moledina S, McKee A, Schulze I-N, Muthurangu V. Analysis of the septal curvature with CMR in the paediatric population with pulmonary hypertension is a useful tool. Journal of Cardiovascular Magnetic Resonance. BioMed Central Ltd; 2012 Feb 1;14(Suppl 1):P83.

209. Barber NJ, Ako EO, Kowalik GT, Steeden JA, Pandya B, Muthurangu V. MR augmented cardiopulmonary exercise testing—a novel approach to assessing cardiovascular function. Physiological Measurement. IOP Publishing; 2015 Sep 23;:85–94.

210. Marshall SP, Smith MS, Weinberger E. Perceived Anxiety of Pediatric Patients to Magnetic Resonance. Clinical Pediatrics. Sage

PublicationsSage CA: Thousand Oaks, CA; 2016 Jul 2;34(1):59–60.

211. Szeszak S, Man R, Love A, Langmack G, Wharrad H, Dineen RA. Animated educational video to prepare children for MRI without sedation: evaluation of the appeal and value. Pediatr Radiol. Springer Berlin Heidelberg; 2016 Nov;46(12):1744–50.

212. Frick MH, Somer T. Base-line effects on response of stroke volume to leg exercise in the supine position. J Appl Physiol. 1964 Jul;19:639–43.

213. Sun X-G, Hansen JE, Oudiz RJ, Wasserman K. Pulmonary function in primary pulmonary hypertension. Journal of the American College of Cardiology. 2003 Mar;41(6):1028–35.

214. Fontan F, Baudet E. Surgical repair of tricuspid atresia. Thorax. 1971 May;26(3):240–8.

215. Pundi KN, Johnson JN, Dearani JA, Pundi KN, Li Z, Hinck CA, et al. 40-Year Follow-Up After the Fontan Operation: Long-Term Outcomes of 1,052 Patients. Journal of the American College of Cardiology. 2015 Oct;66(15):1700–10.

216. Takken T, Tacken MHP, Blank AC, Hulzebos EH, Strengers JLM, Helders PJM. Exercise limitation in patients with Fontan circulation: a review. J Cardiovasc Med (Hagerstown). 2007 Oct;8(10):775–81.

217. Takken T, Hulzebos HJ, Blank AC, Tacken MHP, Helders PJM, Strengers JLM. Exercise prescription for patients with a Fontan circulation: current evidence and future directions. Neth Heart J. 2007;15(4):142–7.

218. Inai K, Saita Y, Takeda S, Nakazawa M, Kimura H. Skeletal muscle hemodynamics and endothelial function in patients after Fontan operation. Am J Cardiol. 2004 Mar;93(6):792–7.

219. Binotto MA, Maeda NY, Lopes AA. Altered endothelial function following the Fontan procedure. Cardiol Young. 2008 Feb;18(1):70–4.

220. Avitabile CM, Leonard MB, Zemel BS, Brodsky JL, Lee D, Dodds K, et al. Lean mass deficits, vitamin D status and exercise capacity in children and young adults after Fontan palliation. Heart. 2014 Nov;100(21):1702–7.

221. Atz AM, Zak V, Mahony L, Uzark K, D'agincourt N, Goldberg DJ, et al. Longitudinal Outcomes of Patients With Single Ventricle After the Fontan Procedure. Journal of the American College of Cardiology. 2017 Jun 6;69(22):2735–44.

222. Hollingsworth KG, de Sousa PL, Straub V, Carlier PG. Towards harmonization of protocols for MRI outcome measures in skeletal muscle studies: consensus recommendations from two TREAT-NMD

NMR workshops, 2 May 2010, Stockholm, Sweden, 1-2 October 2009, Paris, France. Neuromuscul Disord. 2012 Oct 1;22 Suppl 2:S54–67.

223. Brassard P, Bédard E, Jobin J, Rodés-Cabau J, Poirier P. Exercise capacity and impact of exercise training in patients after a Fontan procedure: a review. Can J Cardiol. Pulsus Group; 2006 May 1;22(6):489–95.

224. Sutherland N, Jones B, d'Udekem Y. Should We Recommend Exercise after the Fontan Procedure? Heart Lung Circ. 2015 Aug;24(8):753–68.

225. Jacobsen RM, Ginde S, Mussatto K, Neubauer J, Earing M, Danduran M. Can a Home-based Cardiac Physical Activity Program Improve the Physical Function Quality of Life in Children with Fontan Circulation? Congenit Heart Dis. 2016 Mar;11(2):175–82.

226. Tagliafico A, Bignotti B, Tagliafico G, Martinoli C. Usefulness of IDEAL T2 imaging for homogeneous fat suppression and reducing susceptibility artefacts in brachial plexus MRI at 3.0 T. Radiol Med. Springer Milan; 2016 Jan;121(1):45–53.

227. Borg GA. Psychophysical bases of perceived exertion. Medicine & Science in Sports & Exercise. 1982;14(5):377–81.

228. Ohuchi H, Hasegawa S, Yasuda K, Yamada O, Ono Y, Echigo S. Severely impaired cardiac autonomic nervous activity after the Fontan operation. Circulation. American Heart Association, Inc; 2001 Sep 25;104(13):1513–8.

229. Kouatli AA, Garcia JA, Zellers TM, Weinstein EM, Mahony L. Enalapril does not enhance exercise capacity in patients after Fontan procedure. Circulation. 1997 Sep 2;96(5):1507–12.

230. Burr JF, Bredin SSD, Faktor MD, Warburton DER. The 6-minute walk test as a predictor of objectively measured aerobic fitness in healthy working-aged adults. Phys Sportsmed. 2011 May;39(2):133–9.

231. d'Udekem Y, Fernando N, Plessis du K. Ask not what your Fontan can do for you, ask what you can do for your Fontan! J Thorac Cardiovasc Surg. 2018 Mar 10.

232. Segrera SA, Lawler L, Opotowsky AR, Systrom D, Waxman AB. Open label study of ambrisentan in patients with exercise pulmonary hypertension. Pulmonary Circulation. SAGE PublicationsSage UK: London, England; 2017 Apr;7(2):531–8.

233. Roest AAW, Helbing WA, Kunz P, van den Aardweg JG, Lamb HJ, Vliegen HW, et al. Exercise MR imaging in the assessment of pulmonary regurgitation and biventricular function in patients after tetralogy of fallot repair. Radiology. Radiological Society of North America; 2002 Apr;223(1):204–11.

234. Gatzoulis MA, Clark AL, Cullen S, Newman CG, Redington AN. Right ventricular diastolic function 15 to 35 years after repair of tetralogy of Fallot. Restrictive physiology predicts superior exercise performance. Circulation. 1995 Mar 15;91(6):1775–81.

235. Setser RM, Fischer SE, Lorenz CH. Quantification of left ventricular function with magnetic resonance images acquired in real time. J Magn Reson Imaging. 2000 Sep;12(3):430–8.

236. Tan LK, McLaughlin RA, Lim E, Abdul Aziz YF, Liew YM. Fully automated segmentation of the left ventricle in cine cardiac MRI using neural network regression. J Magn Reson Imaging. John Wiley & Sons, Ltd; 2018 Jan 9;48(1):140–52.

237. Roussakis A, Baras P, Seimenis I, Andreou J, Danias P. Relationship of Number of Phases per Cardiac Cycle and Accuracy of Measurement of Left Ventricular Volumes, Ejection Fraction, and Mass. J Cardiovasc Magn Reson. 2004 Dec 1;6(4):837–44.

238. Pushparajah K, Chubb H, Razavi R. MR-guided Cardiac Interventions. Top Magn Reson Imaging. 2018 Jun;27(3):115–28.

239. van der Graaf M. In vivo magnetic resonance spectroscopy: basic methodology and clinical applications. Eur Biophys J. Springer-Verlag; 2010 Mar;39(4):527–40.

240. Boss A, Kreis R, Saillen P, Zehnder M, Boesch C, Vermathen P. Skeletal muscle 1H MRSI before and after prolonged exercise. II. visibility of free carnitine. Magn Reson Med. 2012 Jan 27;68(5):1368–75.

241. Tevald MA, Foulis SA, Kent JA. Effect of age on in vivo oxidative capacity in two locomotory muscles of the leg. Age (Dordr). Springer Netherlands; 2014;36(5):9713.

242. Fiedler GB, Schmid AI, Goluch S, Schewzow K, Laistler E, Niess F, et al. Skeletal muscle ATP synthesis and cellular H+ handling measured by localized 31P-MRS during exercise and recovery. Scientific Reports. Nature Publishing Group; 2016 Aug 26;6(1):904.

243. Cannon DT, Bimson WE, Hampson SA, Bowen TS, Murgatroyd SR, Marwood S, et al. Skeletal muscle ATP turnover by 31P magnetic resonance spectroscopy during moderate and heavy bilateral knee extension. J Physiol. John Wiley & Sons, Ltd (10.1111); 2014 Dec 1;592(23):5287–300.

244. Murgatroyd SR, Ferguson C, Ward SA, Whipp BJ, Rossiter HB. Pulmonary O 2uptake kinetics as a determinant of high-intensity exercise tolerance in humans. J Appl Physiol (1985). American Physiological Society Bethesda, MD; 2011 Jun;110(6):1598–606.

245. Blanchard J, Blais S, Chetaille P, Bisson M, Counil FP, Girard TH, et al. New Reference Values for Cardiopulmonary Exercise Testing in Children. Medicine & Science in Sports & Exercise. 2018 Jan.

246. Ako E, Barber N, Kowalik GT, Steeden J, Porter J, Walker J, et al. UNDERSTANDING THE CARDIOPULMONARY CIRCULATION IN SICKLE CELL DISEASE: USING AN MR AUGMENTED CARDIOPULMONARY EXERCISE TESTING TECHNIQUE. Journal of the American College of Cardiology. 2016 Apr;67(13):2345.

247. Rhodes J. Impact of Cardiac Rehabilitation on the Exercise Function of Children With Serious Congenital Heart Disease. PEDIATRICS. 2005 Dec 1;116(6):1339–45.

248. Gewillig M, Brown SC, Eyskens B, Heying R, Ganame J, Budts W, et al. The Fontan circulation: who controls cardiac output? Interact Cardiovasc Thorac Surg. 1st ed. 2010 Mar;10(3):428–33.

249. Aiqi Sun, Bo Zhao, Rui Li, Chun Yuan. 4D real-time phase-contrast flow MRI with sparse sampling. Conf Proc IEEE Eng Med Biol Soc. IEEE; 2017 Jul;2017:3252–5.

250. Peterson S, Su JA, Szmuszkovicz JR, Johnson R, Sargent B. Exercise capacity following pediatric heart transplantation: A systematic review. Pediatr Transplant. 2017 Aug;21(5):e12922.

251. Ako E, Barber N, Steeden J, Walker M, Muthurangu V, MR C. A novel non-invasive method of assessing cardiovascular function using magnetic resonance augmented cardiopulmonary exercise testing. Journal of the American College of Cardiology. 2015;65(10):A1139.

Appendix I: Examples of research ethics committee approved recruitment poster, information sheet and consent form.

Hello!

Great Ormond Street Hospital for Children NHS
NHS Foundation Trust

We're looking for **healthy 8 to 16 year olds** to help us understand a heart and lung condition called Pulmonary Hypertension.

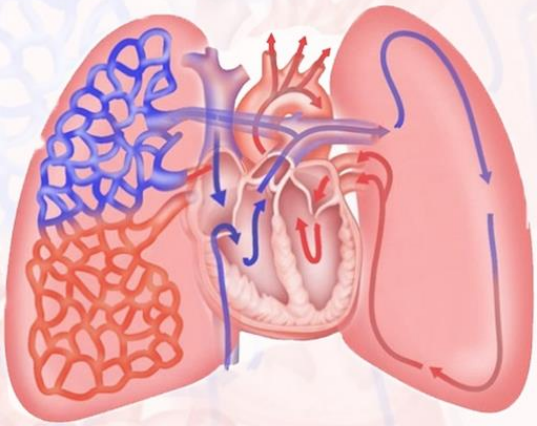

If you would be willing to come to Great Ormond Street Hospital for a **Magnetic Resonance Imaging (MRI)** scan of the heart while exercising, parents & guardians please email Dr Nathaniel Barber at:

nathaniel.barber@gosh.nhs.uk

- MRI scans are completely safe with no radiation exposure involved
- There are no blood tests or needles involved
- The whole visit will last no more than 45 minutes to 1 hour
- Volunteers take home a CD with MRI pictures of their heart

We look forward to hearing from you.

PIS 8-12yrs V3 270314
Rec ref: 14/LO/0720

Participant Information Sheet
Cardiac MRI Exercise Testing

Information for Children aged 10-12

Thank you for thinking about helping us with our research. Before you decide to take part it is important to understand why we are doing the research and what we would ask you to do if decide you would like to help. Don't worry if you don't understand any of the information here. We're also telling your parents or guardian about the research and would be really happy to answer any questions.

Why are we doing the research?

Several heart conditions including Tetralogy of Fallot (a heart condition you were born with and had repaired when you were a baby) can make it harder to exercise as you get older. We want to find out in more detail about how and why this happens.
The research is using the MRI (magnetic) scanner to take pictures of your heart while you exercise.

Why have I been chosen?

You have been chosen because you are a patient with repaired Tetralogy of Fallot at Great Ormond Street Hospital.
Because you're aged 8 to 16 years you're the perfect age to use the MRI exercise bike.

Do I have to take part?

No! It's up to you and your parents or guardians to decide. If you do decide you would like to help then:

1) A doctor will ask your parent or guardian to sign a consent (permission) form.
2) We would also like to offer you the opportunity to sign an assent form (this is like a consent form for children, but we also need your parent or guardian to sign the consent form)
3) If you change your mind and don't want to do it anymore that's fine. You can stop at any time. Just let us or your parent or guardian know. You don't have to tell us the reason for changing your mind.

What will happen if I decide to take part?

You will come to the MRI department at Great Ormond Street Hospital with your parent or guardian.
We will welcome you, check how you are feeling and that you are O.K. to have a scan that day. We will show you the exercise bike and how to use it.
We will use the MRI scanner to take pictures of your heart when you are resting and also when you are using the bike (the bike part will take about 7 minutes). During the scan we will give you some headphones to wear. If you like you can listen to some music. While you're having the scan we will give you a mask to wear that measures what you are breathing (most people find the mask quite comfortable to

wear). All the way through the scan you will be able to talk to your parent or guardian, the doctor and the person controlling the scan.

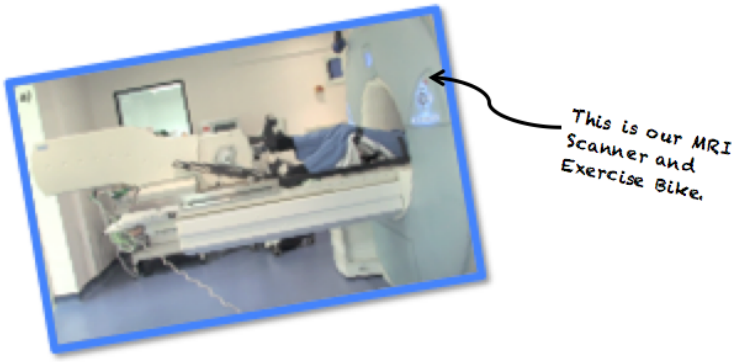

After you have finished you will be free to go home.

What are the benefits of taking part?

There is no individual benefit from helping. We will use the information we get from you to try to improve treatment for your condition in the future. We cannot promise the information we get will help you directly but it might help children in the future with the same problem.

Is it safe?

Yes MRI scanning and exercise testing are both very safe. The MRI scanner uses a giant magnet so we are very careful that only safe materials that won't get stuck to it go into the scanning room.

Sometimes people feel claustrophobic (like the space they're in is too tight) inside the MRI scanner. If this happens to you just let us know and we will stop the scan and help you get out.

Some people can feel their heart beating very fast or feel dizzy or unwell when they exercise. If this happens to you just let us know and we will stop the scan and help you get out.

The MRI scanner can also be quite noisy sometimes (from the parts moving inside) if you haven't been in it before. We will give you some headphones to wear to help.

What will happen if I don't want to carry on with the study?

If you change your mind just let us know and you can stop. You don't have to give a reason for stopping.

What if there's a problem?

If there's any kind of problem just let your parent/guardian or a member of the research team know and we will do our best to sort it out.

Will anyone else know I'm doing this?
No, not unless you want them to. All information collected for the study will be kept strictly confidential (so only people with a right to see it can see it).

What will happen to the results of the research study?
Once the results are ready we will share them with you and with doctors and nurses treating children with heart conditions that can make it harder to exercise. We hope that we will be able to publish the study in Medical Journals (specialist magazines/websites that get read around the world) so that as many people as possible can benefit from what we find out.

Who is organizing and paying for the research?
Great Ormond Street Hospital and the UCL Institute of Cardiovascular Science are organizing this study. This study is being paid for by the Great Ormond Street Hospital Children's Charity.

Who has reviewed the study?
The Research Ethics Committee: NRES Committee London - London Bridge

Thank you for taking the time to read this leaflet.

If you have any Extra Questions:
We'd be really happy to answer any questions. You can ask the person giving you this leaflet or alternatively you or your parent/guardian can contact:

Dr. Vivek Muthurangu, the lead investigator at v.muthurangu@ucl.ac.uk
Or Dr. Nathaniel Barber, Clinical Training Fellow.
Tel: 02074059200 x6840 email nathaniel.barber@ucl.ac.uk
Please ensure to put "MRI-CPET" as the subject.

Great Ormond Street Hospital for Children NHS
NHS Foundation Trust

Consent form
Rec ref:

CONSENT FORM

MR-Augmented Cardiopulmonary Exercise Testing in Pulmonary Hypertension – Fontan Group

Researchers: Dr. Vivek Muthurangu, Dr. Nathaniel Barber
Any questions to: Dr. Vivek Muthurangu, Great Ormond Street Hospital

	Please initial box
I confirm that I have read and understood the information sheet for the above study and have had the opportunity to ask questions.	
I understand that I will be referred to the appropriate medical service in the event of the finding of an abnormality.	
I understand that I can withdraw from this study at any time without giving a reason and that this will have no impact on my clinical care.	
I understand that the data collected may be presented anonymously.	
I understand that relevant sections of my medical notes and data collected during the study, may be looked at by individuals from regulatory authorities or from the NHS Trust, where it is relevant to my taking part in this research. I give permission for these individuals to have access to my records.	
I agree to taking part in the above study.	

Name of Participant	Date	Signature
Name of Consent Taker (If different to researcher)	Date	Signature
Name of Researcher	Date	Signature

Copies 1) For Participant 2) For Researcher 3) For Hospital Notes.

Appendix II: MRI Safety Checklist

Great Ormond Street Hospital: MRI Department

MRI Checklist Form

Name _____ **D.O.B.** _____ **Weight** ____

Hospital No. _____ **Date** ___/___/___ **Height** ____

1. Has your child had any previous MRI studies? ☐ Yes ☐ No
   If yes, please list Body part and date _____

Some of the following may be hazardous to your safety and some may interfere with the MRI examination. Please tick the correct answer for each of the following questions.

1. Have you ever had any heart surgery? ☐ Yes ☐ No

Pacemaker	☐ Yes ☐ No
Internal pacing wires	☐ Yes ☐ No
Vascular stents or clips	☐ Yes ☐ No
Artificial heart valve	☐ Yes ☐ No
Wire surgical staples	☐ Yes ☐ No
Any other heart implant	☐ Yes ☐ No

Which Person(s) have been metal checked to accompany the patient?

2. Have you ever had any head surgery? ☐ Yes ☐ No

Aneurysm clip or coil	☐ Yes ☐ No
Shunt (interventricular)	☐ Yes ☐ No
Shunt (programmable)	☐ Yes ☐ No
Neurostimulator	☐ Yes ☐ No
Cochlear implant	☐ Yes ☐ No
Any other metal head implant	☐ Yes ☐ No

3. Have you ever had spinal surgery? ☐ Yes ☐ No

Metal Rods in your spine	☐ Yes ☐ No
Any other metal spinal implants	☐ Yes ☐ No

4.Have you EVER had any other surgery? ☐ Yes ☐ No

Any metal implants as a result	☐ Yes ☐ No
Do you have a Hickman line	☐ Yes ☐ No

IMPORTANT

Please remove the following items from your person before entering the MRI scanner.

Keys, coins, watch
Credit cards
Rail/tube tickets
Any other metallic items.

IN ADDITION

Do you have any metal in your body as a result of an accident	☐ Yes ☐ No
Ever injured your eye with a metallic object (welding, shavings or foreign body)	☐ Yes ☐ No
Do you have a hearing aid	☐ Yes ☐ No
Do you have any metallic dental work	☐ Yes ☐ No
Do you have any body piercings	☐ Yes ☐ No
Is there any chance that you or your child could be pregnant	☐ Yes ☐ No
Do you have any drug allergies	☐ Yes ☐ No
Do you have any renal problems or impairment	☐ Yes ☐ No
Do you have any tattoos?	☐ Yes ☐ No
Are you breastfeeding?	c Yes c No
What is the date of your LMP?	

Signature of person completing form _____

Name and relationship _____

Signature of MRI personnel completing form _____

Appendix III: Gas Exchange Validation Data

GESV Target Values (VO2, VCO2, RQ, VE) for Gas Exchange Systems (Field Use Only)

1) Enter the Dry Gas Concentrations, the current Relative Humidity, Temperature and Barometric Pressure -- in the blue bordered boxes of the 'TEST DATA' Section.
2) Do not enter data into the yellow boxes on this form -- the yellow boxes will be populated automatically from data you enter into the blue boxes.
3) Enter the Respiratory Rates into the appropriate blue boxes as well as your measured values for the VO2 - STPD, VCO2 - STPD, V_E - STPD or V_E- BTPS.

GESV Settings - CAL DATA

	GESV Settings - CALIBRATION DATA Low Volume (L)	Med. Volume (L)	High Volume (L)	GESV	
nominal volume settings at low, med and high speed	1.0	1.5	1.5	GESV Serial # :	126000044
actual volume at low, med and high speed	0.962	1.478	1.482	Technician:	NAM
volume correction factor	1.038	1.015	1.012	Cal. Date:	
	Resp. Rate	Resp. Rate	Resp. Rate		

CAL DATA Rel Humidity (%)	CAL DATA Temperature °C	CAL DATA Barometer (mm HG)	CAL DATA PH_2O (mm Hg)	10.0 Orifice Flow Rate (L/min - ATPX)	20.0 Orifice Flow Rate (L/min - ATPX)	40.0 Orifice Flow Rate (L/min - ATPX)
9	23	742	21.07	1.678	9.391	15.607

TEST DATA

O2		CO2		GESV Settings - AMBIENT DATA (TEST) Low V_T Volume (L)	Medium V_T Volume (L)	High V_T Volume (L)	Model Number:	790-705-305
Dry Concentration:	20.93%	Dry Concentration:	20.60%	0.962	1.478	1.482	Umbilical Tab:	
Ambient:	20.75%	Ambient:	20.43%				Serial Number:	
				Resp. Rate	Resp. Rate	Resp. Rate	Technician:	

Rel Humidity (%)	TEST DATA Temperature (C)	TEST DATA Barometric Pressure (mmHg)	TEST DATA PH_2O (mmHg)	9.38 Orifice Flow Rate (L/min - ATPX)	19.29 Orifice Flow Rate (L/min - ATPX)	38.51 Orifice Flow Rate (L/min - ATPX)	Setup O2 Calibration Gas 12%	Setup CO2 Calibration Gas 5%
28	24	740	21.07	1.697	9.500	15.788	11.90%	4.96%

% Error Tolerance 7.5% OR Low Absolute Tolerance 0.03

	Low Acceptable	Target	High Acceptable	ACTUAL	
Low (Rest)	O2(L/min - STPD)	O2(L/min - STPD)	O2(L/min - STPD)	O2(L/min - STPD)	PASS
	0.269	0.290	0.312	0.279	
VO2 - STPD Medium (Exercise)	O2(L/min - STPD)	O2(L/min - STPD)	O2(L/min - STPD)	O2(L/min - STPD)	PASS
	1.572	1.700	1.827	1.606	
High (Exercise)	O2(L/min - STPD)	O2(L/min - STPD)	O2(L/min - STPD)	O2(L/min - STPD)	PASS
	2.627	2.840	3.053	2.837	

% Error Tolerance 7.5% OR Low Absolute Tolerance 0.03

	Low Acceptable	Target	High Acceptable	ACTUAL	
Low (Rest)	CO2(L/min - STPD)	CO2(L/min - STPD)	CO2(L/min - STPD)	CO2(L/min - STPD)	PASS
	0.264	0.286	0.307	0.285	
VCO2 - STPD Medium (Exercise)	CO2(L/min - STPD)	CO2(L/min - STPD)	CO2(L/min - STPD)	CO2(L/min - STPD)	PASS
	1.547	1.673	1.798	1.627	
High (Exercise)	CO2(L/min - STPD)	CO2(L/min - STPD)	CO2(L/min - STPD)	CO2(L/min - STPD)	PASS
	2.586	2.796	3.005	2.774	

% Error Tolerance 7.5% OR Low Absolute Tolerance 0.1

Actual RQ is autocalculated from Actual VO2 & VCO2

	Low Acceptable	Target	High Acceptable	ACTUAL	
Low (Rest)	RQ (RER)	RQ (RER)	RQ (RER)	RQ (RER)	PASS
	0.910	0.984	1.058	1.022	
RQ (RER) Medium (Exercise)	RQ (RER)	RQ (RER)	RQ (RER)	RQ (RER)	PASS
	0.910	0.984	1.058	1.013	
High (Exercise)	RQ (RER)	RQ (RER)	RQ (RER)	RQ (RER)	PASS
	0.910	0.984	1.058	0.978	

% Error Tolerance 5.0% OR Low Absolute Tolerance 0.0

VE values in STPD

	Low Acceptable	Target	High Acceptable	ACTUAL	
Low (Rest)	VE(Liters - STPD)	VE(Liters - STPD)	VE(Liters - STPD)		
	7.454	7.846	8.239		
V_E - STPD Medium (Exercise)	VE(Liters - STPD)	VE(Liters - STPD)	VE(Liters - STPD)	VE(Liters - ATPS)	PASS
	23.551	24.791	26.030	24.500	
High (Exercise)	VE(Liters - STPD)	VE(Liters - STPD)	VE(Liters - STPD)	VE(Liters - ATPS)	PASS
	47.144	49.625	52.107	49.500	

% Error Tolerance 3.0% OR Low Absolute Tolerance 0.0

VE values in BTPS

	Low Acceptable	Target	High Acceptable	ACTUAL	
Low (Rest)	VE(Liters - BTPS)	VE(Liters - BTPS)	VE(Liters - BTPS)	VE(Liters - BTPS)	PASS
	9.464	9.756	10.049	9.700	
V_E - BTPS Medium (Exercise)	VE(Liters - BTPS)	VE(Liters - BTPS)	VE(Liters - BTPS)	VE(Liters - BTPS)	PASS
	29.238	30.143	31.047	30.200	
High (Exercise)	VE(Liters - BTPS)	VE(Liters - BTPS)	VE(Liters - BTPS)	VE(Liters - BTPS)	PASS
	58.356	60.160	61.965	60.400	

Gas exchange system validation data for the modified umbilical provided by the manufacturer. All measured gas variables (VO_2, VCO_2) RER and volume measurements at both standard pressure dry (STPD) conditions and body temperature and pressure saturated (BTPS) fell within the same acceptable ranges as the standard length commercial umbilical.